

University of New Hampshire

University of New Hampshire Scholars' Repository

Master's Theses and Capstones

Student Scholarship

Spring 2012

Dissolved organic carbon quantity and quality in North American rivers and streams

Kevin Walker Hanley

University of New Hampshire, Durham

Follow this and additional works at: <https://scholars.unh.edu/thesis>

Recommended Citation

Hanley, Kevin Walker, "Dissolved organic carbon quantity and quality in North American rivers and streams" (2012). *Master's Theses and Capstones*. 702.

<https://scholars.unh.edu/thesis/702>

This Thesis is brought to you for free and open access by the Student Scholarship at University of New Hampshire Scholars' Repository. It has been accepted for inclusion in Master's Theses and Capstones by an authorized administrator of University of New Hampshire Scholars' Repository. For more information, please contact Scholarly.Communication@unh.edu.

DISSOLVED ORGANIC CARBON QUANTITY AND QUALITY IN NORTH
AMERICAN RIVERS AND STREAMS

BY

KEVIN WALKER HANLEY
B.S., McGill University, 2005

THESIS

Submitted to the University of New Hampshire
in Partial Fulfillment of
the Requirements for the Degree of

Master of Science
in
Earth Science

May, 2012

UMI Number: 1518007

All rights reserved

INFORMATION TO ALL USERS

The quality of this reproduction is dependent upon the quality of the copy submitted.

In the unlikely event that the author did not send a complete manuscript and there are missing pages, these will be noted. Also, if material had to be removed, a note will indicate the deletion.

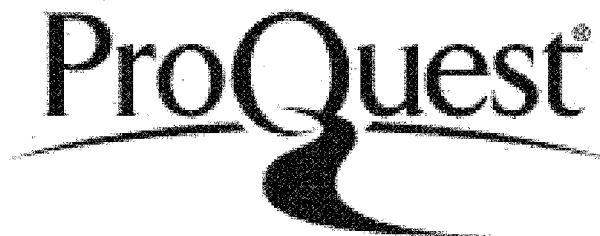


UMI 1518007

Published by ProQuest LLC 2012. Copyright in the Dissertation held by the Author.

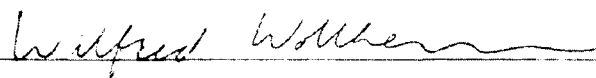
Microform Edition © ProQuest LLC.

All rights reserved. This work is protected against unauthorized copying under Title 17, United States Code.

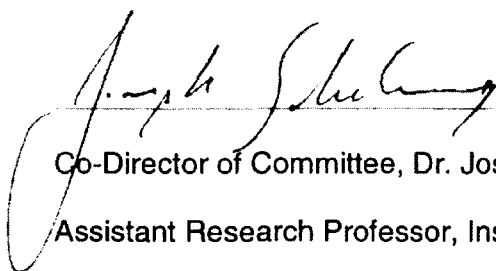


ProQuest LLC
789 East Eisenhower Parkway
P.O. Box 1346
Ann Arbor, MI 48106-1346

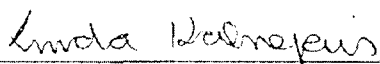
This thesis has been examined and approved.



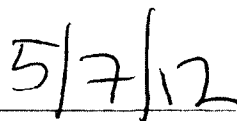
Co-Director of Committee, Dr. Wilfred Wollheim,
Assistant Professor, Earth Systems Research Center and
Department of Natural Resources and the Environment



Co-Director of Committee, Dr. Joseph Salisbury,
Assistant Research Professor, Institute for the Study of Earth,
Oceans, and Space



Dr. Linda Kalnejais, Assistant Professor, Department of
Earth Sciences



Date

ACKNOWLEDGEMENTS

We are grateful to S. Glidden, A. Prusevich, and R. Stewart for data processing assistance, to C. Crawford (USGS) and the field teams of the USGS National Stream Quality Accounting Network and National Water Quality Assessment programs for assistance in fieldwork, and to K. Butler for laboratory assistance. This work was funded by National Aeronautics and Space Administration grants NNX09AU89G and NNH04AA62I, and the U.S. Geological Survey's NASQAN, NAWQA, and National Research Programs. This research was completed in partial fulfillment of the requirements for the degree of M.S. in Earth Science at the University of New Hampshire.

TABLE OF CONTENTS

ACKNOWLEDGEMENTS.....	iii
LIST OF TABLES	v
LIST OF FIGURES.....	vi
ABSTRACT	vii

CHAPTER	PAGE
I. CONTROLS ON DISSOLVED ORGANIC CARBON QUANTITY AND QUALITY IN LARGE NORTH AMERICAN RIVERS.....	1
Methods.....	6
Results.....	12
Discussion	19
II. ASSESSING TEMPORAL VARIABILITY IN DISSOLVED ORGANIC CARBON QUANTITY AND QUALITY FOR SMALL RIVERS IN THE CONTINENTAL UNITED STATES.....	33
Methods.....	36
Results.....	44
Discussion	55
CONCLUSIONS AND FUTURE WORK.....	60
LIST OF REFERENCES	62
APPENDIX	72

LIST OF TABLES

CHAPTER I

Table 1.1	7
Table 1.2	10
Table 1.3	15
Table 1.4	16
Table 1.5	26

CHAPTER I

Table 2.1	38
Table 2.2	49
Table 2.3	53

APPENDIX

Table A.1	73
Table A.2	79
Table A.3	87
Table A.4	92
Table A.5	93
Table A.6	97

LIST OF FIGURES

CHAPTER I

Figure 1.1	6
Figure 1.2	14
Figure 1.3	15
Figure 1.4	17
Figure 1.5 & 1.6	18
Figure 1.7	20
Figure 1.8	21
Figure 1.9	23

CHAPTER II

Figure 2.1	37
Figure 2.2	43
Figure 2.3	46
Figure 2.4	47
Figure 2.5	50
Figure 2.6 & 2.7	51
Figure 2.8	57
Figure 2.9	59

ABSTRACT

DISSOLVED ORGANIC CARBON QUANTITY AND QUALITY IN NORTH AMERICAN RIVERS AND STREAMS

by

Kevin Walker Hanley

University of New Hampshire, May, 2012

The controls on the quantity and chemical composition of dissolved organic carbon (DOC) in freshwater systems are crucial to understanding and managing processes like carbon sequestration, heavy-metal transport, and municipal water sanitization. We analyzed DOC quantity and quality for 17 major North American rivers and the temporal variability of DOC quantity and quality in several thousand small basins. Among large basins, we found positive correlation between wetland-cover and both DOC concentration ($R^2=0.78$; $p<0.0001$) and specific ultraviolet absorbance at 254nm ($SUVA_{254}$; $R^2=0.91$; $p<0.0001$). We found that the role of river networks in altering the annual DOC signal minimal except in systems with long residence times. Among small basins, we found characteristics like runoff, stormflow, and vegetation indices useful in predicting the temporal variability of DOC concentration. Further work should clarify where individual characteristics drive DOC variability and more rigorously define the role of processing in large rivers.

CHAPTER I

CONTROLS ON DISSOLVED ORGANIC CARBON QUANTITY AND QUALITY
IN LARGE NORTH AMERICAN RIVERS

Introduction

Dissolved organic carbon (DOC) quantity and chemical quality in rivers and streams play key biogeochemical roles influencing drinking water quality, heavy metal transport, stream ecosystem processes, coastal eutrophication, and the global carbon cycle [Aiken *et al.*, 2003; Buffam *et al.*, 2001; Cole *et al.*, 2007; Frey and Smith, 2005; Gattuso *et al.*, 1998; Lehtoranta *et al.*, 2009; Sholkovitz, 1976; Siddiqui *et al.*, 1997]. Large rivers are particularly important because they are a major source of material to the coastal ocean and they indicate dynamics across broad regions. However, most previous basin-scale riverine organic carbon studies have focused either on small or individual watersheds, with many finding that bulk DOC variability is related to basin-scale characteristics such as wetland-cover and runoff [Buffam *et al.*, 2007; Chorover and Amistadi, 2001; Clair and Ehrman, 1996; Creed *et al.*, 2003; Dalzell *et al.*, 2007; Gergel *et al.*, 1999; Mulholland and Kuenzler, 1979; Raymond and Hopkinson, 2003]. We sought to address whether the processes that appear to control DOC quantity in small basins also scale to large, continental-scale systems. In addition, current global carbon flux models continue to rely on DOC concentration data of questionable quality, often collected more than 30 years ago [Alexander *et al.*, 1998; Harrison *et al.*, 2005; Lauerwald *et al.*, 2012; Meybeck and Ragu, 1996; Seitzinger *et al.*, 2005]. Here we provide updated estimates of DOC concentration and flux from 17 large rivers in North America that may be used in future modeling efforts.

Interpreting variability in the quantity of DOC and predicting its impact in natural systems is difficult without also taking into account its chemical makeup, or quality. The quality of DOC is largely determined by its source material and past biogeochemical transformations [Schlesinger, 1997]. As a result, DOC is made up of thousands of different molecules with a broad spectrum of compositions, aromaticities, and molecular weights [Maurice et al., 2002]. Because the chemical quality of DOC influences and is influenced by microbial and photolytic processes [Anesio et al., 2005; Miller et al., 2009; Namour and Muller, 1998; Stubbins et al., 2008] knowledge of DOC quality can improve understanding of both the source and fate of DOC in river systems. The chemical makeup of DOC in aquatic systems also influences the transport and bioavailability of heavy metals [Dittman et al., 2010] and anthropogenic organic compounds, interacts with natural and engineered nanoparticles [Aiken et al., 2011], and impacts the production of harmful byproducts of chlorine disinfection during drinking water sanitization [Singer, 1999]. Therefore, a more complete understanding of the quality of DOC in rivers and streams will aid in our interpretation of bulk DOC variability and help to ensure the health and safety of fresh water resources.

Some previous large and continental-scale studies have explored controls on DOC quantity and quality, though each had limitations. *Aitkenhead and McDowell* [2000] found a strong link between soil C:N and DOC flux at the annual scale among biomes ($R^2=0.992$, $p<0.0001$). Despite the strength of this relationship, when it is applied to predicting DOC flux from individual watersheds,

particularly large ones, its utility is limited by the necessity of geospatially extensive soil C:N data. *Frost et al.* [2006] characterized DOC concentration and quality throughout a single large river network. They found that concentration was related to a range of landscape variables including percent wetland-cover and the total drainage area of individual sub-catchments. They also found that the molecular weight of DOC and its aromaticity were related to the percent lake-cover and percent wetland-cover of individual sub-catchments. *Shih et al.* [2010] developed a continental-scale total organic carbon flux model based on a variety of watershed parameters using the SPARROW modeling framework [*Alexander et al.*, 2000]. They found that in-stream processes were significant in controlling both the quantity and quality of DOC. However, implicit in their model was the assumption that all organic carbon in a reach, irrespective of quality, was remineralized at the same rate. This type of model simplification may be adequate to predict bulk organic carbon quantity, but it does not reflect important complexities in the underlying biogeochemical processes and makes the interpretation of model predictions problematic. By not taking into account the spectrum of organic matter quality among different sources the authors likely overestimated the contribution to basin exports by more easily remineralized autochthonous sources and underestimated the more refractory allochthonous sources [*Benner*, 2003; *del Giorgio and Davis*, 2003; *del Giorgio and Pace*, 2008]. Unfortunately, few comparative large-basin DOC studies have been conducted that also incorporate quality. Here we update large-river DOC flux estimates and improve understanding of the processes underlying DOC

variability in freshwater systems by examining DOC quantity together with quality among 17 large rivers throughout temperate North America. We strove to answer several primary research questions:

1. Are the biogeochemical processes underlying the observed relationships between watershed-scale characteristics and DOC quantity among small rivers also important among large and continental-scale systems?
2. Can watershed-scale characteristics explain the variability of DOC quality among large river basins?

Answers to these questions will also help address a third question:

3. How important are in-stream processes accumulated at network scales in altering the quantity and quality of DOC transferred from the continents to the oceans?

Methods

Study Sites

Our study sites included 17 large watersheds from across a wide range of biomes in North America (Figure 1.1, Table 1.1), 11 of which are monitored by the U.S. Geological Survey's National Stream Quality Accounting Network (NASQAN). Basins were selected based on two criteria: large drainage areas ($> 1000 \text{ km}^2$) and complete daily discharge records available for the sampling period. NASQAN locations in Alaska (Yukon River) were excluded to eliminate the confounding influence of permafrost from the analysis. Site information, including geospatial coordinates, contributing drainage area, and most discharge data were acquired through the USGS National Water Information Service (NWIS). Discharge data for the Rio Grande were obtained from the International Boundary and Water Commission [IBWC, 2010]. In all cases, runoff was calculated as discharge divided by drainage area.

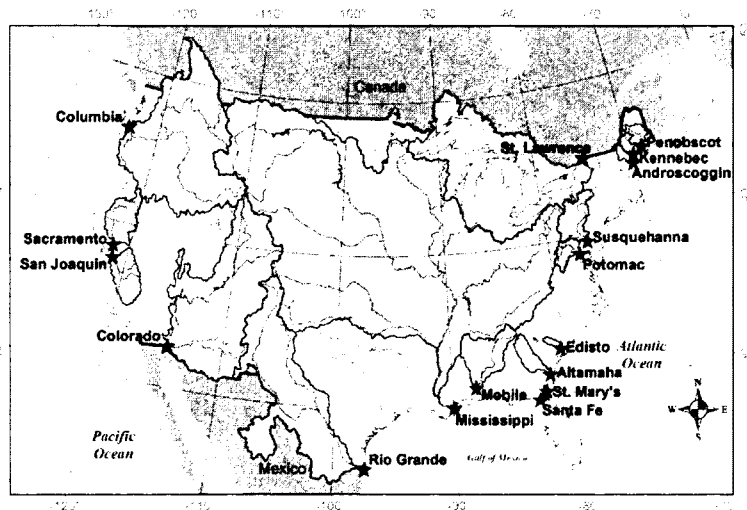


Figure 1.1. Map showing the drainage basins and sampling locations for 17 North American rivers.

Table 1.1. Table showing station information, upstream drainage area, mean runoff, and annual mean values for dissolved organic carbon (DOC), specific ultraviolet absorption at 254 nm (SUVA₂₅₄) and hydrophobic organic acids (HPOA). Rivers are sorted clockwise around the North American coastline starting in the Northeastern United States. *ND* indicates no data available.

Site Number	River Name	Location	Lat	Long	Drainage <i>km²</i>	Wetlands <i>% basin</i>	Runoff <i>cm/yr</i>	DOC yield <i>g yr⁻¹ m⁻²</i>	DOC load <i>kg/day</i>	[DOC] <i>mgC/L</i>	SUVA ₂₅₄ <i>L mgC⁻¹ m⁻¹</i>	HPOA <i>%[DOC]</i>	HPOA Load <i>kg/day</i>
01036390	Penobscot River	Eddington, ME	44.83	-68.70	19460	10.4	80.66	7.55	403000	9.3	3.8	<i>ND</i>	<i>ND</i>
01049265	Kennebec River	North Sidney, ME	44.47	-69.68	13990	6.8	78.12	4.97	191000	6.4	3.6	<i>ND</i>	<i>ND</i>
01059400	Androscoggin River	Brunswick, ME	43.92	-69.97	8894	4.8	88.00	5.31	129000	6.0	3.6	<i>ND</i>	<i>ND</i>
01578310	Susquehanna River	Conowingo, MD	39.66	-76.17	70200	1.2	52.41	1.38	266000	2.7	2.3	0.39	90700
01646580	Potomac River	Washington, D.C.	38.93	-77.12	29970	0.6	39.66	1.64	134000	4.3	2.6	0.36	45000
02175000	Edisto River	Givhans, SC	33.03	-80.39	7071	16.3	16.86	1.96	37900	11.2	4.0	0.66	24000
02226160	Altamaha River	Everett City, GA	31.43	-81.61	36000	10.5	28.76	2.99	297000	10.1	4.2	0.44	128000
02231000	St. Mary's River	MacClenny, FL	30.36	-82.08	1800	32.5	39.01	18.52	92000	46.8	4.7	0.71	65600
02322500	Santa Fe River	Fort White, FL	29.85	-82.72	2634	15.8	34.88	5.54	40000	12.9	4.0	0.66	29300
02470500	Mobile River	Mount Vernon, AL	31.09	-87.98	111030	8.0	25.17	1.36	414000	5.7	3.4	0.52	209000
04264331	St. Lawrence River	Cornwall, ON	45.01	-74.79	773900	6.9	30.58	1.24	1800000	2.8	1.3	0.29	529000
07374525	Mississippi River	Belle Chasse, LA	29.86	-89.98	2930000	3.4	16.44	0.66	5260000	4.0	3.0	0.43	2050000
08475000	Rio Grande	Brownsville, TX	25.88	-97.45	456700	0.5	0.11	0.01	9200	5.9	2.1	0.35	3180
09522000	Colorado River	Morelos Dam, AZ	32.72	-114.72	639000	0.6	0.30	0.01	16700	3.1	1.7	0.37	5490
11303500	San Joaquin River	Vernalis, CA	37.68	-121.27	35058	0.4	5.16	0.19	18400	3.6	2.5	0.44	5160
11447650	Sacramento River	Freeport Bridge, CA	38.46	-121.50	69457	1.2	21.11	0.63	119000	2.9	2.7	0.39	33400
14246900	Columbia River	Qunicy, OR	46.18	-123.18	665400	0.9	30.59	0.65	1180000	2.1	2.7	0.42	461000

For several rivers daily discharge data were available only at a nearby USGS gauging station located on the same mainstem. In these cases, discharge (Q) was scaled by the percent-difference in upstream drainage areas (A) for the nearby and the NASQAN stations:

$$Q_{NASQAN} = Q_{nearby} (A_{NASQAN} / A_{nearby}) \quad (\text{Eq. 1.1})$$

This technique was used for the Altamaha, Potomac, Mobile, Androscoggin, and Penobscot rivers [Hodgkins, 1999]. In order to analyze discharge seasonality among systems, we normalized monthly-mean discharge values for individual basins to their corresponding annual mean discharge. The resulting values were averaged by month to obtain a time-series of normalized mean discharge for all basins.

We calculated percent wetland-cover in each basin using data derived from the National Land Cover Database (NLCD) [Homer *et al.*, 2004]. We aggregated high resolution NLCD wetland data into a 6-minute resolution grid to produce a percent-wetland raster. We used RiverGIS (RGIS), a raster algebra and topological network analysis application, and the STN-6, a simulated topological river network, to calculate the abundance of wetlands upstream of each of our sampling points [Vorosmarty *et al.*, 2000]. Finally, mean latitude was calculated by taking the average latitude of all grid cells in each basin.

Quantity and Quality

Stations were sampled approximately monthly over 2 to 4 year periods between 2002 and 2010 by the U.S. Geological Survey (Table 1.2). We analyzed

for DOC concentration following *Aiken* [1992]. We also measured DOC quality in terms of specific ultraviolet absorbance ($SUVA_{254}$), which is defined as a sample's spectral absorbance at 254 nm (UVA) normalized to its DOC concentration. All samples were analyzed for UVA using a Hewlett-Packard photo-diode array spectrophotometer and $SUVA_{254}$ was calculated by dividing UVA by DOC concentration. We chose $SUVA_{254}$ as the primary measure of quality because, although it does not explicitly quantify lability, it is a good indicator of DOC aromaticity [*Weishaar et al.*, 2003].

We also measured the proportion of bulk DOC as hydrophobic organic acids (HPOA) using XAD-resin fractionation analysis following *Aiken et al.* [1992]. In brief, samples were acidified to pH 2 using HCl and passed through a column of XAD-8 resin. The HPOA fraction was retained on the XAD-8 resin and then back eluted with 0.1 M NaOH. The concentration of HPOA was determined by direct measurement of the eluent and is presented here as a fraction of bulk DOC. XAD fractionation is useful because it allows us to directly identify the hydrophobic and generally more aromatic and allochthonous compounds in the bulk DOC pool such as fulvic and humic acids [*Aiken et al.*, 1979; *Aiken et al.*, 1992].

Table 1.2. Table showing LOADEST model information: R^2 , Nash-Sutcliffe coefficient, and root mean square error are shown for dissolved organic carbon (DOC), specific ultraviolet absorption at 254 nm ($SUVA_{254}$) and hydrophobic organic acids (HPOA). *ND* indicates that no data were available.

River Name	n	Year Begin	Year End	DOC R^2	DOC RMSE	DOC NS	SUVA R^2	SUVA RMSE	SUVA NS	HPOA R^2	HPOA RMSE	HPOA NS
					<i>mgC/L</i>			<i>L mgC⁻¹ m¹</i>			<i>%[DOC]</i>	
Penobscot River	61	2004	2008	0.97	1.8	0.60	0.99	0.2	0.39	<i>ND</i>	<i>ND</i>	<i>ND</i>
Kennebec River	12	2006	2007	0.99	0.5	0.75	0.99	0.1	0.43	<i>ND</i>	<i>ND</i>	<i>ND</i>
Androscoggin River	12	2006	2007	0.99	0.4	0.81	0.99	0.1	0.58	<i>ND</i>	<i>ND</i>	<i>ND</i>
Susquehanna River	22	2008	2010	0.94	0.4	0.39	0.96	0.3	0.09	0.90	0.04	0.18
Potomac River	21	2008	2010	0.99	0.3	0.80	0.99	0.1	0.81	0.99	0.03	0.92
Edisto River	18	2005	2008	0.96	1.6	0.81	0.99	0.2	0.28	0.96	0.04	0.81
Altamaha River	19	2008	2009	0.99	1.1	0.67	0.99	0.3	0.66	0.90	0.11	-0.51
St. Mary's River	31	2002	2006	0.99	8.5	0.68	0.99	0.3	0.17	0.98	0.04	0.67
Santa Fe River	29	2002	2004	0.93	5.3	0.78	0.98	0.4	0.79	0.93	0.07	0.62
Mobile River	25	2008	2010	0.98	0.6	0.71	0.99	0.2	0.72	0.98	0.04	0.36
St. Lawrence River	16	2008	2009	0.93	0.1	0.80	0.74	0.1	0.53	0.68	0.02	0.36
Mississippi River	23	2008	2010	0.94	0.3	0.50	0.99	0.1	0.71	0.98	0.03	0.80
Rio Grande	21	2008	2009	0.99	0.3	0.44	0.98	0.2	0.32	0.98	0.02	0.30
Colorado River	27	2008	2010	0.92	0.4	0.17	0.96	0.1	0.54	0.99	0.03	0.37
San Joaquin River	23	2008	2010	0.90	0.8	0.48	0.98	0.2	0.27	0.81	0.06	0.21
Sacramento River	24	2008	2010	0.95	0.4	0.80	0.97	0.2	0.82	0.97	0.05	0.95
Columbia River	18	2009	2010	0.97	0.2	0.66	0.96	0.3	0.61	0.94	0.03	0.60

For each station we estimated daily values and the flow-weighted overall-mean for the entire sampling period (henceforth simply referred to as "mean") for DOC concentration and $SUVA_{254}$ using LoadRunner, a graphical front-end to the USGS application LOADEST [Booth *et al.*, 2007; Runkel *et al.*, 2004]. LOADEST incorporates daily discharge, seasonality, and measured constituent data to parameterize a multiple-regression model that allows a continuous time series to be estimated from discrete measurements. Root mean square error (*RMSE*) for each basin was calculated as:

$$RMSE = \sqrt{\frac{\sum ([DOC]_{modeled} - [DOC]_{measured})^2}{n}} \quad (\text{Eq. 1.2})$$

Where $[DOC]$ is DOC concentration and n is the number of observations.

Monthly and annual discharge-weighted concentration means were automatically calculated from the daily modeled values, and fluxes were simply the sum of daily concentrations multiplied by daily discharge over the time period of interest. Mean concentration, flux, and yield were calculated by taking the average of the annual means for each basin. In order to compare among watersheds, we divided flux by basin area to obtain DOC yield.

Results

Basin Attributes and Mean DOC Characteristics

Basins ranged in drainage area from 1800 km² for the St. Mary's River in Florida to 2,930,000 km² for the Mississippi River in Louisiana. In total, the watersheds for all the rivers accounted for more than 70% of the land-area of the contiguous United States and 26% of the land area of North America. The most northerly river was the Columbia in Oregon with a mean watershed latitude of 46.1 degrees and the most southerly was the Santa Fe, with a mean watershed latitude of 30.0 degrees. Mean runoff during each basin's sampling period ranged from 0.11 cm/yr for the Rio Grande in Texas to 88.00 cm/yr for the Androscoggin River in Maine. Wetland-cover ranged from 0.5% for the San Joaquin River in California to 32.5% for the St. Mary's River (Table 1.1).

Mean DOC concentrations from LOADEST ranged from 2.1 mgC/L for the Columbia River in Oregon to 46.8 mgC/L for the St. Mary's, while DOC load ranged from 9200 kgC/day for the Rio Grande to 5,260,000 kgC/day for the Mississippi. DOC yield ranged from 0.01 gC yr⁻¹m⁻² for the Colorado and St. Lawrence rivers in Arizona and Ontario, respectively, to 18.5 gC yr⁻¹m⁻² for the St. Mary's. Mean SUVA₂₅₄, ranged from 1.3 L mg C⁻¹ m⁻¹ for the St. Lawrence to 4.7 L mgC⁻¹ m⁻¹ for the St. Mary's. Mean HPOA fraction ranged from 0.29 for the St. Lawrence to 0.72 for the Santa Fe River in Florida, while HPOA load ranged from 3170 kgC/day for the Rio Grande to 2,050,000 kgC/day for the Mississippi.

Total DOC and HPOA flux for all basins studied was 3.80 TgC/yr and 1.34 TgC/yr, respectively (Table 1.1).

All LOADEST models used to estimate mean DOC concentration, SUVA₂₅₄, and HPOA concentration were significant, with $p < 0.0001$ in all cases except the SUVA₂₅₄ and HPOA models for the St. Lawrence ($p=0.0008$ and $p=0.002$, respectively). For DOC, R^2 ranged from 0.90 to 0.99 for DOC and from 0.74 to 0.99 for SUVA₂₅₄, while Nash-Sutcliffe coefficients ranged from 0.17 to 0.81 for DOC and from 0.09 to 0.82 for SUVA₂₅₄. For HPOA, R^2 ranged from 0.68 to 0.99 and Nash-Sutcliffe coefficients ranged from -0.51 (for the Altamaha River in Georgia) to 0.95, indicating that, with the exception of the Altamaha HPOA model, all LOADEST models predicted measured values with more accuracy than a simple mean (Table 1.2).

DOC Quantity Patterns

We found a strong positive correlation between percent wetland-cover and the log-transformed mean DOC concentration ($R^2=0.83$, $p<0.0001$; Figure 2a). However, the shape of this relationship is almost exclusively driven by the wetland-dominated St. Mary's River. When we excluded the St. Mary's as an outlier, variability in untransformed mean DOC concentration was still well explained by percent wetland-cover ($R^2=0.78$, $p<0.0001$; Figure 2b):

$$[DOC] = 0.55 * L_W + 2.769 \quad (\text{Eq. 1.3})$$

where L_W is percent wetland-cover. In this relationship the St. Lawrence falls well below the regression line but is still included in the analysis.

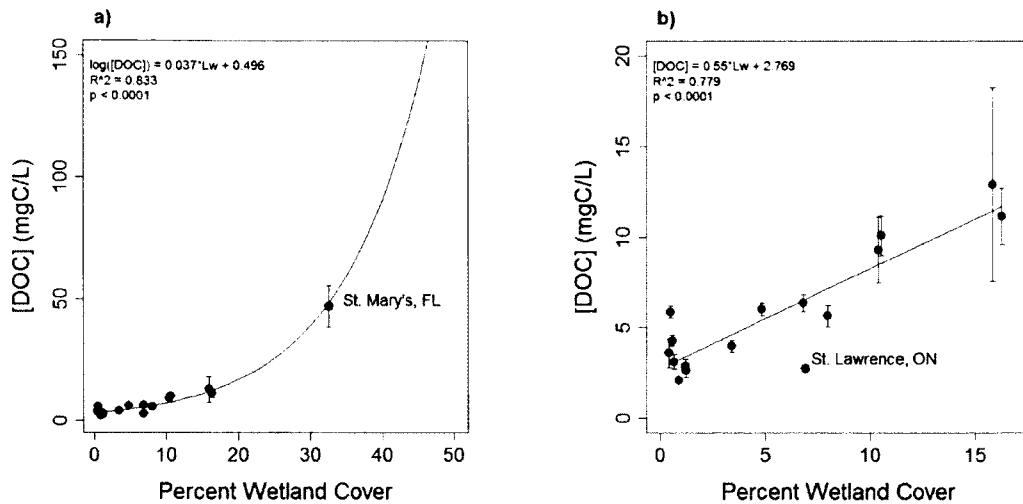


Figure 1.2. Figure showing mean dissolved organic carbon (DOC) concentration vs. percent wetland-cover a) for all sites, with the St. Mary's River highlighted in green and b) excluding St. Mary's River, with the St. Lawrence River highlighted in green. Error bars represent root mean squared error for the LOADEST model and are smaller than the size of the data point in some cases.

In order to investigate seasonality in DOC concentration variability we examined the relationships between percent wetland-cover and monthly-mean DOC concentration among basins. We found that monthly-mean concentration was significantly correlated ($p < 0.05$) with percent wetland-cover for all months, with R^2 ranging from 0.31 to 0.80 (Table 1.3).

We found no significant relationship between mean annual runoff (RO) and mean DOC concentration among basins. However, we did find a significant positive correlation between mean DOC yield and runoff when the St. Marys was again excluded as an outlier ($R^2 = 0.63$, $p < 0.0001$; Figure 1.3):

$$DOC_{yield} = 0.068 * RO - 0.129 \quad (\text{Eq. 1.4})$$

Within individual systems, around half of basins exhibited a significant positive correlation between discrete DOC concentration and daily runoff. In these basins runoff explained between 11 percent and 62 percent of concentration variability (Table 1.4). We found no correlation between the statistical significance of these relationships and a basin's percent wetland-cover or mean annual runoff.

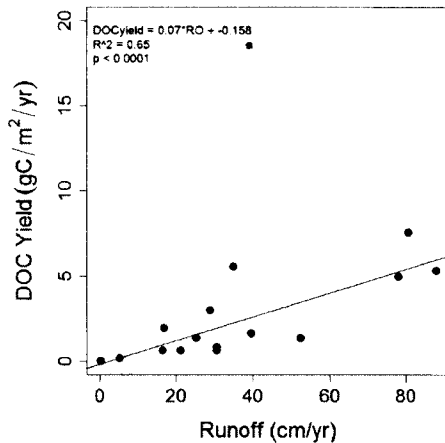


Figure 1.3. Figure showing mean dissolved organic carbon (DOC) yield vs. runoff for all sites (black), excluding St. Mary's River (green) from the linear regression.

Table 1.3. Table showing the equations for the relationships between percent wetland-cover (L_w) and monthly-mean dissolved organic carbon (DOC) concentration or monthly-mean specific ultraviolet absorption at 254 nm ($SUVA_{254}$). Monthly DOC relationships include all rivers except the St. Mary's and monthly $SUVA_{254}$ relationships include all rivers except the St. Lawrence and Colorado.

Month	DOC formula	R ²	p-value	SUVA ₂₅₄ formula	R ²	p-value
Jan	[DOC] = 0.36*L _w + 3.23	0.63	< 0.001	SUVA = 1.04*log(L _w) + 2.729	0.83	< 0.001
Feb	[DOC] = 0.40*L _w + 2.92	0.78	< 0.001	SUVA = 1.15*log(L _w) + 2.599	0.88	< 0.001
Mar	[DOC] = 0.75*L _w + 1.96	0.63	< 0.001	SUVA = 1.24*log(L _w) + 2.587	0.93	< 0.001
Apr	[DOC] = 0.53*L _w + 2.59	0.80	< 0.001	SUVA = 1.19*log(L _w) + 2.592	0.89	< 0.001
May	[DOC] = 0.24*L _w + 3.52	0.31	0.015	SUVA = 1.02*log(L _w) + 2.66	0.75	< 0.001
Jun	[DOC] = 0.46*L _w + 2.81	0.75	< 0.001	SUVA = 1.11*log(L _w) + 2.607	0.79	< 0.001
Jul	[DOC] = 0.44*L _w + 2.87	0.69	< 0.001	SUVA = 1.21*log(L _w) + 2.469	0.86	< 0.001
Aug	[DOC] = 0.49*L _w + 2.89	0.75	< 0.001	SUVA = 1.29*log(L _w) + 2.425	0.88	< 0.001
Sep	[DOC] = 0.75*L _w + 2.19	0.73	< 0.001	SUVA = 1.36*log(L _w) + 2.426	0.83	< 0.001
Oct	[DOC] = 0.38*L _w + 3.44	0.42	0.004	SUVA = 1.32*log(L _w) + 2.502	0.84	< 0.001
Nov	[DOC] = 0.33*L _w + 3.32	0.36	0.008	SUVA = 1.25*log(L _w) + 2.55	0.87	< 0.001
Dec	[DOC] = 0.36*L _w + 3.17	0.46	0.002	SUVA = 1.21*log(L _w) + 2.623	0.85	< 0.001

Table 1.4. Table showing within-basin runoff (RO) relationships for dissolved organic carbon (DOC) concentration and specific ultraviolet absorption at 254 nm (SUVA₂₅₄). Basins without a significant relationship are labeled *N/S*.

River Name	Runoff-DOC formula	R ²	p-value	Runoff-SUVA ₂₅₄ formula	R ²	p-value
Penobscot River	[DOC] = 0.01*RO + 8.46	0.11	0.004	<i>N/S</i>	<i>N/S</i>	0.119
Kennebec River	[DOC] = -0.01*RO + 7.40	0.28	0.043	<i>N/S</i>	<i>N/S</i>	0.275
Androscoggin River	<i>N/S</i>	<i>N/S</i>	0.191	<i>N/S</i>	<i>N/S</i>	0.915
Susquehanna River	<i>N/S</i>	<i>N/S</i>	0.963	<i>N/S</i>	<i>N/S</i>	0.227
Potomac River	<i>N/S</i>	<i>N/S</i>	0.706	<i>N/S</i>	<i>N/S</i>	0.058
Edisto River	[DOC] = 0.27*RO + 4.63	0.40	0.003	<i>N/S</i>	<i>N/S</i>	0.055
Altamaha River	[DOC] = 0.03*RO + 8.53	0.18	0.022	SUVA = 0.01*RO + 3.89	0.27	0.006
St. Mary's River	<i>N/S</i>	<i>N/S</i>	0.336	<i>N/S</i>	<i>N/S</i>	0.101
Santa Fe River	[DOC] = 0.17*RO + 2.78	0.62	< 0.001	SUVA = 0.01*RO + 3.76	0.10	0.045
Mobile River	<i>N/S</i>	<i>N/S</i>	0.443	SUVA = 0.01*RO + 3.06	0.35	0.001
St. Lawrence River	[DOC] = 0.06*RO + 0.97	0.38	0.005	<i>N/S</i>	<i>N/S</i>	0.89
Mississippi River	<i>N/S</i>	<i>N/S</i>	0.086	SUVA = 0.02*RO + 2.57	0.27	0.007
Rio Grande	<i>N/S</i>	<i>N/S</i>	0.06	SUVA = 2.05*RO + 1.85	0.16	0.043
Colorado River	[DOC] = 1.67*RO + 2.56	0.14	0.029	SUVA = 0.95*RO + 1.35	0.20	0.011
San Joaquin River	<i>N/S</i>	<i>N/S</i>	0.583	<i>N/S</i>	<i>N/S</i>	0.107
Sacramento River	[DOC] = 0.06*RO + 1.37	0.50	< 0.001	SUVA = 0.04*RO + 1.67	0.71	< 0.001
Columbia River	[DOC] = 0.02*RO + 1.47	0.47	0.001	SUVA = 0.02*RO + 1.96	0.27	0.017

DOC Quality Patterns

Percent wetland-cover also appeared to be an important variable in controlling DOC quality. We found a strong positive correlation between the logarithm of percent wetland-cover and mean SUVA₂₅₄ among the large rivers in our data set (R²=0.54, p=0.0005; Figure 1.4). In this case, the St. Lawrence and Colorado rivers were outliers, exhibiting far lower SUVA₂₅₄ than expected based on their wetland-cover. The St. Mary's was not an outlier for SUVA₂₅₄. When the St. Lawrence and Colorado rivers were excluded from the regression, the relationship between percent wetland-cover and SUVA₂₅₄ improved (R²=0.90, p<0.0001; Figure 1.4):

$$SUVA_{254} = 1.17 * \log(L_W) + 2.65 \quad (\text{Eq. 5})$$

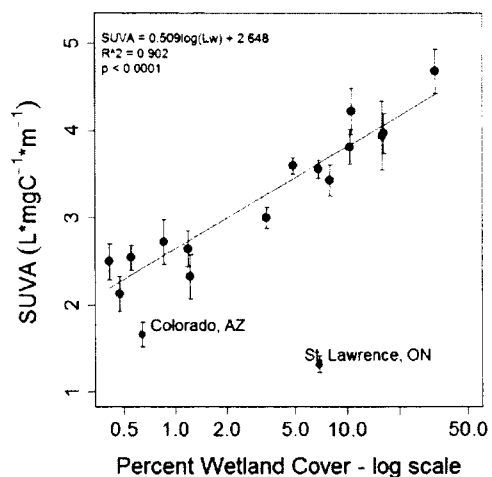


Figure 1.4. Figure showing mean specific ultraviolet absorption at 254 nm (SUVA₂₅₄) vs. percent wetland-cover for all basins. X-axis is log-scale and excluded outliers are in green. Final model is in black. Model before the outliers were excluded is shown in dotted grey. Error bars represent root mean squared error for the LOADEST model.

We also examined the relationships between percent wetland-cover and monthly-mean SUVA₂₅₄ among basins and found that monthly-mean SUVA₂₅₄ was significantly correlated ($p < 0.001$) with percent wetland-cover for all months with R^2 ranging from 0.75 to 0.93 (Table 1.3). These relationships exhibited little seasonal variability and were more highly significant than the monthly DOC concentration relationships.

We found no statistically significant relationship between mean runoff and SUVA₂₅₄ among basins, with or without outliers (Figure 1.5). Within individual systems, around half of basins exhibited a significant positive correlation between discrete SUVA₂₅₄ and daily runoff, with runoff explaining between 10 percent and 71 percent of variability (Table 1.4). Basins with a significant relationship tended to be in the south and the west, whereas northern and eastern rivers did not tend to show significance. As with DOC concentration, we found no correlation between the statistical significance of these relationships and a basin's percent wetland-cover.

HPOA as a percentage of bulk DOC was positively correlated with $SUVA_{254}$ measurements in individual grab samples across 14 basins where both measurements were made ($R^2=0.89$, $p<0.0001$; Figure 1.6). Within individual basins, the relationship with $SUVA_{254}$ was significant for all but three systems (Mobile, Mississippi, and Colorado) with R^2 ranging from 0.24 for the St. Mary's to 0.87 for the neighboring Santa Fe. As a result, HPOA patterns were very similar to $SUVA_{254}$.

Figure 1.5. Figure showing mean specific ultraviolet absorption at 254 nm ($SUVA_{254}$) vs. mean runoff for all basins. Excluded outliers (St. Lawrence and Colorado) are shown in green.

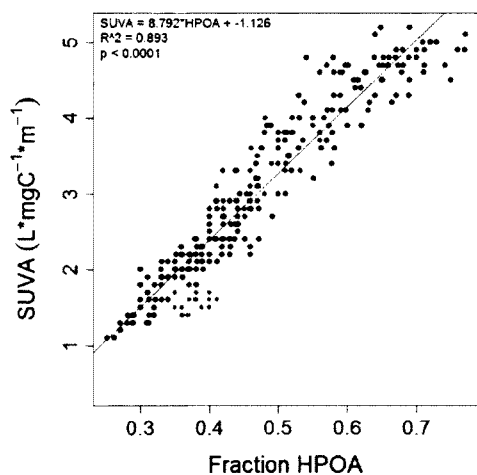
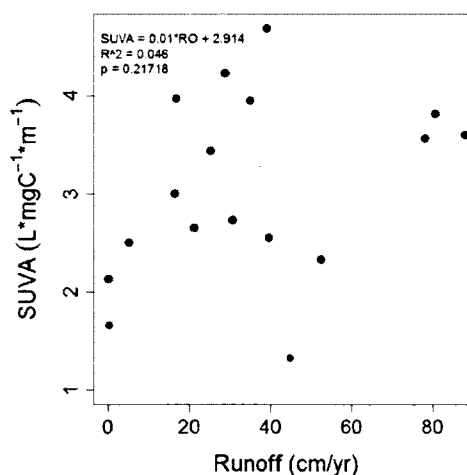


Figure 1.6. Fraction of dissolved organic carbon (DOC) as hydrophobic organic acid (HPOA) vs. specific ultraviolet absorption at 254 nm ($SUVA_{254}$) for discrete measurements from all basins. Measurements from rivers where the within-basin relationship between HPOA and $SUVA_{254}$ was not significant (see Table 5) are shown as colored dots: Colorado River in green, Mississippi River in blue, and Mobile River in red.

Discussion

DOC Quantity

We identified a significant positive relationship between basin wetland-cover and mean DOC concentration among large watersheds that was consistent with what has been reported for small basins [Buffam *et al.*, 2007; Creed *et al.*, 2003; Eckhardt and Moore, 1990; Gergel *et al.*, 1999; Gorham *et al.*, 1998; Raymond and Hopkinson, 2003]. Similar observations previously made among small basins have typically been explained by the hypothesis that runoff from a wetland to a stream channel would be less likely to have intersected the mineral soil horizon than runoff from non-wetland systems. These flow paths are important because DOC builds up in wetlands due to anaerobic conditions while DOC in subsurface flow intersecting the mineral horizon is more likely to be removed from solution by microbial processing and adsorption [Aitkenhead-Peterson *et al.*, 2003; Buffam *et al.*, 2007; Eckhardt and Moore, 1990; Tipping *et al.*, 1999]. We found that these small-basin patterns also occurred in large river systems, indicating that the control exerted by wetlands on the source of riverine DOC was also evident in large and continental scale systems.

Although percent wetland cover is a powerful explanatory variable, substantial DOC concentration variability remained among the seven least wetland-dominated watersheds. These watersheds are geographically diverse and include the San Joaquin, Rio Grande, Potomac, Colorado, Columbia, Sacramento, and Susquehanna rivers which range from 0.4 to 1.2% wetland

cover and possess a mean DOC concentration of 3.5 ± 1.3 mgC/L. Among these basins, we found that mean watershed latitude was negatively correlated with DOC concentration ($R^2=0.71$, $p=0.011$; Figure 1.7), indicating that climate effects may dominate DOC concentration variability among low-wetland systems at the annual scale, but that wetland controls eclipse climate effects in basins where wetlands are more extensive.

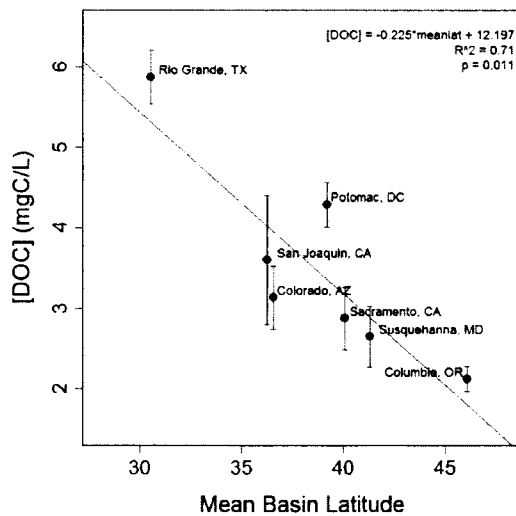


Figure 1.7. Figure showing mean dissolved organic carbon (DOC) concentration vs. mean watershed latitude for systems with less than 2% wetland cover. Error bars represent root mean squared error for the LOADEST model.

As in previous studies, we analyzed seasonal patterns in wetland-concentration relationships to help identify potential driving mechanisms. Typically, previous small-basin studies focused on a series of snapshots within the annual cycle. For example, *Buffam et al.* [2007] observed that the slope of the relationship between wetlands and DOC was steepest during a period of baseflow, suggesting dilution of DOC in high-wetland regions and increased DOC concentration in low-wetland regions during the spring flood (Figure 1.8). *Eckhardt and Moore* [1990], *Raymond and Hopkinson* [2003], and *Gorham et al.*

[1998] observed no clear seasonal pattern in the slopes of wetland-DOC relationships, though *Eckhardt and Moore* [1990] did find that streams draining low-wetland catchments exhibited a positive response in DOC concentration to rising runoff, a result consistent with *Buffam et al.* [2007]. *Boyer et al.* [1997] observed similar patterns and suggested as an explanation that the spring flood could lead to increased flushing of DOC from organic surface soil horizons that were previously hydrologically disconnected.

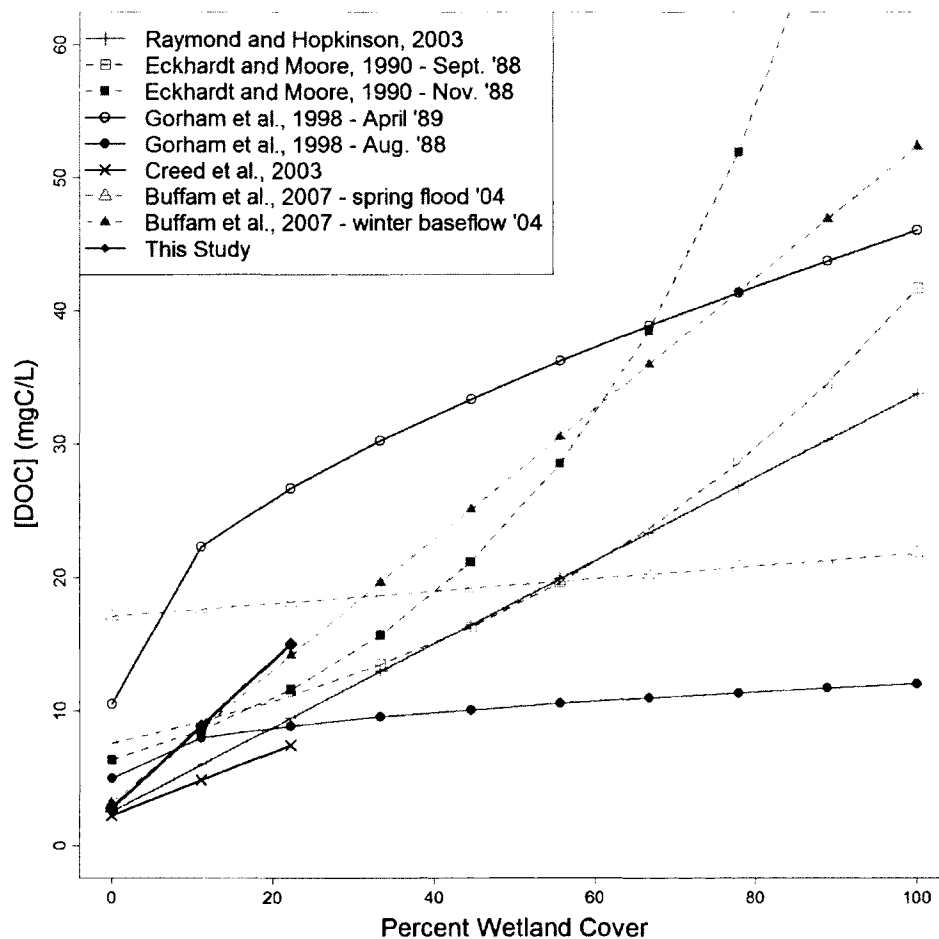


Figure 1.8. Figure showing dissolved organic carbon (DOC) concentration vs. percent wetland-cover relationships from this (red diamonds) and five previous small-basin studies.

When we examined the slopes of the DOC concentration vs. percent wetland-cover relationships for individual months throughout the year, we found some evidence to support the hypothesis that the spring flood drove rising DOC concentration in low-wetland systems and dilution of DOC in high-wetland systems. We observed a consistent mean slope of 0.37 ± 0.03 between October and February, with a sharp rise to 0.75 in March (Figure 1.9a). This initial rise in slope was followed by a fall through April to 0.24 in May in apparent response to rising monthly-mean runoff, which was consistent with *Buffam et al.* [2007]. Slope returned to a consistent mean of 0.46 ± 0.02 through June, July, and August before spiking again to 0.75 in September. The y-intercepts of these relationships were closely negatively correlated with the slopes ($R^2=0.92$, $p<0.0001$; Figure 9b), which was also consistent with *Buffam et al.* [2007]. However, in contrast to the previously described hypothesis, daily discharge drove an increase in DOC concentration only within some individual large basins (Table 1.4) and no correlation was found between the statistical significance of these relationships and percent wetland-cover. For example, the high slopes observed in March and September were primarily driven by spikes in monthly mean DOC concentration in the Altamaha river, a high-wetland system, in response to elevated monthly-mean discharge. Thus, evidence in large watersheds is inconclusive with respect to the hypothesis presented by *Buffam et al.* [2007].

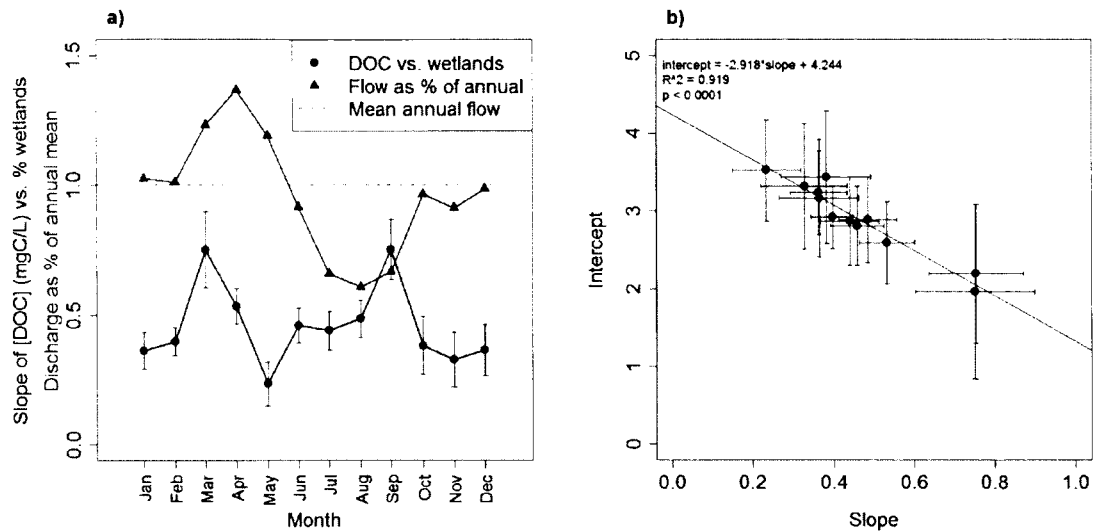


Figure 1.9. Figure showing a) slopes of the relationships between monthly-mean dissolved organic carbon (DOC) concentration and percent wetland-cover (plotted in black) and normalized monthly-mean discharge as a percent of mean annual flow (plotted in blue). b) Slope vs. intercept for the relationships between monthly-mean DOC concentration and percent wetland-cover. All error bars represent standard error.

Mean runoff appeared to control variation in DOC yield among large basins at the annual scale (Fig. 1.3) without directly influencing DOC concentration [Mulholland and Kuenzler, 1979; Mulholland and Watts, 1982]. The lack of a significant relationship between mean DOC concentration and mean runoff indicated that the controls exerted on mean yield by runoff were unrelated to the factors controlling mean concentration. Rather, when predicting DOC flux at annual scales from large rivers, annual runoff should be considered a vector, rather than an explanatory variable for concentration.

In this study, we sampled across the hydrograph and estimated fluxes using LOADEST, which led to DOC flux estimates that differed from those made previously. The 17 rivers systems in this study generated a total DOC flux of 3.80

TgC/yr, which constituted only 9% of the total DOC flux from the entire North American continent as estimated by *Ludwig et al.* [1996] (41.18 TgC/yr), yet these 17 rivers accounted for approximately 13% of total North American discharge [*Benke and Cushing*, 2005]. The low fraction of total flux from these 17 rivers when compared to the total North American flux estimated by *Ludwig et al.* [1996] may be partially due to their use of a mean DOC concentration value of 8.79 mgC/L for the Mississippi River [*Leenheer*, 1982], which is more than double the mean concentration found here (4.0 mgC/L). The Mississippi is particularly important because it is the largest river in North America and it accounts for nearly half of total discharge and DOC flux from the 17 rivers in this study, so even small percentage errors in its concentration can lead to a large absolute error in the estimation of flux. It is possible that such over-estimates of riverine DOC flux could contribute to the "missing terrestrial carbon" often noted in oceanographic carbon-cycle studies [*Bianchi*, 2011].

More recent studies also base their models partly on concentration values from data sources which have not been updated in over thirty years and often present mean DOC concentrations based on only 2 to 4 measurements per year [*Alexander et al.*, 1998; *Harrison et al.*, 2005; *Lauerwald et al.*, 2012; *Meybeck and Ragu*, 1996; *Seitzinger et al.*, 2005]. For example, *Seitzinger et al.* [2005] and *Harrison et al.* [2005] use DOC concentration measurements for the Mississippi River recorded from 1978-1984, arriving at a mean concentration of 6.7 mgC/L ($n=14$). However, we examined the USGS National Water Information System for historic DOC concentration measurements from the same gauging

station and found only a single value that exceeded 5 mgC/L since 1997 and a median DOC concentration of 3.7 mgC/L ($n=84$), indicating that there may be significant error in the historic DOC records that are still being used in current models. By sampling for multiple years across the hydrograph, employing strict QAQC, and estimating fluxes using the LOADEST model, we present a clearer, updated picture of the quantity of DOC recently delivered by these large rivers to estuaries and the coastal ocean.

DOC Quality

Basin-scale wetland cover played a major role in controlling mean DOC quality among large basins. It was clear that higher percent wetland cover drove an increase in mean $SUVA_{254}$. The role of wetlands in controlling $SUVA_{254}$ among large basins appears to be related to the previously discussed hypothesis that subsurface flow through mineral versus organic soil horizons can control DOC concentration variability. Saturated, anaerobic conditions common in wetland soils can inhibit organic matter remineralization and lead to the persistence of semi-labile aromatic compounds in subsurface flow that would drive up $SUVA_{254}$ in the rivers and streams to which it is discharged [Guillemette and del Giorgio, 2011]. In the absence of wetlands, extensive microbial processing and the preferential sorption of strongly UV-absorbing, aromatic DOC molecules onto mineral soils, and, in some specialized cases, onto sediments and particles within the stream channel, would drive down $SUVA_{254}$ [Chorover and Amistadi, 2001; McKnight et al., 2002; McKnight et al., 1992; Meier et al.,

1999; Perez et al., 2011; Tipping et al., 1999]. Thus, if subsurface flow paths are less likely to intersect mineral horizons in watersheds with extensive wetland cover, less of the aromatic, strongly UV-absorbing DOC would be removed and DOC with a higher SUVA₂₅₄ would be more likely to enter river systems.

The significant positive correlation between SUVA₂₅₄ and the HPOA fraction of bulk DOC (Fig. 1.6) was unsurprising because the HPOA is typically considered to comprise aquatic fulvic and humic acids possessing a high molecular weight and aromaticity [Aiken et al., 1979]. These results suggest that SUVA₂₅₄ may be a useful surrogate for HPOA in organic carbon modeling applications. However, this relationship broke down within some individual basins (Mobile, Mississippi, and Colorado; Table 1.5), indicating that non-aromatic hydrophobic acids may drive HPOA in some cases and that care should be taken when utilizing SUVA₂₅₄ as a proxy for HPOA.

Table 1.5. Table showing within-basin relationships between hydrophobic organic acid (HPOA) and specific ultraviolet absorbance at 254 nm (SUVA₂₅₄). Basins without a significant relationship are labeled *N/S*. *ND* indicates that no data were available.

River Name	HPOA-SUVA ₂₅₄ formula	R ²	p-value
Penobscot River	<i>ND</i>	<i>ND</i>	<i>ND</i>
Kennebec River	<i>ND</i>	<i>ND</i>	<i>ND</i>
Androscoggin River	<i>ND</i>	<i>ND</i>	<i>ND</i>
Susquehanna River	SUVA = 4.795*HPOA + 0.346	0.64	< 0.001
Potomac River	SUVA = 6.584*HPOA + -0.306	0.58	0.003
Edisto River	SUVA = 4.988*HPOA + 1.061	0.54	0.001
Altamaha River	SUVA = 8.267*HPOA + -0.577	0.39	< 0.001
St. Mary's River	SUVA = 2.738*HPOA + 2.826	0.24	0.003
Santa Fe River	SUVA = 7.245*HPOA + -0.19	0.87	< 0.001
Mobile River	<i>N/S</i>	<i>N/S</i>	0.201
St. Lawrence River	SUVA = 5.243*HPOA + -0.18	0.64	< 0.001
Mississippi River	<i>N/S</i>	<i>N/S</i>	0.346
Rio Grande	SUVA = 6.013*HPOA + -0.102	0.48	0.001
Colorado River	<i>N/S</i>	<i>N/S</i>	0.199
San Joaquin River	SUVA = 4.807*HPOA + 0.43	0.40	0.009
Sacramento River	SUVA = 8.07*HPOA + -0.825	0.76	< 0.001
Columbia River	SUVA = 8.754*HPOA + -1.143	0.56	0.003

Network-scale processing

It was somewhat surprising that the terrestrial wetland signal was so clear at the continental scale. We expected this signal to be masked or muted in large rivers by in-stream processes like photodegradation, microbial processing, and sorption accumulating through the river network. However, percent wetland-cover explained much of the DOC concentration and SUVA₂₅₄ variability among basins at the annual scale. When we compared the concentration vs. wetland relationship observed here (Eq. 1.3) to those observed in previous studies [Buffam *et al.*, 2007; Creed *et al.*, 2003; Eckhardt and Moore, 1990; Gergel *et al.*, 1999; Gorham *et al.*, 1998; Raymond and Hopkinson, 2003], we found little obvious difference in absolute concentration, slope, or intercept (Figure 1.8). Specifically, over the range of percent wetland-cover values studied here, the slope was greater than those found in most previous small basin studies but fell between the highest and lowest, demonstrating little evidence for within-network processing at annual scales.

While wetland abundance was clearly related to SUVA₂₅₄ in large watersheds, the presence of large lakes and reservoirs appeared to alter this pattern, as suggested by the Colorado and St. Lawrence river outliers. Waters in Lakes Mead and Powell on the Colorado River have a combined residence time of approximately 5 years [USBR-LC; USBR-UC] and in Lake Ontario on the St. Lawrence, approximately 6 years [Beltran *et al.*, 1995]. We suspected that the long residence times for water in the two outlier rivers (Colorado and St. Lawrence) might have driven down SUVA₂₅₄ by autochthonous production of

lower SUVA₂₅₄ DOC, photodegradation, and microbial processing [*Spencer et al.*, in press]. Previous studies suggest that in the Colorado River artificially flooded canyons like Lake Powell act as a trap for both organic and inorganic material entering from the major upstream river. Over time, sediments settle and organic matter can be remineralized or adsorbed onto precipitating calcite [*Reynolds*, 1978]. Water discharged from Glen Canyon Dam is left nutrient-rich and nearly free of suspended particles. Unsurprisingly, these conditions facilitate autochthonous production of weakly UV-absorbing DOC [*Henderson et al.*, 2008] in the downstream reach [*Stanford*, 1990]. Conversely, this interpretation is not always supported in the literature for the St. Lawrence: based on an isotopic analysis of watershed soil-carbon, DOC, POC, and DIC, *Helie and Hillaire-Marcel* [2006] reported an underlying terrestrial DOC signal with some autochthonously driven variability only in the summer months.

Extensive photodegradation of DOC during the long Great Lakes residence time and limited autochthonous production could help to explain the apparent conundrum in the St. Lawrence River of DOC with very low SUVA₂₅₄ values that also retain a terrestrial isotopic signal. Photodegradation acts primarily by breaking up strongly UV-absorbing molecules like terrestrial humic and fulvic acids [*Moran and Zepp*, 1997; *Waiser and Robarts*, 2004], which drives down SUVA₂₅₄ over time. Photodegradation of DOC has also been observed to result in an increase in its lability, leading to greater microbial remineralization [*Anesio et al.*, 2005]. Thus, in addition to driving down SUVA₂₅₄

in the St. Lawrence, photodegradation could also provide an explanation for the comparatively low DOC concentration that we observed there (Figure 1.2b).

SUVA₂₅₄ end members identified in this study were similar to those found in the literature [Spencer *et al.*, 2008; Weishaar *et al.*, 2003]. We identified a maximum mean SUVA₂₅₄ of $4.7 \pm 0.3 \text{ L mgC}^{-1} \text{ m}^{-1}$ and an HPOA fraction of $71 \pm 4 \%$, for the wetland-dominated St. Mary's River. The highest mean SUVA₂₅₄ values previously reported ranged from 3.2 to $5.3 \text{ L mgC}^{-1} \text{ m}^{-1}$ for aquatic humic substances [Weishaar *et al.*, 2003]. The lower end member was more difficult to estimate because as percent wetland-cover in Equation 1.5 approached zero, so did predicted mean SUVA₂₅₄. Mean SUVA₂₅₄ for the six basins with less than 2% wetland-cover (Colorado River excluded) was $2.5 \pm 0.2 \text{ L mgC}^{-1} \text{ m}^{-1}$, significantly higher than groundwater and microbially-dominated SUVA₂₅₄ end members found by Stets *et al.* [2010] which ranged from 0.9 to $2.1 \text{ L mgC}^{-1} \text{ m}^{-1}$. However, mean SUVA₂₅₄ for the St. Lawrence and Colorado rivers were 1.3 and $1.7 \text{ L mgC}^{-1} \text{ m}^{-1}$, respectively. If network-scale processing played a major role in driving SUVA₂₅₄ by breaking down aromatic allochthonous DOC, we would expect very low wetland systems to exhibit SUVA₂₅₄ values similar to previously identified end members or values from long residence time systems. Rather, these results support the hypothesis proposed by *del Giorgio and Pace* [2008] and *Richey et al.* [1990] which suggested that labile autochthonous material may be rapidly recycled while more refractory, generally allochthonous DOC is delivered to the coastal ocean.

We did not find evidence to support the contention by *Shih et al.* [2010] that approximately 60% of organic matter in rivers with high mean discharge ($> 17.85 \text{ m}^3 \text{ s}^{-1}$) was autochthonous. All rivers in this study, with the exception of the Rio Grande, fall within this category and terrestrial wetland signals were strong, with percent wetland-cover explaining 90% of the variability in DOC quality (Eq. 1.5) and nearly 80% of the variability in quantity (Eq. 1.3). Although the comparison between TOC and DOC is not direct, at annual scales DOC tends to make up the majority of organic matter in rivers [*Meybeck*, 1982]. We believe that *Shih et al.* [2010] may have overestimated the contribution of autochthonous sources at the mouths of the largest river systems because they assumed the same degradation constant to all organic matter in a given reach, whether it was recalcitrant allochthonous material or more labile autochthonous material. The longer a bulk DOC pool is subjected to degradation under this assumption, the greater the percent-difference between predicted labile DOC and actual labile DOC would become. Consider a conceptual model where ten units of slowly degrading organic material (OM_A) and ten units of quickly degrading organic material (OM_B) are loaded into the headwaters of a small stream. Transfer efficiency (TE) is defined as the fraction of DOC in a particular reach that is delivered downstream,

$$TE = \exp(-k t) \quad (\text{Eq. 1.6})$$

where k is a reaction rate expressed in units of time^{-1} and t is a residence time. *Shih et al.* [2010] found a mean reaction rate of 0.0338 day^{-1} . If we assume that quickly and slowly degrading organic matter have reaction rates three standard

deviations below and above that mean, respectively, OM_A would have a k of 0.0228 day^{-1} and OM_B a k of 0.0448 day^{-1} . With a residence time of ten days, we would expect to be left with 6.39 units of OM_A and 7.96 units of OM_B . However, if we subject both OM_A and OM_B to the same mean reaction rate, the model predicts 7.13 units of each remaining. Although both models predict approximately 14 units of bulk organic material at the stream mouth, the contribution of the quickly degrading OM_A is over-estimated in the second case by 0.74 units, or 11.6%. If we assume the reach is larger, with a residence time of 30 days, the over-estimation grows to 1.02 units, or 39.1%. Although the absolute over-estimation of OM_A eventually decreases at very long residence times where the bulk pool approaches zero, the percent over-estimation of OM_A continues to increase. Thus, a degradation model that subjects both labile and recalcitrant organic matter to equivalent degradation rates through time will over-predict the influence of the quickly degrading, photosynthetically-derived pool by increasing percentages in larger basins with longer residence times.

We found that in large systems lacking long-term surface water storage, DOC concentration and quality in terms of $SUVA_{254}$ were well predicted by percent wetland-cover. The current evidence suggests that for these systems at annual scales, in-stream processes like autochthonous production, microbial remineralization, and photodegradation play a subordinate role in driving DOC quantity and quality compared to processes that load allochthonous DOC into the river system, with new production being quickly recycled by the microbial community rather than delivered in large quantities to the coastal ocean [del

Giorgio and Pace, 2008; Richey et al., 1990]. However, this finding is based on a relatively weak test that compares mean annual DOC vs. wetland relationships in large basins with snapshots from small basins in a variety of regions. In addition, few comparative DOC quality studies in small basins have been conducted. Finally, the tendency of smaller basins in this analysis to possess greater wetland coverage complicates the interpretation of our results because it is difficult to divorce the impact of basin size from wetlands. In order to fully evaluate the role of network-scale processing in driving annual DOC quantity and quality exported from large basins, more comprehensive, synoptic study of DOC and DOC quality changes from small headwaters to large rivers throughout river networks should be conducted.

CHAPTER II

ASSESSING TEMPORAL VARIABILITY IN DISSOLVED ORGANIC CARBON QUANTITY AND QUALITY FOR SMALL RIVERS IN THE CONTINENTAL UNITED STATES

Introduction

Dissolved organic carbon (DOC) and its chemical quality are fundamental players in the biogeochemistry of aquatic systems and have been the subject of a great deal of study. For example, riverine DOC represents an important connection in the global carbon cycle [*Battin et al.*, 2009; *Cole et al.*, 2007], is a crucial parameter in municipal water treatment [*Singer*, 1999], remains central to understanding the transport and bioavailability of heavy metals [*Aiken et al.*, 2011; *Dittman et al.*, 2010], and may hold the key to developing satellite-based measurement of DOC concentration ($[DOC]$) in the coastal ocean [*Salisbury et al.*, 2011]. Current continental-scale modeling efforts have made significant progress in predicting mean annual fluxes and concentrations of bulk DOC for North American rivers and streams [*Lauerwald et al.*, 2012; *Ludwig et al.*, 1996; *Seitzinger et al.*, 2005; *Shih et al.*, 2010]. However, the chemical quality of continental DOC flux has rarely been addressed and the within-year variability of both DOC quantity and quality have not been modeled. A spatially explicit model with a temporal resolution in days that encompassed both DOC quantity and quality could have immediate impacts on the previously mentioned fields of study, but a number of challenges remain. Primarily, the temporal variability of DOC loading to the aquatic system from the terrestrial environment must be quantified, and in addition, within-channel biogeochemical processing and production must be properly constrained. [*Anesio et al.*, 2005; *Moran and Zepp*, 1997; *Stubbins et al.*, 2008; *Waiser and Roberts*, 2004].

In this paper, we investigated the transfer of DOC over time from the terrestrial to the aquatic environment by analyzing temporal variability in DOC concentration and quality for numerous small, headwater basins in the United States Geological Survey's (USGS) National Water Information Service (NWIS). We addressed two primary questions: what time-varying basin-scale characteristics are related to DOC concentration and quality variability in small basins? Second, can static basin-scale attributes of these systems tell us anything about how the dominant time-varying predictors might be applied more generally?

Methods

In this study we developed a database of DOC quantity and quality measurements in terms of $[DOC]$ and specific ultraviolet absorbance at 254nm ($SUVA_{254}$) at river and stream gauging stations in the conterminous United States. We joined this database with several different continuous time-varying basin attributes, including daily discharge, ratio of stormflow to total discharge, and a variety of remotely-sensed basin-attributes. Next, in small individual basins we examined relationships between these time-varying attributes and both DOC concentration and $SUVA_{254}$. Finally, we investigated a variety of static basin-attributes for how they might help to explain the role of the time-varying attributes in controlling DOC variability.

Database Development

We obtained DOC concentration data for 7982 rivers and streams from the National Water Information Service (NWIS; <http://waterdata.usgs.gov/>) managed by the United States Geological Survey (USGS; Figure 2.1), which were recorded as early as August 23, 1958 and as recently as October 10, 2009. We excluded concentrations greater than 65 mgC/L, which were reported at only 55 stations and were mostly recorded by the early 1980's, before strict QA/QC had been commonly implemented for DOC measurements, and the accuracy of such extraordinarily high values is suspect. The NWIS also provided historic daily discharge records for 2304 of these stations, as well as $SUVA_{254}$ data for 560

stations. We excluded $SUVA_{254}$ measurements greater than $6 \text{ L mg C}^{-1} \text{ m}^{-1}$ from analysis because such high values are more likely due to interference in UV absorbance at 254 nm by dissolved iron than the DOC itself [Weishaar *et al.*, 2003]. We also excluded $SUVA_{254}$ values below the threshold of $0.6 \text{ L mg C}^{-1} \text{ m}^{-1}$, which is well below previously observed microbial and groundwater end members [Stets *et al.*, 2010], and is generally observed only in oceanic systems.

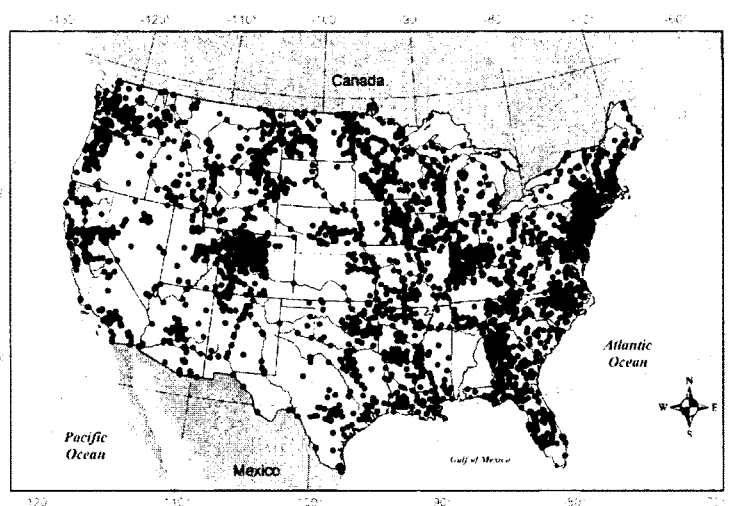


Figure 2.1. Map showing sampling locations for NWIS gauging stations.

We imported latitude and longitude data from the NWIS to ESRI's ArcGIS 9.10 in order to georeference all stations; basins were distributed throughout the conterminous United States. We also merged the NWIS station data with the GAGES database ($n=6785$) [Falcone *et al.*, 2010], which provided annual-mean or static basin-scale data which covered soils, watershed climatology, hydrology, infrastructure, and topography for 1378 out of 7982 basins.

We used ArcGIS to perform a spatial join between our georeferenced NWIS data and the topological stream network from the National Hydrography

Dataset (NHDplus) [USGS, 2006]. In this join each NWIS station was spatially associated with a single NHDplus stream-segment, which was in turn associated with a variety of upstream basin attributes. We used these associations to extract a number of attributes from the NHDplus, including cumulative upstream drainage area (A_{NHD}) and the cumulative upstream percent-cover for 21 different land cover categories from the 1992 National Land Cover Database (NLCD) [Homer *et al.*, 2004]. These 21 categories were simplified to six basic land-cover types: forest, agriculture, urban, wetland, grassland, and shrubland (Table 2.1).

Table 2.1. Table showing landcover categories for the National Land Cover Database and the simplified categories used in this study.

#	NLCD (1992) Categories	Simplified Categories
21	Low Intensity Residential	Urban
22	High Intensity Residential	
23	Commercial/Industrial/Transportation	
85	Urban/Recreational Grasses	
41	Deciduous Forest	Forest
42	Evergreen Forest	
43	Mixed Forest	
51	Shrubland	Shrubland
71	Grassland/Herbaceous	Grassland
81	Pasture/Hay	Agricultural
82	Row Crops	
83	Small Grains	
84	Fallow	
91	Woody Wetlands	Wetlands
92	Emergent Herbaceous Wetlands	

We also used the spatial join between the NWIS dataset and the NHDplus to generate watershed-boundary polygons. We used an NHDplus tool, BasinDelineator v2.009, to generate these polygons for each NHDplus stream segment associated with a station in our database. We populated fields in the NWIS dataset with an ID number and the contributing area of each watershed

polygon (A_P). Finally, we derived a raster mask from the vector-based polygons generated by BasinDelineator.

Moderate Resolution Imaging Spectroradiometer (MODIS) data sets were obtained from several sources and were available starting in February of 2000. We investigated continuously available remotely-sensed indices that we considered likely to be associated with DOC variability. These included Gross Primary Production (GPP) and Land Surface Temperature for night and day ($NLST$ and $DLST$, respectively) [LPDAAC, 2000], as well as Enhanced Vegetation Index (EVI) and Land Surface Water Index ($LSWI$) [Xiao *et al.*, 2009]. We calculated mean land surface temperature for each system (mean LST) as the average of $NLST$ and $DLST$. All MODIS products were available at an 8-day temporal resolution. These gridded data sets were clipped using the previously generated raster-based watershed polygons in order to calculate basin-mean MODIS values at every time step for each station. After generating basin-mean MODIS values at an 8-day interval, we interpolated across the 7-day gaps using the linear method of the *interpTS* function, in the *Water Quality (wq)* library for R 2.12.2 [RDCT, 2011]. In addition, antecedent values for all time-varying watershed parameters, including GPP , EVI , $LSWI$, $DLST$, $NLST$, and stream discharge were calculated as the mean of the preceding 32 day periods. Finally, we merged daily and antecedent MODIS values with the NWIS data set by station and date.

In some cases, the area of the generated polygon (A_P) was different than the drainage area reported in the NWIS (A_{USGS}). In order to restrict analysis to

systems where the calculated MODIS index values accurately reflected the watersheds upstream of each station we calculated the percent difference for the areas of the generated polygons with respect to the NWIS reported drainage area (R_{UP} ; Equation 2.1). Disparity also existed between A_{USGS} and the cumulative upstream drainage areas extracted from the NHDplus tables (A_{NHD}). It was important to calculate the percent difference between A_{USGS} and A_{NHD} (R_{UN} ; Equation 2.2) because land-cover values were directly extracted from the NHDplus and are associated with A_{NHD} rather than being a product of the generated polygons. Finally, in cases where a drainage area was not available from the NWIS, we calculated the percent difference between A_{NHD} and A_P (R_{NP} ; Equation 2.3):

$$R_{UP} = \left(\frac{|A_{USGS} - A_P|}{A_{USGS}} \right) \cdot 100 \quad (\text{Eq. 2.1})$$

$$R_{UN} = \left(\frac{|A_{USGS} - A_{NHD}|}{A_{USGS}} \right) \cdot 100 \quad (\text{Eq. 2.2})$$

$$R_{NP} = \left(\frac{|A_{NHD} - A_P|}{A_{NHD}} \right) \cdot 100 \quad (\text{Eq. 2.3})$$

Small Basin Analysis

Analysis of DOC in small basins is important for identifying controls on headwater DOC concentration and thus the loading of DOC from the terrestrial environment to downstream river systems. We defined small basins as those with drainage areas less than 100 km² because minimal biogeochemical processing would have had the opportunity to occur in such small streams and

because grid-cells in current continental DOC flux modeling tools are, at a 6 arcminute resolution, of a comparable scale [Vorosmarty *et al.*, 2000]. Of the 7982 initial basins, a subset of 3046, called the Small Basin Subset (SBS) had total drainage areas less than 100 km² and also had R_{UC} , R_{UP} , and R_{NP} less than 100% (Figure 2.2). Historic daily discharge records from the NWIS concurrent with [DOC] measurements were available for 265 stations in the SBS and SUVA₂₅₄ data were available in the SBS for 318 stations. GAGES data were available for only 164 SBS streams, limiting availability of some static basin-attribute data. MODIS coverage was available for approximately 1000 stations.

We expected the fraction of daily discharge as either stormflow or baseflow to be related to DOC quantity and quality variability because stormflow is more likely to be overland or in organic upper soil horizons while baseflow is more likely to be derived from deeper groundwater sources. Therefore, we applied a hydrograph separation algorithm to the historic discharge records from small watersheds where daily discharge records were complete for at least a full year and were concurrent with [DOC] measurements. We followed Eckhardt [2005] in order to obtain daily fractions of total discharge as both stormflow and baseflow. Eckhardt [2008] noted that this method is only appropriate for use on small watersheds, thus, we did not extend the hydrograph separation analysis to systems with drainage areas larger than 100 km². A daily stormflow ratio (S_R) was calculated as the daily stormflow divided by total daily discharge.

We analyzed regressions between DOC concentration and each individual basin's daily discharge, $LSWI$, GPP , mean LST , and their 32-day antecedents, as

well as daily S_R for all stations in the SBS where the appropriate variables were available. We also analyzed regressions between $SUVA_{254}$ and each of these variables. The relationships between $[DOC]$ and both Q and GPP took the form of Equation 2.4, which is based on logarithmic transformations of both $[DOC]$ and the predictor variable in a simple linear regression. Equation 2.5, which represents the relationships between $[DOC]$ and S_R , EVI , $LSWI$, and mean LST , is based on a logarithmic transformation of only $[DOC]$. Equation 2.6 is based on the logarithmic transformation of only the predictor variable and represents the relationship between $SUVA_{254}$ and both Q and GPP_{32} . Finally, Equation 2.7 is based on a simple linear regression without transformation and represents the relationship between $SUVA_{254}$ and S_R :

$$[DOC] = \beta \cdot x^m \quad (\text{Eq. 2.4})$$

$$[DOC] = \beta \cdot e^{xm} \quad (\text{Eq. 2.5})$$

$$SUVA_{254} = m \cdot \log(x) + \beta \quad (\text{Eq. 2.6})$$

$$SUVA_{254} = m \cdot x + \beta \quad (\text{Eq. 2.7})$$

Where x is the predictor variable (Q , GPP , or S_R) and both m and β are regression coefficients. In all cases log-transformations were performed so that the variables in question met the assumption of a normal distribution in a linear regression.

We also used "box-and-whisker" type plots to investigate what static basin-scale properties could help us understand controls on the parameters that governed time-varying DOC. Among the basin-scale properties we tested were GAGES-derived attributes: slope of the basin, northness of the slope aspect,

eastness of the slope aspect, soil permeability, soil organic matter content, clay content of soil, soil depth, % of precipitation as snow, relative humidity, and air temperature. We also tested several static basin-scale attributes derived from the NWIS and the NHDplus: % wetland cover, % forest cover, latitude, runoff, and basin area. We generated box-and-whisker plots using R 2.12.2. The boxes in these plots were "notched", where the width of the notch above and below the median (W_N) was calculated following [Chambers *et al.*, 1983] (Equation 2.8):

$$W_N = \frac{\pm 1.58 \cdot IQR}{\sqrt{n}} \quad (\text{Eq. 2.8})$$

Where IQR is the interquartile range and n is the number of observations.

Chambers et al. [1983] considered a lack of overlap between these notches to be strong evidence that the medians of the two populations differ.

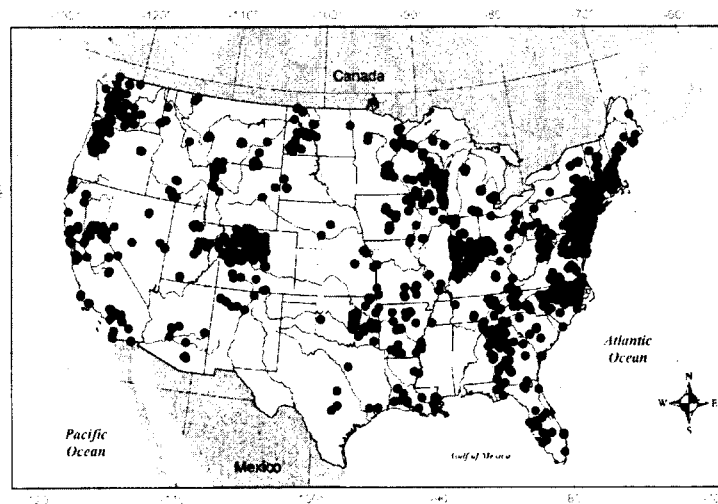


Figure 2.2. Map showing the sampling locations for the United States Geological Survey's National Water Information Service gauging stations in the Small Basin Subset.

Results

Static Characteristics of Small Basins

Stations in the SBS ($n=3046$) were distributed throughout the conterminous United States. Station latitude ranged from 27.209 degrees in Florida to 48.927 degrees in Washington. The drainage areas of small basins ranged from 0.25 km² in Nevada County, California to 99.8 km² in Sumpter County, Georgia. Median drainage area was 27.7 km² and mean drainage area was 33.6 km².

Land-cover ranged from 0% to more than 96% for most land-cover categories, including forested, urban, agricultural, and shrublands, with means of 50.9%, 11.9%, 21.3%, and 4.5%, respectively. Grasslands and wetlands reached maximums of 85% and 74% with means of 5.5% and 3.9%, respectively. From the GAGES database of mean basin properties, slope ranged from 0% to 51.4% with a mean of 10.4% \pm 14.1% and a median of 3.8%, indicating a highly skewed distribution. Both the eastness and northness of the basin aspect ranged from -1 to 1, indicating basins facing in all directions, from directly east to directly west, and directly south to directly north. For soil properties, permeability ranged from 1.3 cm/hr to 31.5 cm/hr with a mean of 12.7 cm/hr \pm 8.9 cm/hr and a median of 12.2 cm/hr. Average organic matter content of soils ranged from 0.2% to 13.0% with a mean of 1.6% \pm 1.8% and a median of 0.9%, indicating a skewed distribution. Mean basin soil depth ranged from 48.8 cm to 153.4 cm with a mean of 126.7 cm \pm 28.9 cm and a median of 139.2 cm. Clay content of soils ranged

from 3.40% to 53.1% with a mean of $16.2\% \pm 10.1\%$ and a median of 14.2%. For climatology, the percent of precipitation as snow ranged from 0% to 66.5 % with a mean of $20.4\% \pm 18.1\%$ and a median of 17.3%. Relative humidity ranged from 43.3% to 80.5% with a mean of $65.8\% \pm 6.7\%$ and a median of 67.0%. Finally, average basin temperature ranged from $-1.6\text{ }^{\circ}\text{C}$ to $22.4\text{ }^{\circ}\text{C}$ with a mean of $10.8\text{ }^{\circ}\text{C} \pm 5.1\text{ }^{\circ}\text{C}$ and a median of $11.0\text{ }^{\circ}\text{C}$.

Time-Varying Characteristics of Small Basins

DOC concentration had a log-normal distribution and ranged from 0.3 mgC/L to 60.0 mgC/L, with a geometric mean of $2.7\text{ mgC/L} \pm 2.4\text{ mgC/L}$. Where available, SUVA_{254} ranged from $0.6\text{ L mg C}^{-1}\text{ m}^{-1}$ to $5.9\text{ L mg C}^{-1}\text{ m}^{-1}$, with an overall mean of $3.8\text{ L mg C}^{-1}\text{ m}^{-1} \pm 1.3\text{ L mg C}^{-1}\text{ m}^{-1}$.

Historic daily discharge records overlapping DOC concentration measurements were available for 265 gauging stations in the SBS. Mean daily discharge values for streams in the SBS were log-normally distributed and ranged from $0.002\text{ m}^3/\text{s}$ to $23.049\text{ m}^3/\text{s}$ with a geometric mean of $0.564\text{ m}^3/\text{s} \pm 4.243\text{ m}^3/\text{s}$, indicating a highly skewed distribution. Following hydrograph separation analysis [Eckhardt, 2005] we calculated a mean S_R for each basin which ranged from 0 to .93, with an overall mean of 0.31 ± 0.20 and a median of 0.26. These results indicated that mean total streamflow in individual basins ranged from being composed of entirely baseflow to almost entirely stormflow. Antecedents of discharge and S_R demonstrated similar range, probability distribution, mean, and median as the daily values.

MODIS indices *EVI*, *GPP*, *LSWI*, and *LST* had a variety of probability distributions (Figure 2.3) and all exhibited significant intercorrelation (Figure 2.4). Antecedent values for MODIS indices were similarly distributed and intercorrelated. Because the intercorrelation of predictor variables in a linear regression can confound interpretation of the role of those variables, we sought to select a single MODIS index as a best predictor of DOC concentration and $SUVA_{254}$ in our final calculations.

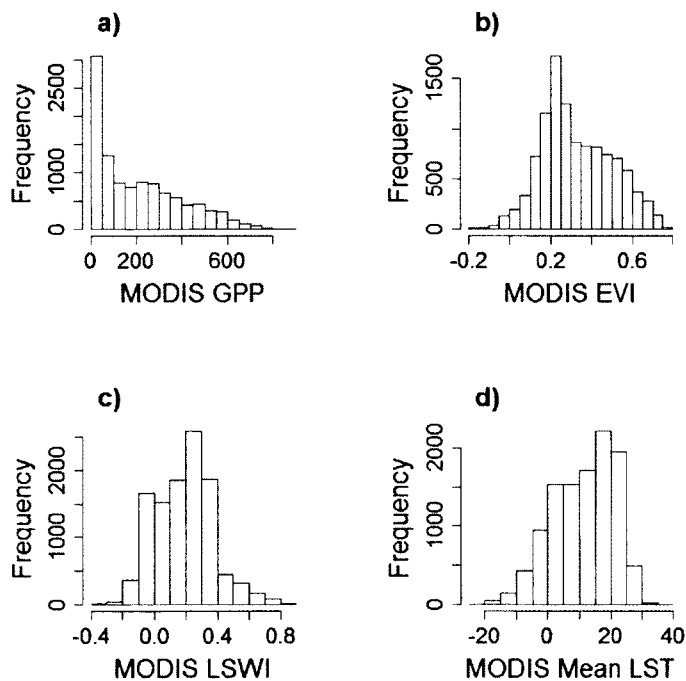


Figure 2.3. Figure showing probability distributions for various MODIS indices used in this study. a) Gross Primary Production, b) Enhanced Vegetation Index, c) Land Surface Water Index, and d) mean Land Surface Temperature.

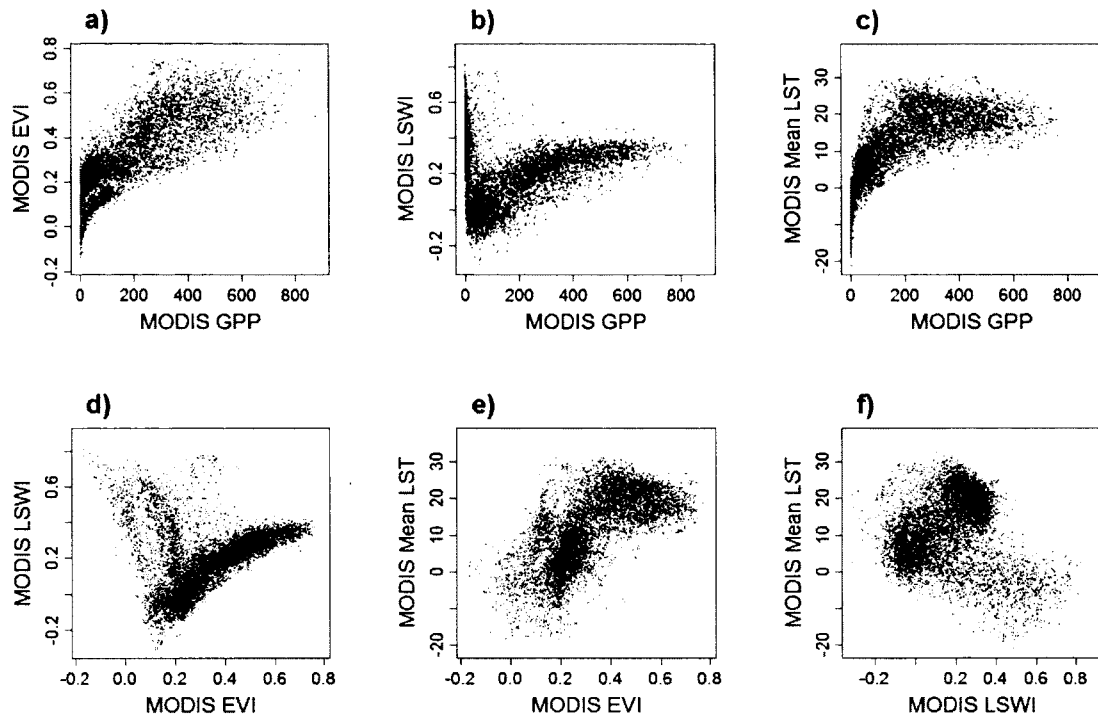


Figure 2.4. Figure showing the intercorrelation of MODIS indices used in this study. a) Enhanced Vegetation Index (EVI) vs. Gross Primary Production (GPP), b) Land Surface Water Index (LSWI) vs. GPP, c) mean Land Surface Temperature (LST) vs GPP, d) LSWI vs. EVI, e) LST vs EVI, and f) LST vs. LSWI.

DOC Controls

We found significant (p -value < 0.05) relationships between $[DOC]$ and the various time-varying basin-scale characteristics, including discharge, MODIS indices, and S_R (Table 2.2). Discharge was significantly correlated with $[DOC]$ at 121 out of 265 stations (Table A.1), while its 32-day antecedent was only significant at 78 out of 265 stations. 110 of the 121 basins where discharge was a significant predictor of $[DOC]$ had positively sloped relationships, while 11 were negatively sloped. This indicated that rising discharge was generally associated

with a rise in DOC concentration, which is a phenomenon that has been observed in previous studies [Agren et al., 2010; Eckhardt and Moore, 1990; Raymond and Saiers, 2010].

In the case of MODIS indices, the relationship between $[DOC]$ and daily GPP was significant for 76 out of 349 individual stations, while its 32-day antecedent (GPP_{32}) was significant for 95 out of 344 (Table A.2). Of these 95 relationships, 78 were positively sloped, indicating a generally positive response in $[DOC]$ to GPP_{32} . Other MODIS indices were correlated with $[DOC]$ in similar numbers of basins (Table 2.2). We selected GPP_{32} as the MODIS index for use in our final analysis because it was a significant predictor of $[DOC]$ in the greatest number of individual basins, though only slightly, and it had a clear log-normal distribution which allowed it to meet the assumptions of a linear regression under logarithmic transformation. In addition, GPP had only positive values which made the transformation comparatively simple. The seasonal variability of GPP in individual basins also has a theoretical basis for inclusion as a control on DOC as primary production is the ultimate source of natural organic matter.

Daily S_R was significantly correlated with $[DOC]$ at 80 out of 200 stations (Table A.3). Of these 80 relationships 77 were positively sloped, indicating that a higher ratio of stormflow to total streamflow generally results in higher DOC concentrations. When we restricted analysis to basins and times where all three predictor variables (Q , GPP_{32} , and S_R) were available ($n=66$; Table 2.3), we noted that only 12 basins lacked a relationship with one of the predictors and that substantial overlap occurred among the three (Figure 2.5).

Predictor	vs. $[DOC]$		vs. $SUVA_{254}$	
	$p < 0.05$	$p > 0.05$	$p < 0.05$	$p > 0.05$
Q	121	144	6	13
Q32	78	187	5	14
SR	80	120	2	17
SR32	49	150	3	16
GPP	74	270	27	139
GPP32	95	249	32	134
EVI	69	291	36	144
EVI32	88	272	34	146
LSWI	57	303	24	160
LSWI32	52	308	17	167
LST	80	285	34	146
LST32	94	271	33	147

Table 2.2. Table showing the number of significant and non-significant relationships between time-varying basin attributes and both dissolved organic carbon concentration ($[DOC]$) and specific ultraviolet absorbance at 254nm ($SUVA_{254}$) for individual basins.

In the box-and-whisker plots, we found several static basin characteristics that were useful in explaining the controls exerted by the different time-varying parameters. In basins where discharge was vs. was not a significant predictor of DOC, notches for aspect northness and soil depth did not overlap (Figures 2.6 and 2.7). These results indicated that the basins with discharge as a significant predictor of $[DOC]$ are likely to be more southerly-facing and to have deeper soils than those basins where Q is not a significant predictor. We found no other static basin characteristics with the same type of explanatory power because all other notches overlapped when comparing populations of basins where Q , GPP_{32} , and S_R were significant or non-significant predictors of $[DOC]$.

Box-and-whisker plots were also used to investigate why some basins exhibited positively sloped relationships between the time-varying predictors and $[DOC]$ while others exhibited negatively sloped relationships. We found that basins where discharge was positively correlated with $[DOC]$ were likely to have a higher percent forest-cover than basins with negative correlations (Figure 2.8). In addition, we found that basins where GPP_{32} was positively correlated with

[DOC] were likely to have a higher percent wetland-cover and percent agricultural-cover and lower percent shrubland-cover than basins with a negative correlation (Figure 2.9).

We also found significant relationships (p -value < 0.05) between $SUVA_{254}$ and the three primary time-varying attributes (Table 2.2). Q was significantly correlated with $SUVA_{254}$ at 6 out of 19 stations (Table A.4), GPP_{32} was significantly correlated with $SUVA_{254}$ at 32 out of 166 stations (Table A.5), and S_R was significantly correlated with $SUVA_{254}$ at 2 out of 19 stations (Table A.6).

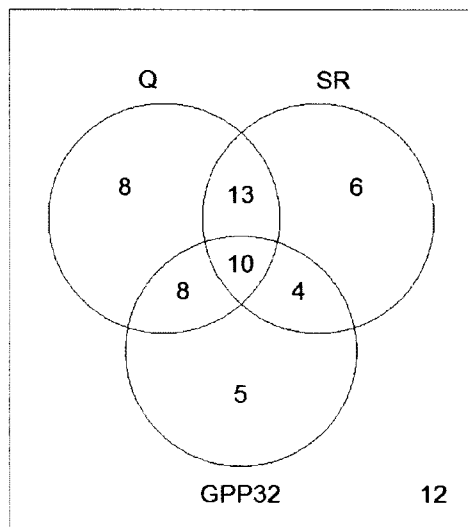


Figure 2.5. Venn diagram showing the overlap between significant time-varying predictor variables for dissolved organic carbon concentration in individual basins. Predictors include 32-day antecedents of discharge (Q) and gross primary production (GPP), as well as stormflow ratio (S_R). Bottom right is the number of basins where none of the three are significant predictors.

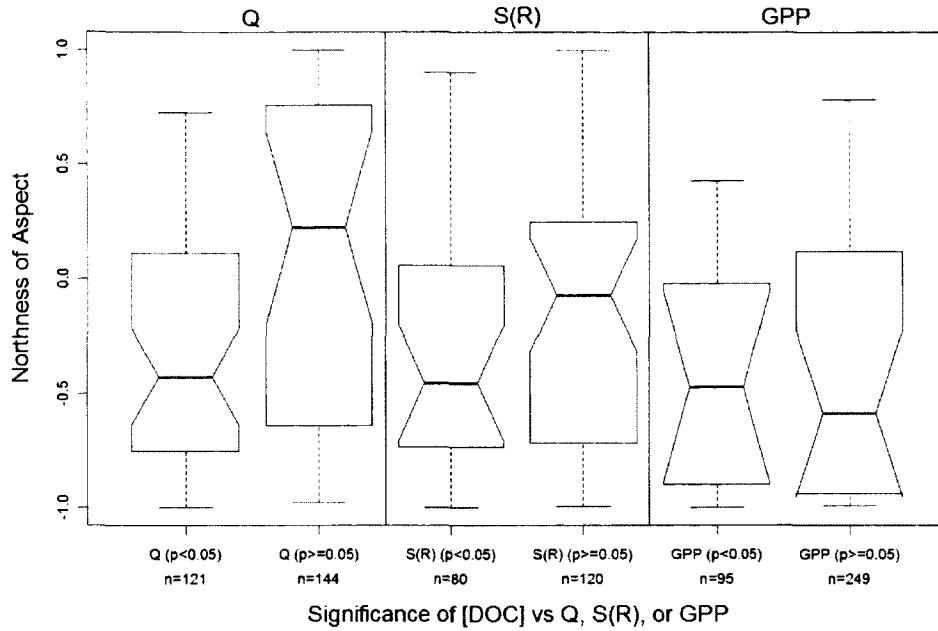


Figure 2.6. Box-and-whisker plot of aspect northness for basins where the three time-varying predictors were and were not correlated with dissolved organic carbon concentration (*[DOC]*). For discharge (Q), notches do not overlap, indicating a significant difference in the medians.

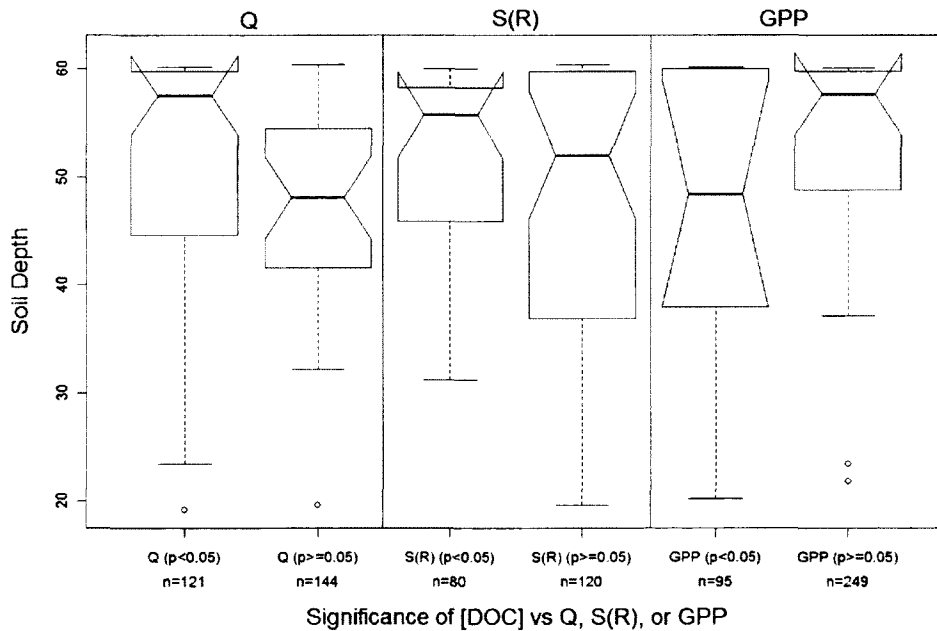


Figure 2.7 Box-and-whisker plot of soil depth for basins where the three time-varying predictors were and were not correlated with dissolved organic carbon concentration (*[DOC]*). For discharge (Q), notches do not overlap, indicating a significant difference in the medians.

Table 2.3. Table showing basin information for 66 basins where discharge (Q), antecedent gross primary production (GPP_{32}), and stormflow ratio (S_R) are all available on the same dates as at least four dissolved organic carbon (DOC) measurements. Discharge and SR are computed as basin means over the entire time-period available. The last three columns represent whether the time-varying predictor in question (Q , GPP_{32} , or S_R) are significantly correlated with $[DOC]$.

Station ID	County, State	Lat. <i>DD</i>	Long. <i>DD</i>	Drainage <i>km²</i>	Discharge <i>m³/s</i>	S_R	Wetland <i>%</i>	Forest <i>%</i>	Ag. <i>%</i>	Urban <i>%</i>	Grass <i>%</i>	Shrub <i>%</i>	Q <i>p < 0.05 vs. [DOC]</i>	GPP_{32}	S_R
01095220	Worcester County, Massachusetts	42.411	-71.792	81.8	1.6	0.207	8.2	76.5	8.5	5.4	0.0	0.0	Y	N	Y
01102345	Essex County, Massachusetts	42.469	-71.007	53.9	0.9	0.192	9.5	29.6	0.0	60.5	0.0	0.0	Y	N	N
01362380	Ulster County, New York	42.098	-74.317	81.6	2.8	0.169	0.0	98.3	0.2	1.5	0.0	0.0	Y	Y	Y
01394500	Union County, New Jersey	40.688	-74.312	66.0	0.9	0.196	0.9	28.9	0.5	69.7	0.0	0.0	Y	N	Y
01407760	Monmouth County, New Jersey	40.203	-74.066	16.7	0.3	0.187	9.0	25.7	4.3	56.5	0.0	0.0	Y	Y	N
01410150	Burlington County, New Jersey	39.623	-74.441	21.0	0.5	0.177	5.9	91.6	0.3	2.0	0.0	0.0	Y	N	N
01410810	Camden County, New Jersey	39.696	-74.940	20.0	0.4	0.177	12.7	31.0	21.2	35.2	0.0	0.0	Y	N	Y
01410820	Camden County, New Jersey	39.669	-74.913	96.6	1.9	0.176	17.2	42.5	15.8	23.4	0.0	0.0	Y	N	N
01411300	Cape May County, New Jersey	39.307	-74.821	79.8	1.2	0.174	12.4	73.4	4.1	3.4	0.0	0.0	Y	N	N
01412800	Cumberland County, New Jersey	39.473	-75.256	72.5	1.0	0.173	4.0	13.4	80.4	2.2	0.0	0.0	Y	N	Y
01421618	Delaware County, New York	42.361	-74.663	37.0	0.9	0.188	0.0	73.0	26.6	0.5	0.0	0.0	Y	Y	Y
01422747	Delaware County, New York	42.173	-75.122	64.0	1.4	0.188	0.0	71.8	27.1	1.0	0.0	0.0	Y	Y	Y
01434017	Ulster County, New York	41.925	-74.541	59.3	2.1	0.148	0.0	99.5	0.4	0.1	0.0	0.0	Y	Y	Y
01434025	Ulster County, New York	41.995	-74.501	9.6	0.3	0.166	0.0	100.0	0.0	0.0	0.0	0.0	Y	Y	Y
01434498	Sullivan County, New York	41.920	-74.575	87.5	3.2	0.160	0.0	99.6	0.3	0.0	0.0	0.0	Y	Y	Y
01466500	Burlington County, New Jersey	39.885	-74.505	6.1	0.1	0.304	5.7	85.4	0.2	0.0	0.0	0.0	Y	N	N
01467150	Camden County, New Jersey	39.903	-75.021	44.0	0.9	0.179	3.6	25.0	7.5	60.7	0.0	0.0	Y	Y	N
01493112	Kent County, Maryland	39.257	-75.940	15.9	0.3	0.167	4.5	4.9	90.2	0.4	0.0	0.0	Y	N	Y
01493500	Kent County, Maryland	39.280	-76.014	32.9	0.3	0.177	5.0	4.0	90.0	1.0	0.0	0.0	Y	N	Y
01591000	Montgomery County, Maryland	39.238	-77.056	90.1	1.1	0.152	3.3	33.3	62.8	0.6	0.0	0.0	Y	Y	Y
02172300	Aiken County, South Carolina	33.753	-81.602	40.4	0.6	0.165	5.7	71.8	19.9	0.4	0.0	0.0	Y	N	Y
02306774	Hillsborough County, Florida	28.066	-82.566	45.3	0.4	0.261	24.9	4.3	2.9	43.9	9.0	0.1	Y	N	N
02338523	Heard County, Georgia	33.341	-85.227	43.5	0.6	0.156	0.0	92.4	7.4	0.1	0.0	0.0	Y	N	Y
03353637	Marion County, Indiana	39.667	-86.196	44.0	0.6	0.353	0.2	3.8	43.3	52.6	0.0	0.0	Y	Y	Y

03361638	Hancock County, Indiana	39.843	-85.825	7.2	0.1	0.609	0.0	0.7	98.3	1.1	0.0	0.0	Y	Y	N
03448800	Buncombe County, North Carolina	35.619	-82.308	11.0	0.5	0.169	0.1	77.5	0.4	21.9	0.0	0.0	Y	N	Y
04087030	Waukesha County, Wisconsin	43.173	-88.104	89.9	0.9	0.191	3.3	15.3	56.3	23.8	0.9	0.0	Y	N	Y
04087088	Milwaukee County, Wisconsin	43.055	-88.046	47.1	0.4	0.167	3.0	15.2	0.6	77.9	3.3	0.0	Y	N	N
04087204	Milwaukee County, Wisconsin	42.925	-87.870	64.7	0.7	0.203	1.5	11.8	34.8	49.1	2.8	0.0	Y	Y	N
05014300	Glacier County, Montana	48.795	-113.679	37.6	2.4	0.185	0.7	24.2	0.0	0.0	20.9	28.7	Y	Y	Y
05451080	Hamilton County, Iowa	42.544	-93.589	31.1	0.4	0.164	0.3	0.4	95.3	1.5	2.5	0.0	Y	N	Y
05540275	Du Page County, Illinois	41.726	-88.164	25.6	0.3	0.258	0.4	3.7	62.1	33.8	0.1	0.0	Y	Y	N
06187915	Park County, Montana	45.003	-110.001	80.8	1.6	0.220	0.0	73.2	0.0	0.1	4.0	9.9	Y	Y	N
07362587	Saline County, Arkansas	34.797	-92.933	69.9	3.2	0.335	0.0	99.5	0.1	0.0	0.0	0.0	Y	N	Y
09306242	Rio Blanco County, Colorado	39.920	-108.472	81.8	0.0	0.332	0.1	46.8	0.0	0.2	19.8	32.8	Y	Y	N
10343500	Nevada County, California	39.432	-120.237	27.2	0.3	0.182	0.0	86.4	0.0	0.0	2.5	11.1	Y	Y	N
11262900	Merced County, California	37.263	-120.906	89.3	2.9	0.231	36.4	0.1	26.4	0.7	35.9	0.4	Y	N	N
12128000	King County, Washington	47.696	-122.275	31.3	0.3	0.167	0.2	7.8	0.0	88.6	0.9	2.4	Y	Y	Y
14161500	Lane County, Oregon	44.210	-122.256	62.4	3.4	0.174	0.0	97.1	0.0	0.0	1.3	1.0	Y	N	Y
01102500	Middlesex County, Massachusetts	42.447	-71.139	64.0	0.9	0.198	4.2	26.3	0.0	69.0	0.0	0.0	N	N	N
01105000	Norfolk County, Massachusetts	42.177	-71.201	89.9	1.7	0.204	9.5	50.6	2.1	37.5	0.0	0.0	N	N	N
01367800	Sussex County, New Jersey	41.163	-74.675	40.9	0.9	0.188	4.8	40.6	53.8	0.8	0.0	0.0	N	Y	N
01398000	Hunterdon County, New Jersey	40.473	-74.828	66.6	1.1	0.194	1.2	31.3	60.2	7.2	0.0	0.0	N	N	Y
01464907	Bucks County, Pennsylvania	40.229	-75.120	69.4	1.5	0.189	0.2	35.5	31.5	32.4	0.0	0.0	N	N	Y
01479820	Chester County, Pennsylvania	39.817	-75.692	73.3	1.2	0.156	0.8	33.9	54.3	11.0	0.0	0.0	N	N	N
01482500	Salem County, New Jersey	39.644	-75.330	37.8	0.6	0.187	3.1	15.6	76.1	5.0	0.0	0.0	N	N	N
01673638	King William County, Virginia	37.627	-76.963	22.8	0.2	0.212	4.8	80.3	9.4	0.1	0.0	0.0	N	Y	N
02087580	Wake County, North Carolina	35.719	-78.752	54.4	1.3	0.256	2.3	59.3	8.8	28.5	0.0	0.0	N	Y	Y
0209096970	Wayne County, North Carolina	35.479	-77.910	7.8	0.1	0.308	15.6	43.1	41.1	0.0	0.0	0.0	N	Y	N
0209173190	Greene County, North Carolina	35.525	-77.563	1.5	0.0	0.840	18.7	35.1	46.2	0.0	0.0	0.0	N	Y	N
0209173200	Greene County, North Carolina	35.531	-77.559	74.1	0.5	0.489	28.9	29.7	40.7	0.5	0.0	0.0	N	Y	N
0209741955	Durham County, North Carolina	35.872	-78.913	54.6	1.0	0.204	5.3	61.8	1.1	29.6	0.0	0.0	N	N	N
02097464	Orange County, North Carolina	35.924	-79.115	21.6	0.2	0.249	0.2	81.9	15.9	1.9	0.0	0.0	N	N	Y
02172305	Aiken County, South Carolina	33.718	-81.607	79.5	0.6	0.162	6.2	72.8	16.4	0.3	0.0	0.0	N	N	N
02314274	Charlton County, Georgia	30.804	-82.418	12.2	2.0	0.185	64.9	33.9	0.1	0.0	0.0	0.1	N	N	N
02336635	Cobb County, Georgia	33.803	-84.521	81.6	1.5	0.150	0.0	57.8	1.4	39.6	0.0	0.0	N	N	N
04087159	Milwaukee County, Wisconsin	42.998	-87.926	48.7	0.7	0.186	0.3	3.5	0.0	96.2	0.1	0.0	N	N	N

04087214	Milwaukee County, Wisconsin	42.945	-88.014	38.1	0.5	0.250	0.5	14.0	1.9	81.1	2.4	0.0	N	N	N
07083000	Lake County, Colorado	39.172	-106.389	61.1	0.8	0.138	0.0	30.7	0.0	0.0	37.2	2.2	N	Y	Y
072632962	Pulaski County, Arkansas	34.881	-92.681	22.5	0.7	0.350	0.0	98.5	0.7	0.0	0.0	0.0	N	N	N
072632971	Pulaski County, Arkansas	34.890	-92.647	6.6	0.2	0.402	0.0	99.4	0.6	0.0	0.0	0.0	N	N	N
10167800	Salt Lake County, Utah	40.614	-111.842	95.8	0.5	0.258	0.1	44.3	1.6	12.9	3.4	30.6	N	N	Y
10336778	El Dorado County, California	38.909	-119.961	31.5	0.2	0.131	0.0	66.5	0.0	1.0	11.3	17.5	N	Y	Y
14201300	Marion County, Oregon	45.101	-122.821	38.8	0.6	0.248	0.1	2.7	88.9	1.0	0.7	0.0	N	N	Y
14205400	Washington County, Oregon	45.681	-123.070	87.5	2.1	0.161	0.0	92.1	1.0	0.0	0.0	0.2	N	N	Y
14206950	Washington County, Oregon	45.404	-122.754	81.6	1.2	0.184	0.4	28.4	5.2	56.3	2.2	5.0	N	Y	Y

Discussion

In order to better understand the temporal variability of DOC flux from the terrestrial environment to the aquatic, we analyzed the within-basin response of $[DOC]$ to several time-varying predictors for individual streams in the SBS. When we analyzed within-basin response to three time-varying predictors (Q , S_R , GPP_{32}) we found that $[DOC]$ was often controlled by discharge ($n=121$). These relationships were generally positively sloped ($n=110$), indicating that increasing discharge had a concentrating effect on DOC. This was expected because previous studies have found that with increasing runoff, more of a watershed can become hydrologically connected to the stream. If runoff increased, previously disconnected portions of the watershed, particularly in organic upper soil horizons, could be flushed of DOC [Boyer *et al.*, 1997]. The deeper soils associated with basins where Q was a significant predictor of $[DOC]$ (Figure 2.7) provide some support for this hypothesis in that systems with deep soils can accommodate a greater rise in runoff before all soils are fully hydrologically connected.

Several basins ($n=11$) exhibited a negative slope, indicating a diluting effect. In these cases the watersheds may have already been fully hydrologically connected such that when runoff increased, the volume of water in the system rose while the absolute quantity of DOC transferred to the aquatic system remained the same, resulting in dilution. We expected such basins to be dominated by wetlands, which have been previously associated with a diluting

effect [Buffam *et al.*, 2007], but found no significant difference in median wetland-cover when comparing systems with positively vs. negatively sloped relationships. However, it is interesting to note that the population of basins with negatively sloped relationships had significantly lower percent forest-cover than the population of basins with positively sloped relationships (Figure 2.8), but it is unclear how this may be related to diluting versus concentrating hydrological processes.

The role of S_R in controlling $[DOC]$ in the SBS was also apparent. Out of 80 systems where S_R was a significant predictor of $[DOC]$, 77 exhibited a positive relationship. These results support the hypothesis discussed in Chapter 1 that DOC is removed from solution in the deep subsurface by microbial degradation and adsorption to mineral surfaces. When S_R is high, overland flow and shallow subsurface flow through organic soil horizons become more likely and high concentrations of minimally degraded organic compounds can be added to solution. Conversely, when S_R is low, most streamflow has its origin in deeper groundwater of low concentration and low $SUVA_{254}$. Thus, we expected $SUVA_{254}$ to exhibit a similar response to S_R as $[DOC]$, but $SUVA_{254}$ was significantly correlated with S_R in only 2 out of 19 basins.

The third time-varying parameter, 32-day antecedent GPP, was also a statistically significant predictor of $[DOC]$ in a large number of basins ($n=95$). We interpreted these results as an indication that in some watersheds DOC transfer to the aquatic system can be partially controlled by the seasonality of terrestrial primary production. We found that the regression between $[DOC]$ and

GPP_{32} was positively sloped in 78 basins, confirming an overall positive relationship. However, we did find significant negative relationships in 17 basins. The population of basins with a positively sloped relationship between GPP_{32} and $[DOC]$ had significantly higher percent wetland and agricultural-cover and significantly lower percent shrubland-cover than those basins with a negative relationship (Figure 2.9), however it is yet unclear what processes might drive these negative relationships between GPP_{32} and $[DOC]$.

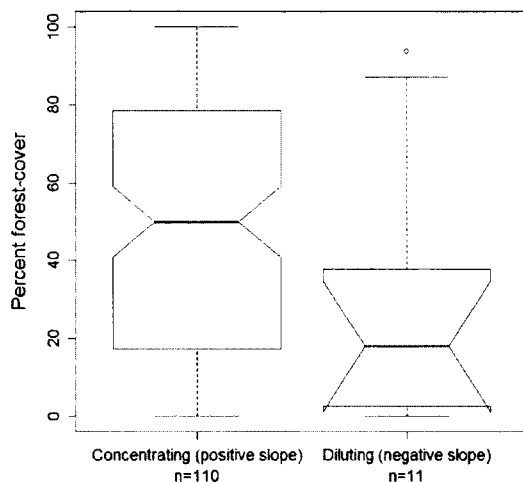


Figure 2.8. "Box and whisker" plot showing the difference in percent forest-cover among populations of basins where the $[DOC]$ vs. Q relationship is concentrating (positive slope) or diluting (negative slope).

Understanding the temporal variability of DOC quantity and quality in the aquatic environment is crucial to understanding many biogeochemical processes. Efforts to model this variability have thus far been hampered by the lack of time-varying DOC loading data at a continental scale. However, directly quantifying the loading of DOC from the terrestrial environment to the aquatic environment is complex because of the numerous sources of DOC to aquatic systems. Such sources include the microbial processing of direct litter fall and other particulate organic matter [Ziegler and Fogel, 2003], autochthonous primary production, and

DOC carried to aquatic systems by groundwater flow, overland flow, and direct precipitation. In order to study DOC loading to aquatic systems we considered DOC quantity in small headwater streams to be representative of an aggregation of these different sources. However, for this aggregation of DOC in headwater streams to be an appropriate proxy for terrestrial loading to the aquatic system we must assume that *in situ* autochthonous production in the headwaters is low. Therefore, we focused on small basins, which are less likely to have significant accumulation of autochthonous production [Vannote *et al.*, 1980]. Second, we must assume that the biogeochemical processing which does occur will be dominated by decomposition of labile organic compounds in direct litter fall and labile autochthonous DOC rather than the more refractory terrestrial DOC. This assumption also has some basins in the River Continuum Concept [Vannote *et al.*, 1980] and studies continue to show preferential microbial remineralization of labile POC and labile autochthonous DOC [Guillemette and del Giorgio, 2011; Koehler *et al.*, 2012; Vahatalo *et al.*, 2010; Ziegler and Fogel, 2003]. However, even in very small streams, microbes do not exclusively consume particulate and autochthonous organic carbon; some allochthonous DOC will always be remineralized. Thus, any terrestrial DOC flux estimates based on these analyses, even in small basins, should be considered a lower bound.

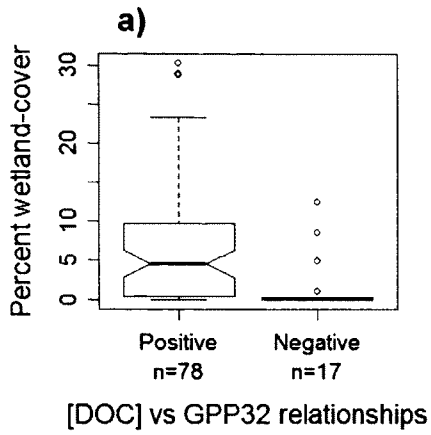
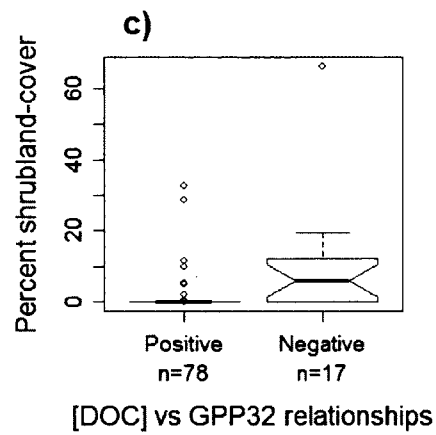
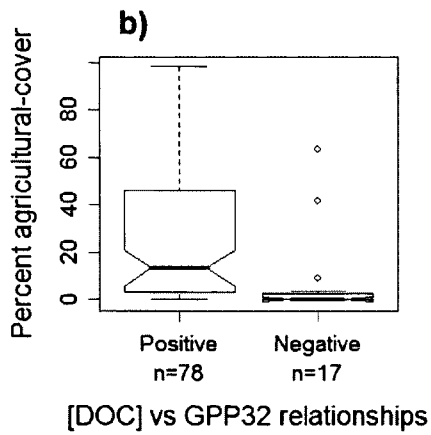


Figure 2.9. "Box and whisker" plot showing the difference among populations of basins where the $[DOC]$ vs. GPP_{32} relationship is positive or negative with respect to a) percent wetland-cover, b) percent agricultural-cover, and c) percent shrubland-cover.



CONCLUSIONS AND FUTURE WORK

We estimated mean DOC quantity and quality in 17 large and diverse North American rivers and demonstrated that wetlands play an integral role in controlling both DOC concentration and quality. These observations suggested that over mean annual time scales, river networks typically do not greatly alter terrestrial source signals except in basins with high residence times. We found that runoff does not drive DOC concentration variability among basins at the annual scale, but that it does within some individual systems. These results supply valuable insight into the controls on mean DOC quantity and quality at broad spatial and temporal scales and provide annual estimates of DOC flux and quality for several of the largest rivers in temperate North America.

We also found significant relationships between DOC concentration and several time-varying predictors among small watersheds. We found that DOC concentration is strongly related to stream discharge, the ratio of stormflow to total stream discharge, and antecedent MODIS gross primary production for the basin. These relationships were found within individual basins and will provide the groundwork in future efforts to model temporal DOC quantity and quality variability at a continental scale. However, further work is still needed to identify the types of basins where each of the three time-varying predictors is applicable.

In order to better understand the source and fate of DOC in the environment future efforts should include improved sampling of headwater DOC quantity and quality in conjunction with large river sampling. Further studies should continue to work towards unraveling the hydrological processes that drive DOC variability within basins, the subsurface biogeochemical reactions that drive baseflow chemistry, and the biological and geochemical processing that drive DOC quantity and quality over time.

REFERENCES

Agren, A., M. Haei, S. J. Kohler, K. Bishop, and H. Laudon (2010), Regulation of stream water dissolved organic carbon (DOC) concentrations during snowmelt; the role of discharge, winter climate and memory effects, *Biogeosciences*, 7(9), 2901-2913.

Aiken, G. R. (1992), Chloride interference in the analysis of dissolved organic carbon by the wet oxidation method, *Environ Sci Technol*, 26(12), 2435-2439.

Aiken, G. R., H. Hsu-Kim, and J. N. Ryan (2011), Influence of Dissolved Organic Matter on the Environmental Fate of Metals, Nanoparticles, and Colloids, *Environ Sci Technol*, 45(8), 3196-3201.

Aiken, G. R., E. M. Thurman, R. L. Malcolm, and H. F. Walton (1979), Comparison of Xad Macroporous Resins for the Concentration of Fulvic-Acid from Aqueous-Solution, *Anal Chem*, 51(11), 1799-1803.

Aiken, G. R., D. M. Mcknight, K. A. Thorn, and E. M. Thurman (1992), Isolation of Hydrophilic Organic-Acids from Water Using Nonionic Macroporous Resins, *Org Geochem*, 18(4), 567-573.

Aiken, G. R., M. Haitzer, J. N. Ryan, and K. Nagy (2003), Interactions between dissolved organic matter and mercury in the Florida Everglades, *J Phys Iv*, 107, 29-32.

Aitkenhead-Peterson, J. A., W. H. McDowell, and J. C. Neff (2003), Sources, production and regulation of allochthonous dissolved organic matter inputs to surface waters, in *Aquatic Ecosystems: Interactivity of Dissolved Organic Matter*, edited, p. 519, Academic Press, London, UK.

Aitkenhead, J. A., and W. H. McDowell (2000), Soil C : N ratio as a predictor of annual riverine DOC flux at local and global scales, *Global Biogeochem Cy*, 14(1), 127-138.

Alexander, R. B., R. A. Smith, and G. E. Schwarz (2000), Effect of stream channel size on the delivery of nitrogen to the Gulf of Mexico, *Nature*, 403(6771), 758-761.

Alexander, R. B., J. R. Slack, A. S. Ludtke, K. K. Fitzgerald, and T. L. Schertz (1998), Data from selected US Geological Survey national stream water quality monitoring networks, *Water Resour Res*, 34(9), 2401-2405.

Anesio, A. M., W. Graneli, G. R. Aiken, D. J. Kieber, and K. Mopper (2005), Effect of humic substance photodegradation on bacterial growth and respiration in lake water, *Appl Environ Microb*, 71(10), 6267-6275.

Battin, T. J., S. Luysaert, L. A. Kaplan, A. K. Aufdenkampe, A. Richter, and L. J. Tranvik (2009), The boundless carbon cycle, *Nat Geosci*, 2(9), 598-600.

Beltran, R., L. Botts, P. Brown, T. Clarke, D. Cowell, K. Fuller, and B. Krushelnicki (1995), *The Great Lakes: An Environmental Atlas and Resource Book*, edited, Government of Canada and United States Environmental Protection Agency.

Benke, A. C., and C. E. Cushing (2005), *Rivers of North America*, xxiii, 1144 p. pp., Elsevier/Academic Press, Amsterdam ; Boston.

Benner, R. (2003), Molecular indicators of the bioavailability of dissolved organic matter, in *Aquatic Ecosystems: Interactivity of Dissolved Organic Matter*, edited, p. 519, Academic Press, London, UK.

Bianchi, T. S. (2011), The role of terrestrially derived organic carbon in the coastal ocean: A changing paradigm and the priming effect, *Proc. Natl. Acad. Sci. U. S. A.*, 108(49), 19473-19481.

Booth, G., P. Raymond, and N. H. Oh (2007), *LoadRunner*, edited, Yale University, New Haven, CT.

Boyer, E. W., G. M. Hornberger, K. E. Bencala, and D. M. McKnight (1997), Response characteristics of DOC flushing in an alpine catchment, *Hydrol Process*, 11(12), 1635-1647.

Buffam, I., J. N. Galloway, L. K. Blum, and K. J. McGlathery (2001), A stormflow/baseflow comparison of dissolved organic matter concentrations and bioavailability in an Appalachian stream, *Biogeochemistry*, 53(3), 269-306.

Buffam, I., H. Laudon, J. Temnerud, C. M. Morth, and K. Bishop (2007), Landscape-scale variability of acidity and dissolved organic carbon during spring flood in a boreal stream network, *J Geophys Res-Biogeophys*, 112(G1).

Chambers, J. M., W. S. Cleveland, B. Kleiner, and P. A. Tukey (1983), *Graphical Methods in Data Analysis*, Wadsworth & Brooks/Cole.

Chorover, J., and M. K. Amistadi (2001), Reaction of forest floor organic matter at goethite, birnessite and smectite surfaces, *Geochim Cosmochim Acta*, 65(1), 95-109.

Clair, T. A., and J. M. Ehrman (1996), Variations in discharge and dissolved organic carbon and nitrogen export from terrestrial basins with changes in climate: A neural network approach, *Limnol Oceanogr*, 41(5), 921-927.

Cole, J. J., et al. (2007), Plumbing the global carbon cycle: Integrating inland waters into the terrestrial carbon budget, *Ecosystems*, 10(1), 171-184.

Creed, I. F., S. E. Sanford, F. D. Beall, L. A. Molot, and P. J. Dillon (2003), Cryptic wetlands: integrating hidden wetlands in regression models of the export of dissolved organic carbon from forested landscapes, *Hydrol Process*, 17(18), 3629-3648.

Dalzell, B. J., T. R. Filley, and J. M. Harbor (2007), The role of hydrology in annual organic carbon loads and terrestrial organic matter export from a midwestern agricultural watershed, *Geochim Cosmochim Acta*, 71(6), 1448-1462.

del Giorgio, P. A., and J. Davis (2003), Patterns in dissolved organic matter lability and consumption across aquatic ecosystems, in *Aquatic Ecosystems: Interactivity of Dissolved Organic Matter*, edited, p. 519, Academic Press, London, UK.

del Giorgio, P. A., and M. L. Pace (2008), Relative independence of dissolved organic carbon transport and processing in a large temperate river: The Hudson River as both pipe and reactor, *Limnol Oceanogr*, 53(1), 185-197.

Dittman, J. A., J. B. Shanley, C. T. Driscoll, G. R. Aiken, A. T. Chalmers, J. E. Towse, and P. Selvendiran (2010), Mercury dynamics in relation to dissolved organic carbon concentration and quality during high flow events in three northeastern US streams, *Water Resour Res*, 46.

Eckhardt, B. W., and T. R. Moore (1990), Controls on Dissolved Organic-Carbon Concentrations in Streams, Southern Quebec, *Can J Fish Aquat Sci*, 47(8), 1537-1544.

Eckhardt, K. (2005), How to construct recursive digital filters for baseflow separation, *Hydrol Process*, 19(2), 507-515.

Eckhardt, K. (2008), A comparison of baseflow indices, which were calculated with seven different baseflow separation methods, *J Hydrol*, 352(1-2), 168-173.

Falcone, J. A., D. M. Carlisle, D. M. Wolock, and M. R. Meador (2010), GAGES: A stream gage database for evaluating natural and altered flow conditions in the conterminous United States, *Ecology*, 91(2), 621-621.

Frey, K. E., and L. C. Smith (2005), Amplified carbon release from vast West Siberian peatlands by 2100, *Geophys Res Lett*, 32(9).

Frost, P. C., J. H. Larson, C. A. Johnston, K. C. Young, P. A. Maurice, G. A. Lamberti, and S. D. Bridgman (2006), Landscape predictors of stream dissolved organic matter concentration and physicochemistry in a Lake Superior river watershed, *Aquat Sci*, 68(1), 40-51.

Gattuso, J. P., M. Frankignoulle, and R. Wollast (1998), Carbon and carbonate metabolism in coastal aquatic ecosystems, *Annu Rev Ecol Syst*, 29, 405-434.

Gergel, S. E., M. G. Turner, and T. K. Kratz (1999), Dissolved organic carbon as an indicator of the scale of watershed influence on lakes and rivers, *Ecol Appl*, 9(4), 1377-1390.

Gorham, E., J. K. Underwood, J. A. Janssens, B. Freedman, W. Maass, D. H. Waller, and J. G. Ogden (1998), The chemistry of streams in southwestern and central Nova Scotia, with particular reference to catchment vegetation and the influence of dissolved organic carbon primarily from wetlands, *Wetlands*, 18(1), 115-132.

Guillemette, F., and P. A. del Giorgio (2011), Reconstructing the various facets of dissolved organic carbon bioavailability in freshwater ecosystems, *Limnol Oceanogr*, 56(2), 734-748.

Harrison, J. A., N. Caraco, and S. P. Seitzinger (2005), Global patterns and sources of dissolved organic matter export to the coastal zone: Results from a spatially explicit, global model, *Global Biogeochem Cy*, 19(4).

Helie, J. F., and C. Hillaire-Marcel (2006), Sources of particulate and dissolved organic carbon in the St Lawrence River: isotopic approach, *Hydrol Process*, 20(9), 1945-1959.

Henderson, R. K., A. Baker, S. A. Parsons, and B. Jefferson (2008), Characterisation of algogenic organic matter extracted from cyanobacteria, green algae and diatoms, *Water Res*, 42(13), 3435-3445.

Hodgkins, G. A. (1999), Estimating the magnitude of peak flows for streams in Maine for selected recurrence intervals *Rep.*, 1-45 pp, U.S. Geological Survey.

Homer, C., C. Q. Huang, L. M. Yang, B. Wylie, and M. Coan (2004), Development of a 2001 National Land-Cover Database for the United States, *Photogramm Eng Rem S*, 70(7), 829-840.

IBWC (2010), Rio Grande Stream Gauge, edited, International Boundary and Water Commission.

Koehler, B., E. von Wachenfeldt, D. Kothawala, and L. J. Tranvik (2012), Reactivity continuum of dissolved organic carbon decomposition in lake water, *J Geophys Res-Bioge*, 117.

Lauerwald, R., J. Hartmann, W. Ludwig, and N. Moosdorf (2012), Assessing the nonconservative fluvial fluxes of dissolved organic carbon in North America, *J. Geophys. Res.*, 117(G1), G01027.

Leenheer, J. (1982), United States Geological Survey data information service, in *Transport of Carbon and Minerals in Major World Rivers*, edited by E. T. Degens, pp. 355-356, Universitat Hamburg, Hamburg.

Lehtoranta, J., P. Ekholm, and H. Pitkanen (2009), Coastal Eutrophication Thresholds: A Matter of Sediment Microbial Processes, *Ambio*, 38(6), 303-308.

LPDAAC, N. L. P. D. A. A. C. (2000), MODIS/Terra Surface Reflectance 8-Day L3 Global 500m SIN Grid V005.

Ludwig, W., J. L. Probst, and S. Kempe (1996), Predicting the oceanic input of organic carbon by continental erosion, *Global Biogeochem Cy*, 10(1), 23-41.

Maurice, P. A., M. J. Pullin, S. E. Cabaniss, Q. H. Zhou, K. Namjesnik-Dejanovic, and G. R. Aiken (2002), A comparison of surface water natural organic matter in raw filtered water samples, XAD, and reverse osmosis isolates, *Water Res*, 36(9), 2357-2371.

McKnight, D. M., G. M. Hornberger, K. E. Bencala, and E. W. Boyer (2002), In-stream sorption of fulvic acid in an acidic stream: A stream-scale transport experiment, *Water Resour Res*, 38(1).

Mcknight, D. M., K. E. Bencala, G. W. Zellweger, G. R. Aiken, G. L. Feder, and K. A. Thorn (1992), Sorption of Dissolved Organic-Carbon by Hydrous Aluminum and Iron-Oxides Occurring at the Confluence of Deer Creek with the Snake River, Summit County, Colorado, *Environ Sci Technol*, 26(7), 1388-1396.

Meier, M., K. Namjesnik-Dejanovic, P. A. Maurice, Y. P. Chin, and G. R. Aiken (1999), Fractionation of aquatic natural organic matter upon sorption to goethite and kaolinite, *Chem Geol*, 157(3-4), 275-284.

Meybeck, M. (1982), CARBON, NITROGEN, AND PHOSPHORUS TRANSPORT BY WORLD RIVERS, *Am. J. Sci.*, 282(4), 401-450.

Meybeck, M., and A. Ragu (1996), River discharges to the oceans: An assessment of suspended solids, major ions, and nutrients, in *Environment and Assessment*, edited by U. E. Programme, pp. 1-245, Nairobi.

Miller, M. P., D. M. McKnight, S. C. Chapra, and M. W. Williams (2009), A model of degradation and production of three pools of dissolved organic matter in an alpine lake, *Limnol Oceanogr*, 54(6), 2213-2227.

Moran, M. A., and R. G. Zepp (1997), Role of photoreactions in the formation of biologically labile compounds from dissolved organic matter, *Limnol Oceanogr*, 42(6), 1307-1316.

Mulholland, P. J., and E. J. Kuenzler (1979), Organic-carbon export from upland and forested wetland watersheds, *Limnol Oceanogr*, 24(5), 960-966.

Mulholland, P. J., and J. A. Watts (1982), TRANSPORT OF ORGANIC-CARBON TO THE OCEANS BY RIVERS OF NORTH-AMERICA - A SYNTHESIS OF EXISTING DATA, *Tellus*, 34(2), 176-186.

Namour, P., and M. C. Muller (1998), Fractionation of organic matter from wastewater treatment plants before and after a 21-day biodegradability test: A physical-chemical method for measurement of the refractory part of effluents, *Water Res*, 32(7), 2224-2231.

Perez, M. A. P., P. Moreira-Turcq, H. Gallard, T. Allard, and M. F. Benedetti (2011), Dissolved organic matter dynamic in the Amazon basin: Sorption by mineral surfaces, *Chem Geol*, 286(3-4), 158-168.

Raymond, P. A., and C. S. Hopkinson (2003), Ecosystem modulation of dissolved carbon age in a temperate marsh-dominated estuary, *Ecosystems*, 6(7), 694-705.

Raymond, P. A., and J. E. Saiers (2010), Event controlled DOC export from forested watersheds, *Biogeochemistry*, 100(1-3), 197-209.

RDCT, R. D. C. T. (2011), R: A Language and Environment for Statistical Computing.

Reynolds, R. C. (1978), POLYPHENOL INHIBITION OF CALCITE PRECIPITATION IN LAKE POWELL, *Limnol Oceanogr*, 23(4), 585-597.

Richey, J. E., J. I. Hedges, A. H. Devol, P. D. Quay, R. Victoria, L. Martinelli, and B. R. Forsberg (1990), BIOGEOCHEMISTRY OF CARBON IN THE AMAZON RIVER, *Limnol Oceanogr*, 35(2), 352-371.

Runkel, R. L., C. G. Crawford, and T. A. Cohn (2004), Load Estimator (LOADEST): A FORTRAN Program for Estimating Constituent Loads in Streams

and Rivers, in *United States Geological Survey Techniques and Methods*, edited, p. 69.

Salisbury, J., D. Vandemark, J. Campbell, C. Hunt, D. Wisser, N. Reul, and B. Chapron (2011), Spatial and temporal coherence between Amazon River discharge, salinity, and light absorption by colored organic carbon in western tropical Atlantic surface waters, *J Geophys Res-Oceans*, 116.

Schlesinger, W. H. (1997), *Biogeochemistry : an analysis of global change*, 2nd ed., xiii, 588 p. pp., Academic Press, San Diego, Calif.

Seitzinger, S. P., J. A. Harrison, E. Dumont, A. H. W. Beusen, and A. F. Bouwman (2005), Sources and delivery of carbon, nitrogen, and phosphorus to the coastal zone: An overview of Global Nutrient Export from Watersheds (NEWS) models and their application, *Global Biogeochem Cy*, 19(4).

Shih, J. S., R. B. Alexander, R. A. Smith, E. W. Boyer, G. E. Schwarz, and S. Chung (2010), An initial SPARROW model of land use and in-stream controls on total organic carbon in streams of the conterminous United States *Rep.*, 22 pp.

Sholkovitz, E. R. (1976), Flocculation of dissolved organic and inorganic matter during mixing of river water and seawater, *Geochim Cosmochim Acta*, 40(7), 831-845.

Siddiqui, M. S., G. L. Amy, and B. D. Murphy (1997), Ozone enhanced removal of natural organic matter from drinking water sources, *Water Res*, 31(12), 3098-3106.

Singer, P. C. (1999), Humic substances as precursors for potentially harmful disinfection by-products, *Water Sci Technol*, 40(9), 25-30.

Spencer, R. G. M., K. D. Butler, and G. R. Aiken (in press), Chromophoric dissolved organic matter and dissolved organic carbon properties of rivers in the U.S.A.

Spencer, R. G. M., G. R. Aiken, K. P. Wickland, R. G. Striegl, and P. J. Hernes (2008), Seasonal and spatial variability in dissolved organic matter quantity and composition from the Yukon River basin, Alaska, *Global Biogeochem Cy*, 22(4).

Stanford, J. A. a. W., J. V. (1990), Limnology of Lake Powell and the chemistry of the Colorado River *Rep.*, 279 pp, Washington, D.C.

Stets, E. G., R. G. Striegl, and G. R. Aiken (2010), Dissolved organic carbon export and internal cycling in small, headwater lakes, *Global Biogeochem Cy*, 24.

Stubbins, A., V. Hubbard, G. Uher, C. S. Law, R. C. Upstill-Goddard, G. R. Aiken, and K. Mopper (2008), Relating carbon monoxide photoproduction to dissolved organic matter functionality, *Environ Sci Technol*, 42(9), 3271-3276.

Tipping, E., et al. (1999), Climatic influences on the leaching of dissolved organic matter from upland UK Moorland soils, investigated by a field manipulation experiment, *Environ Int*, 25(1), 83-95.

USBR-LC Water Resources Group - Lower Colorado Region, edited, United States Bureau of Reclamation.

USBR-UC Water Resources Group - Upper Colorado Region, edited, United States Bureau of Reclamation.

USGS (2006), National Hydrography Dataset (NHDplus).

Vahatalo, A. V., H. Aarnos, and S. Mantyniemi (2010), Biodegradability continuum and biodegradation kinetics of natural organic matter described by the beta distribution, *Biogeochemistry*, 100(1-3), 227-240.

Vannote, R. L., G. W. Minshall, K. W. Cummins, J. R. Sedell, and C. E. Cushing (1980), RIVER CONTINUUM CONCEPT, *Can J Fish Aquat Sci*, 37(1), 130-137.

Vorosmarty, C. J., B. M. Fekete, M. Meybeck, and R. B. Lammers (2000), Global system of rivers: Its role in organizing continental land mass and defining land-to-ocean linkages, *Global Biogeochem Cy*, 14(2), 599-621.

Waiser, M. J., and R. D. Robarts (2004), Photodegradation of DOC in a shallow prairie wetland: evidence from seasonal changes in DOC optical properties and chemical characteristics, *Biogeochemistry*, 69(2), 263-284.

Weishaar, J. L., G. R. Aiken, B. A. Bergamaschi, M. S. Fram, R. Fujii, and K. Mopper (2003), Evaluation of specific ultraviolet absorbance as an indicator of the chemical composition and reactivity of dissolved organic carbon, *Environ Sci Technol*, 37(20), 4702-4708.

Xiao, X., C. Biradar, C. Czarnecki, T. Alabi, and M. Keller (2009), A Simple Algorithm for Large-Scale Mapping of Evergreen Forests in Tropical America, Africa and Asia, *Remote Sensing*, 1(3), 355-374.

Ziegler, S. E., and M. L. Fogel (2003), Seasonal and diel relationships between the isotopic compositions of dissolved and particulate organic matter in freshwater ecosystems, *Biogeochemistry*, 64(1), 25-52.

APPENDIX

Table A.1. Table showing the regression equations, R^2 , and p -value for dissolved organic carbon (DOC) vs. 32-day antecedent discharge (Q32) in individual basins.

USGS Station #	Location	Regression equation	R^2	p
01095220	Worcester County, Massachusetts	[DOC] = 4.6 * Q^(0.128)	0.210	0.003
01102345	Essex County, Massachusetts	[DOC] = 7.14 * Q^(0.071)	0.113	0.024
01172680	Worcester County, Massachusetts	[DOC] = 8.496 * Q^(0.283)	0.399	0.004
01174050	Worcester County, Massachusetts	[DOC] = 4.687 * Q^(-0.146)	0.434	0.000
01174565	Franklin County, Massachusetts	[DOC] = 2.924 * Q^(0.119)	0.134	0.001
01174575	Franklin County, Massachusetts	[DOC] = 2.684 * Q^(-0.122)	0.078	0.023
01184490	Hartford County, Connecticut	[DOC] = 3.469 * Q^(0.292)	0.172	0.004
01187800	Litchfield County, Connecticut	[DOC] = 3.251 * Q^(0.305)	0.280	0.036
01362380	Ulster County, New York	[DOC] = 1.424 * Q^(0.171)	0.247	0.000
01390500	Bergen County, New Jersey	[DOC] = 2.63 * Q^(0.341)	0.593	0.000
01394500	Union County, New Jersey	[DOC] = 3.726 * Q^(0.208)	0.238	0.000
01399690	Hunterdon County, New Jersey	[DOC] = 3.739 * Q^(0.333)	0.520	0.000
01399700	Hunterdon County, New Jersey	[DOC] = 3.115 * Q^(0.331)	0.345	0.000
01407760	Monmouth County, New Jersey	[DOC] = 5.106 * Q^(0.23)	0.161	0.010
01410150	Burlington County, New Jersey	[DOC] = 8.296 * Q^(0.928)	0.474	0.000
01410784	Camden County, New Jersey	[DOC] = 14.696 * Q^(0.548)	0.448	0.000
01410810	Camden County, New Jersey	[DOC] = 17.347 * Q^(0.728)	0.445	0.000
01410820	Camden County, New Jersey	[DOC] = 6.749 * Q^(0.713)	0.497	0.000
01411300	Cape May County, New Jersey	[DOC] = 8.462 * Q^(1.18)	0.669	0.008
01412800	Cumberland County, New Jersey	[DOC] = 3.106 * Q^(0.679)	0.524	0.000
01421618	Delaware County, New York	[DOC] = 2.976 * Q^(0.126)	0.211	0.000
01422738	Delaware County, New York	[DOC] = 2.665 * Q^(0.076)	0.101	0.000
01422747	Delaware County, New York	[DOC] = 1.676 * Q^(0.19)	0.347	0.000
01434013	Ulster County, New York	[DOC] = 1.13 * Q^(0.398)	0.622	0.000
01434017	Ulster County, New York	[DOC] = 1.124 * Q^(0.392)	0.582	0.000
0143402265	Ulster County, New York	[DOC] = 1.036 * Q^(0.241)	0.451	0.000
01434025	Ulster County, New York	[DOC] = 2.558 * Q^(0.235)	0.352	0.000
01434105	Ulster County, New York	[DOC] = 2.192 * Q^(0.258)	0.103	0.003
01434176	Ulster County, New York	[DOC] = 0.778 * Q^(0.304)	0.471	0.000
01434498	Sullivan County, New York	[DOC] = 0.836 * Q^(0.319)	0.586	0.000
01466500	Burlington County, New Jersey	[DOC] = 112.014 * Q^(0.973)	0.605	0.000
01467019	Burlington County, New Jersey	[DOC] = 9.846 * Q^(0.217)	0.178	0.029
01467150	Camden County, New Jersey	[DOC] = 3.972 * Q^(0.132)	0.153	0.000
01478000	New Castle County, Delaware	[DOC] = 6.93 * Q^(0.159)	0.268	0.006
01480300	Chester County, Pennsylvania	[DOC] = 8.192 * Q^(0.522)	0.611	0.000
014806318	Chester County, Pennsylvania	[DOC] = 7.65 * Q^(0.679)	0.360	0.001
01480675	Chester County, Pennsylvania	[DOC] = 8.609 * Q^(0.159)	0.367	0.008
01493112	Kent County, Maryland	[DOC] = 4.521 * Q^(0.41)	0.456	0.000
01493500	Kent County, Maryland	[DOC] = 6.185 * Q^(0.092)	0.064	0.036
01527050	Steuben County, New York	[DOC] = 6.105 * Q^(0.243)	0.131	0.000
01572000	Schuykill County, Pennsylvania	[DOC] = 2.33 * Q^(0.167)	0.196	0.000
01576771	Lancaster County, Pennsylvania	[DOC] = 13.254 * Q^(0.205)	0.122	0.000
01576772	Lancaster County, Pennsylvania	[DOC] = 11.637 * Q^(0.149)	0.073	0.002

01591000	Montgomery County, Maryland	[DOC] = 2.331 * Q^(0.267)	0.259	0.000
01594710	St Mary	[DOC] = 6.936 * Q^(0.282)	0.628	0.000
01621050	Rockingham County, Virginia	[DOC] = 5.879 * Q^(0.266)	0.110	0.013
01654000	Fairfax County, Virginia	[DOC] = 3.595 * Q^(0.152)	0.141	0.023
02082731	Franklin County, North Carolina	[DOC] = 5.892 * Q^(0.087)	0.154	0.015
02083833	Pitt County, North Carolina	[DOC] = 5.584 * Q^(0.224)	0.209	0.000
02090625	Wayne County, North Carolina	[DOC] = 13.408 * Q^(0.198)	0.667	0.000
02091960	Beaufort County, North Carolina	[DOC] = 11.22 * Q^(-0.162)	0.623	0.038
02123567	Montgomery County, North Carolina	[DOC] = 11.967 * Q^(0.608)	0.486	0.049
02143040	Burke County, North Carolina	[DOC] = 1.443 * Q^(0.357)	0.154	0.004
021603257	Greenville County, South Carolina	[DOC] = 1.869 * Q^(0.243)	0.403	0.000
02172300	Aiken County, South Carolina	[DOC] = 5.114 * Q^(0.142)	0.117	0.025
02174250	Orangeburg County, South Carolina	[DOC] = 5.484 * Q^(0.219)	0.783	0.000
02300700	Hillsborough County, Florida	[DOC] = 12.145 * Q^(0.192)	0.573	0.000
02306774	Hillsborough County, Florida	[DOC] = 19.279 * Q^(0.13)	0.638	0.000
02332830	Hall County, Georgia	[DOC] = 2.091 * Q^(0.465)	0.558	0.000
02335870	Cobb County, Georgia	[DOC] = 2.019 * Q^(0.291)	0.541	0.000
02337500	Carroll County, Georgia	[DOC] = 1.559 * Q^(0.45)	0.534	0.000
02338523	Heard County, Georgia	[DOC] = 1.441 * Q^(0.209)	0.145	0.015
03039925	Somerset County, Pennsylvania	[DOC] = 1.176 * Q^(0.128)	0.061	0.012
03144270	Coshocton County, Ohio	[DOC] = 6.589 * Q^(0.237)	0.262	0.000
03144289	Coshocton County, Ohio	[DOC] = 7.194 * Q^(0.189)	0.146	0.012
03201600	Vinton County, Ohio	[DOC] = 5.455 * Q^(0.21)	0.120	0.005
03353600	Marion County, Indiana	[DOC] = 4.958 * Q^(0.078)	0.164	0.023
03353637	Marion County, Indiana	[DOC] = 3.92 * Q^(0.075)	0.118	0.000
03361638	Hancock County, Indiana	[DOC] = 7.373 * Q^(0.216)	0.476	0.000
03373530	Orange County, Indiana	[DOC] = 2.835 * Q^(0.26)	0.281	0.001
03448800	Buncombe County, North Carolina	[DOC] = 2.372 * Q^(0.413)	0.701	0.006
04071795	Shawano County, Wisconsin	[DOC] = 13.59 * Q^(0.1)	0.265	0.004
040851325	Brown County, Wisconsin	[DOC] = 23.977 * Q^(0.347)	0.629	0.037
04086175	Sheboygan County, Wisconsin	[DOC] = 11.263 * Q^(-0.101)	0.318	0.026
04087030	Waukesha County, Wisconsin	[DOC] = 8.828 * Q^(0.218)	0.596	0.000
04087070	Milwaukee County, Wisconsin	[DOC] = 8.583 * Q^(0.121)	0.666	0.001
04087088	Milwaukee County, Wisconsin	[DOC] = 6.846 * Q^(0.171)	0.373	0.021
04087204	Milwaukee County, Wisconsin	[DOC] = 7.238 * Q^(0.089)	0.221	0.000
04288230	Lamoille County, Vermont	[DOC] = 6.691 * Q^(0.467)	0.627	0.012
05014300	Glacier County, Montana	[DOC] = 0.749 * Q^(0.121)	0.205	0.000
05427948	Dane County, Wisconsin	[DOC] = 12.956 * Q^(0.256)	0.302	0.002
05451080	Hamilton County, Iowa	[DOC] = 5.773 * Q^(0.085)	0.178	0.000
05540275	Du Page County, Illinois	[DOC] = 4.606 * Q^(-0.054)	0.147	0.005
06058900	Jefferson County, Montana	[DOC] = 5.735 * Q^(0.699)	0.888	0.000
06187915	Park County, Montana	[DOC] = 1.12 * Q^(0.158)	0.542	0.000
06339560	Mercer County, North Dakota	[DOC] = 16.208 * Q^(0.072)	0.070	0.008
06340580	Mercer County, North Dakota	[DOC] = 14.432 * Q^(-0.083)	0.205	0.015
06340780	Mercer County, North Dakota	[DOC] = 15.569 * Q^(-0.085)	0.161	0.020
06355310	Bowman County, North Dakota	[DOC] = 16.474 * Q^(-0.13)	0.389	0.000
06404800	Custer County, South Dakota	[DOC] = 32.648 * Q^(0.483)	0.450	0.041
06404998	Custer County, South Dakota	[DOC] = 39.462 * Q^(0.664)	0.722	0.002

06611800	Jackson County, Colorado	[DOC] = 7.92 * Q^(0.228)	0.470	0.000
06714400	Clear Creek County, Colorado	[DOC] = 3.823 * Q^(1.855)	0.677	0.014
06879650	Riley County, Kansas	[DOC] = 5.145 * Q^(0.252)	0.423	0.001
06929315	Texas County, Missouri	[DOC] = 1.905 * Q^(0.334)	0.817	0.000
07249100	Mccurtain County, Oklahoma	[DOC] = 6.109 * Q^(0.139)	0.278	0.010
07362587	Saline County, Arkansas	[DOC] = 2.551 * Q^(0.266)	0.529	0.000
07381590	St. Mary Parish, Louisiana	[DOC] = 1.819 * Q^(0.118)	0.143	0.007
09046530	Summit County, Colorado	[DOC] = 0.924 * Q^(0.275)	0.444	0.000
09153290	Mesa County, Colorado	[DOC] = 4.187 * Q^(-0.111)	0.255	0.000
09244464	Routt County, Colorado	[DOC] = 38.115 * Q^(0.223)	0.549	0.014
09244470	Routt County, Colorado	[DOC] = 19.435 * Q^(-0.125)	0.919	0.006
09250600	Moffat County, Colorado	[DOC] = 11.088 * Q^(0.159)	0.220	0.018
09306242	Rio Blanco County, Colorado	[DOC] = 11.326 * Q^(0.132)	0.040	0.017
09310575	Carbon County, Utah	[DOC] = 5.236 * Q^(0.365)	0.894	0.010
10172000	Salt Lake County, Utah	[DOC] = 41.979 * Q^(0.665)	0.393	0.023
10244950	White Pine County, Nevada	[DOC] = 4.22 * Q^(0.48)	0.195	0.049
10343500	Nevada County, California	[DOC] = 3.004 * Q^(0.404)	0.555	0.000
11058500	San Bernardino County, California	[DOC] = 11.275 * Q^(0.641)	0.845	0.002
11063680	San Bernardino County, California	[DOC] = 8.629 * Q^(0.65)	0.933	0.005
11262900	Merced County, California	[DOC] = 9.567 * Q^(0.176)	0.172	0.025
11447360	Sacramento County, California	[DOC] = 8.65 * Q^(0.069)	0.190	0.004
12108500	King County, Washington	[DOC] = 3.071 * Q^(0.547)	0.563	0.000
12113375	King County, Washington	[DOC] = 5.134 * Q^(-0.111)	0.312	0.000
12128000	King County, Washington	[DOC] = 4.801 * Q^(0.208)	0.191	0.001
12212100	Whatcom County, Washington	[DOC] = 2.823 * Q^(0.337)	0.570	0.000
12416000	Kootenai County, Idaho	[DOC] = 5.764 * Q^(0.629)	0.477	0.035
12447390	Okanogan County, Washington	[DOC] = 1.843 * Q^(0.313)	0.592	0.000
14161500	Lane County, Oregon	[DOC] = 0.824 * Q^(0.108)	0.103	0.000
14203750	Washington County, Oregon	[DOC] = 0.912 * Q^(0.278)	0.541	0.000
401707105395000	Larimer County, Colorado	[DOC] = 1.003 * Q^(0.093)	0.020	0.023
01022800	Hancock County, Maine	[DOC] = 3.337 * Q^(-0.028)	0.012	0.295
01097480	Middlesex County, Massachusetts	[DOC] = 5.095 * Q^(-0.044)	-0.072	0.580
01101000	Essex County, Massachusetts	[DOC] = 7.956 * Q^(0.014)	-0.307	0.823
01102500	Middlesex County, Massachusetts	[DOC] = 4.661 * Q^(0.023)	-0.003	0.398
01104460	Middlesex County, Massachusetts	[DOC] = 4.536 * Q^(0.019)	-0.160	0.608
01105000	Norfolk County, Massachusetts	[DOC] = 6.684 * Q^(0)	-0.031	0.991
01172800	Worcester County, Massachusetts	[DOC] = 9.583 * Q^(-0.062)	-0.018	0.407
01208873	Fairfield County, Connecticut	[DOC] = 2.617 * Q^(0.067)	0.006	0.284
01304000	Suffolk County, New York	[DOC] = 2.701 * Q^(-0.107)	-0.075	0.893
01356190	Schenectady County, New York	[DOC] = 4.598 * Q^(-0.061)	0.064	0.051
01367800	Sussex County, New Jersey	[DOC] = 3.422 * Q^(0.024)	-0.042	0.743
01372051	Dutchess County, New York	[DOC] = 4.009 * Q^(-0.056)	0.052	0.146
01376500	Westchester County, New York	[DOC] = 3.569 * Q^(-0.079)	-0.061	0.556
01377500	Bergen County, New Jersey	[DOC] = 3.676 * Q^(0.269)	0.114	0.240
01381500	Morris County, New Jersey	[DOC] = 2.911 * Q^(0.072)	0.004	0.294
01393450	Union County, New Jersey	[DOC] = 4.042 * Q^(-0.044)	-0.031	0.728
01398000	Hunterdon County, New Jersey	[DOC] = 2.924 * Q^(-0.031)	0.012	0.137
01399500	Morris County, New Jersey	[DOC] = 4.062 * Q^(0.005)	-0.033	0.948

01403400	Somerset County, New Jersey	[DOC] = 5.405 * Q^(0.375)	0.099	0.316
01410787	Camden County, New Jersey	[DOC] = 4.313 * Q^(-0.098)	-0.014	0.403
01463620	Mercer County, New Jersey	[DOC] = 4.172 * Q^(-0.011)	-0.043	0.806
01464907	Bucks County, Pennsylvania	[DOC] = 4.85 * Q^(0.018)	-0.006	0.416
01467081	Burlington County, New Jersey	[DOC] = 4.62 * Q^(0.003)	-0.034	0.956
01478137	Chester County, Pennsylvania	[DOC] = 22.842 * Q^(0.089)	-0.007	0.378
01479820	Chester County, Pennsylvania	[DOC] = 5.042 * Q^(0.597)	0.131	0.295
01480095	New Castle County, Delaware	[DOC] = 7.642 * Q^(0.033)	-0.015	0.459
01480637	Chester County, Pennsylvania	[DOC] = 16.108 * Q^(0.337)	0.099	0.135
01482500	Salem County, New Jersey	[DOC] = 7.121 * Q^(0.084)	0.028	0.197
01484100	Kent County, Delaware	[DOC] = 0.292 * Q^(-0.569)	0.349	0.174
01559795	Bedford County, Pennsylvania	[DOC] = 1.165 * Q^(-0.217)	0.048	0.223
01571490	Cumberland County, Pennsylvania	[DOC] = 2.041 * Q^(0.237)	0.021	0.149
01573095	Lebanon County, Pennsylvania	[DOC] = 1.477 * Q^(0.206)	0.041	0.178
01594670	Calvert County, Maryland	[DOC] = 6.024 * Q^(0.021)	0.001	0.282
01659500	Stafford County, Virginia	[DOC] = 3.99 * Q^(0.079)	-0.287	0.765
01673638	King William County, Virginia	[DOC] = 4.528 * Q^(-0.151)	-0.047	0.432
02084164	Pitt County, North Carolina	[DOC] = 8.298 * Q^(0.035)	-0.017	0.495
02084317	Beaufort County, North Carolina	[DOC] = 4.365 * Q^(-0.087)	-0.115	0.499
02084540	Beaufort County, North Carolina	[DOC] = 24.69 * Q^(-0.16)	0.037	0.303
0208524090	Durham County, North Carolina	[DOC] = 8.027 * Q^(0.097)	0.128	0.228
02086849	Durham County, North Carolina	[DOC] = 12.709 * Q^(-0.093)	-0.105	0.489
02087580	Wake County, North Carolina	[DOC] = 5.956 * Q^(0.028)	0.083	0.067
02090960	Wayne County, North Carolina	[DOC] = 12.456 * Q^(0.257)	0.440	0.134
0209096970	Wayne County, North Carolina	[DOC] = 9.212 * Q^(0.026)	-0.071	0.514
0209173190	Greene County, North Carolina	[DOC] = 10.789 * Q^(0.104)	0.081	0.091
0209173200	Greene County, North Carolina	[DOC] = 15.532 * Q^(0.018)	0.002	0.313
02091970	Craven County, North Carolina	[DOC] = 16.676 * Q^(-0.058)	0.070	0.247
02096842	Orange County, North Carolina	[DOC] = 15.32 * Q^(0.158)	0.082	0.231
02096846	Orange County, North Carolina	[DOC] = 5.69 * Q^(-0.038)	-0.191	0.852
0209741955	Durham County, North Carolina	[DOC] = 8.93 * Q^(0.094)	0.282	0.207
02097464	Orange County, North Carolina	[DOC] = 5.693 * Q^(0.069)	0.034	0.244
02105524	Bladen County, North Carolina	[DOC] = 13.049 * Q^(-0.019)	-0.158	0.843
02172305	Aiken County, South Carolina	[DOC] = 5.539 * Q^(0.007)	-0.017	0.973
02314274	Charlton County, Georgia	[DOC] = 49.248 * Q^(-0.028)	-0.155	0.598
02315392	Columbia County, Florida	[DOC] = 39.263 * Q^(0.079)	0.172	0.147
02336635	Cobb County, Georgia	[DOC] = 1.686 * Q^(0.398)	0.515	0.066
02358685	Liberty County, Florida	[DOC] = 4.332 * Q^(0.025)	-0.110	0.930
03015795	Warren County, Pennsylvania	[DOC] = 1.851 * Q^(-0.02)	-0.036	0.765
03037525	Indiana County, Pennsylvania	[DOC] = 1.955 * Q^(0.01)	-0.028	0.797
03039930	Somerset County, Pennsylvania	[DOC] = 0.972 * Q^(-0.059)	-0.002	0.341
03110983	Jefferson County, Ohio	[DOC] = 6.653 * Q^(0.084)	0.037	0.131
03201660	Vinton County, Ohio	[DOC] = 4.185 * Q^(0.112)	0.006	0.286
03201700	Vinton County, Ohio	[DOC] = 3.957 * Q^(0.101)	0.018	0.153
03207962	Pike County, Kentucky	[DOC] = 2.392 * Q^(0.037)	-0.041	0.651
03207965	Pike County, Kentucky	[DOC] = 3.417 * Q^(-0.013)	-0.048	0.855
03282075	Lee County, Kentucky	[DOC] = 3.385 * Q^(0.043)	-0.037	0.574
03282100	Estill County, Kentucky	[DOC] = 3.153 * Q^(0.099)	0.063	0.142

03283370	Powell County, Kentucky	[DOC] = 2.101 * Q [^] (-0.048)	-0.009	0.375
03353551	Marion County, Indiana	[DOC] = 5.547 * Q [^] (0.048)	0.112	0.076
03450000	Buncombe County, North Carolina	[DOC] = 2.561 * Q [^] (0.264)	0.128	0.137
04024315	Douglas County, Wisconsin	[DOC] = 35.924 * Q [^] (0.742)	0.669	0.057
04026349	Bayfield County, Wisconsin	[DOC] = 7.207 * Q [^] (0.497)	-0.134	0.520
04087159	Milwaukee County, Wisconsin	[DOC] = 6.835 * Q [^] (0.174)	0.044	0.248
04087214	Milwaukee County, Wisconsin	[DOC] = 6.935 * Q [^] (0.049)	0.196	0.112
04256485	Herkimer County, New York	[DOC] = 2.508 * Q [^] (-0.023)	-0.226	0.791
05288470	Anoka County, Minnesota	[DOC] = 24.048 * Q [^] (0.151)	0.257	0.064
05288705	Hennepin County, Minnesota	[DOC] = 6.585 * Q [^] (0.01)	-0.014	0.721
05357215	Vilas County, Wisconsin	[DOC] = 5.1 * Q [^] (0.051)	-0.014	0.648
05357225	Vilas County, Wisconsin	[DOC] = 7.602 * Q [^] (0.116)	-0.001	0.342
05487550	Jasper County, Iowa	[DOC] = 5.874 * Q [^] (0.091)	-0.019	0.389
05569968	Fulton County, Illinois	[DOC] = 3.39 * Q [^] (-0.113)	0.064	0.288
05570330	Fulton County, Illinois	[DOC] = 8.279 * Q [^] (0.109)	-0.082	0.519
05595226	St Clair County, Illinois	[DOC] = 3.945 * Q [^] (-0.411)	0.356	0.124
06061900	Jefferson County, Montana	[DOC] = 2.601 * Q [^] (0.144)	0.233	0.154
06279790	Park County, Wyoming	[DOC] = 3.857 * Q [^] (0.335)	0.142	0.101
06279795	Park County, Wyoming	[DOC] = 2.461 * Q [^] (0.233)	0.153	0.103
06307525	Big Horn County, Montana	[DOC] = 18.457 * Q [^] (0.164)	-0.215	0.626
06307528	Rosebud County, Montana	[DOC] = 76.191 * Q [^] (0.475)	0.283	0.207
06339180	Dunn County, North Dakota	[DOC] = 24.463 * Q [^] (0.009)	-0.080	0.857
06340540	Mercer County, North Dakota	[DOC] = 14.396 * Q [^] (-0.05)	0.024	0.273
06340890	McLean County, North Dakota	[DOC] = 25.109 * Q [^] (0.088)	-0.006	0.380
06342040	Oliver County, North Dakota	[DOC] = 15.31 * Q [^] (0.022)	-0.051	0.685
06720330	Adams County, Colorado	[DOC] = 26.14 * Q [^] (0.098)	0.016	0.245
06720415	Adams County, Colorado	[DOC] = 9.897 * Q [^] (-0.074)	0.003	0.298
07031692	Shelby County, Tennessee	[DOC] = 6.273 * Q [^] (0.011)	-0.008	0.440
07083000	Lake County, Colorado	[DOC] = 1.034 * Q [^] (0.106)	0.023	0.082
07232024	Pittsburg County, Oklahoma	[DOC] = 11.734 * Q [^] (0.002)	-0.062	0.944
07246615	Le Flore County, Oklahoma	[DOC] = 8.059 * Q [^] (0.104)	0.006	0.300
07247550	Latimer County, Oklahoma	[DOC] = 8.428 * Q [^] (-0.054)	-0.001	0.336
07248620	Le Flore County, Oklahoma	[DOC] = 3.052 * Q [^] (0.094)	-0.011	0.381
07249422	Le Flore County, Oklahoma	[DOC] = 8.823 * Q [^] (0.018)	-0.102	0.786
072632962	Pulaski County, Arkansas	[DOC] = 5.458 * Q [^] (-0.019)	-0.108	0.873
072632971	Pulaski County, Arkansas	[DOC] = 4.677 * Q [^] (0.285)	0.024	0.293
072632982	Pulaski County, Arkansas	[DOC] = 5.817 * Q [^] (0.014)	-0.108	0.869
09243700	Routt County, Colorado	[DOC] = 8.204 * Q [^] (0.057)	-0.027	0.466
09243800	Routt County, Colorado	[DOC] = 9.025 * Q [^] (-0.041)	-0.045	0.503
09243900	Routt County, Colorado	[DOC] = 9.573 * Q [^] (-0.016)	-0.095	0.834
09244415	Routt County, Colorado	[DOC] = 9.617 * Q [^] (0.056)	0.146	0.189
09244460	Routt County, Colorado	[DOC] = 9.725 * Q [^] (0.065)	-0.124	0.586
09250510	Moffat County, Colorado	[DOC] = 12.858 * Q [^] (0.033)	-0.068	0.595
09250610	Moffat County, Colorado	[DOC] = 11.332 * Q [^] (0.039)	-0.018	0.399
09306025	Rio Blanco County, Colorado	[DOC] = 27.791 * Q [^] (0.239)	-0.123	0.583
09306235	Rio Blanco County, Colorado	[DOC] = 10.566 * Q [^] (0.052)	-0.019	0.586
09306240	Rio Blanco County, Colorado	[DOC] = 15.731 * Q [^] (0.056)	-0.029	0.457
09306244	Rio Blanco County, Colorado	[DOC] = 10.683 * Q [^] (-0.009)	-0.090	0.941

09310600	Carbon County, Utah	[DOC] = 5.581 * Q^(0.196)	0.009	0.312
09310700	Carbon County, Utah	[DOC] = 5.493 * Q^(0.205)	0.090	0.129
09313965	Carbon County, Utah	[DOC] = 6.468 * Q^(-0.027)	-0.162	0.887
09313975	Carbon County, Utah	[DOC] = 2.912 * Q^(-0.201)	0.061	0.166
09313985	Carbon County, Utah	[DOC] = 3.734 * Q^(-0.135)	-0.102	0.505
09314374	Emery County, Utah	[DOC] = 13.781 * Q^(0.225)	-0.064	0.546
09317919	Emery County, Utah	[DOC] = 2.51 * Q^(-0.069)	-0.017	0.402
09317920	Emery County, Utah	[DOC] = 4.633 * Q^(-0.049)	-0.161	0.871
09324200	Emery County, Utah	[DOC] = 5.292 * Q^(0.043)	-0.139	0.878
09331850	Sevier County, Utah	[DOC] = 3.472 * Q^(-0.033)	-0.124	0.928
09367685	San Juan County, New Mexico	[DOC] = 7.037 * Q^(0.042)	-0.145	0.644
10167499	Salt Lake County, Utah	[DOC] = 3.204 * Q^(0.103)	0.042	0.296
10167800	Salt Lake County, Utah	[DOC] = 2.645 * Q^(0.055)	0.029	0.188
10170250	Salt Lake County, Utah	[DOC] = 9.333 * Q^(0.312)	0.003	0.323
10249300	Nye County, Nevada	[DOC] = 3.143 * Q^(0.141)	0.110	0.105
10249900	Esmeralda County, Nevada	[DOC] = 1.942 * Q^(-0.279)	-0.056	0.585
10254970	Imperial County, California	[DOC] = 4.607 * Q^(0.519)	-0.152	0.668
10336626	El Dorado County, California	[DOC] = 1.755 * Q^(0.101)	-0.188	0.829
10336778	El Dorado County, California	[DOC] = 3.181 * Q^(0.444)	0.155	0.207
11482468	Humboldt County, California	[DOC] = 3.884 * Q^(-0.007)	-0.033	0.898
11532620	Del Norte County, California	[DOC] = 2.183 * Q^(0.112)	0.067	0.181
12103380	King County, Washington	[DOC] = 0.986 * Q^(0.179)	0.086	0.094
12185300	Snohomish County, Washington	[DOC] = 0.758 * Q^(0.003)	-0.010	0.957
14201300	Marion County, Oregon	[DOC] = 3.784 * Q^(0.004)	-0.014	0.845
14205400	Washington County, Oregon	[DOC] = 1.128 * Q^(-0.033)	-0.007	0.395
14206950	Washington County, Oregon	[DOC] = 3.883 * Q^(-0.02)	-0.009	0.474
14211500	Multnomah County, Oregon	[DOC] = 3.834 * Q^(-0.048)	0.122	0.190
14222980	Cowlitz County, Washington	[DOC] = 2.028 * Q^(-0.128)	-0.052	0.693
401723105400000	Larimer County, Colorado	[DOC] = 0.628 * Q^(-0.001)	-0.004	0.986
401733105392404	Larimer County, Colorado	[DOC] = 0.901 * Q^(-0.023)	-0.073	0.521

Table A.2. Table showing the regression equations, R^2 , and p -value for dissolved organic carbon concentration (DOC) vs. 32-day antecedent MODIS gross primary production index (GPP32) in individual basins.

USGS Station	Location	Regression equation	R^2	p
01022805	Hancock County, Maine	[DOC] = 0.009 * GPP32 ^(1.141)	0.589	0.046
01106468	Plymouth County, Massachusetts	[DOC] = 0.867 * GPP32 ^(0.326)	0.761	0.006
01170970	Hampshire County, Massachusetts	[DOC] = 0.865 * GPP32 ^(0.081)	0.507	0.002
01209710	Fairfield County, Connecticut	[DOC] = 2.259 * GPP32 ^(0.091)	0.250	0.002
0131199010	Hamilton County, New York	[DOC] = 6.734 * GPP32 ^(0.085)	0.273	0.005
0131199022	Hamilton County, New York	[DOC] = 3.406 * GPP32 ^(0.217)	0.429	0.047
01362380	Ulster County, New York	[DOC] = 1.166 * GPP32 ^(0.094)	0.099	0.000
01367780	Sussex County, New Jersey	[DOC] = 2.141 * GPP32 ^(0.094)	0.524	0.026
01367800	Sussex County, New Jersey	[DOC] = 2.421 * GPP32 ^(0.09)	0.228	0.002
01367902	Sussex County, New Jersey	[DOC] = 1.055 * GPP32 ^(0.204)	0.859	0.000
01368825	Sussex County, New Jersey	[DOC] = 2.918 * GPP32 ^(0.163)	0.623	0.012
01379200	Somerset County, New Jersey	[DOC] = 2.952 * GPP32 ^(0.058)	0.093	0.037
01380100	Morris County, New Jersey	[DOC] = 2.474 * GPP32 ^(0.076)	0.261	0.001
01382960	Passaic County, New Jersey	[DOC] = 1.389 * GPP32 ^(0.162)	0.425	0.047
01388720	Morris County, New Jersey	[DOC] = 3.726 * GPP32 ^(0.08)	0.292	0.000
01399295	Morris County, New Jersey	[DOC] = 0.705 * GPP32 ^(0.25)	0.656	0.009
01400530	Monmouth County, New Jersey	[DOC] = 0.793 * GPP32 ^(0.183)	0.589	0.016
01400808	Mercer County, New Jersey	[DOC] = 2.123 * GPP32 ^(0.156)	0.221	0.038
01400860	Mercer County, New Jersey	[DOC] = 2.374 * GPP32 ^(0.147)	0.316	0.007
01401700	Somerset County, New Jersey	[DOC] = 1.705 * GPP32 ^(0.124)	0.456	0.039
01405340	Middlesex County, New Jersey	[DOC] = 0.608 * GPP32 ^(0.295)	0.593	0.000
01407210	Monmouth County, New Jersey	[DOC] = 0.852 * GPP32 ^(0.249)	0.579	0.017
01407760	Monmouth County, New Jersey	[DOC] = 1.589 * GPP32 ^(0.15)	0.127	0.020
01408009	Monmouth County, New Jersey	[DOC] = 0.783 * GPP32 ^(0.266)	0.229	0.002
01408598	Ocean County, New Jersey	[DOC] = 2.091 * GPP32 ^(0.135)	0.294	0.049
01409387	Burlington County, New Jersey	[DOC] = 2.623 * GPP32 ^(0.182)	0.120	0.021
0140940950	Camden County, New Jersey	[DOC] = 1.44 * GPP32 ^(0.227)	0.527	0.000
01411196	Atlantic County, New Jersey	[DOC] = 20.124 * GPP32 ^(-0.231)	0.099	0.033
01411400	Cape May County, New Jersey	[DOC] = 8.006 * GPP32 ^(0.137)	0.203	0.003
01411444	Cumberland County, New Jersey	[DOC] = 4.51 * GPP32 ^(0.147)	0.143	0.013
01412005	Cumberland County, New Jersey	[DOC] = 10.21 * GPP32 ^(-0.219)	0.444	0.042
01413013	Cumberland County, New Jersey	[DOC] = 0.946 * GPP32 ^(0.244)	0.538	0.023
01421618	Delaware County, New York	[DOC] = 2.272 * GPP32 ^(0.075)	0.146	0.000
01422738	Delaware County, New York	[DOC] = 1.64 * GPP32 ^(0.069)	0.198	0.000
01422747	Delaware County, New York	[DOC] = 1.626 * GPP32 ^(0.039)	0.035	0.000
01434017	Ulster County, New York	[DOC] = 1.238 * GPP32 ^(0.062)	0.124	0.011
01434025	Ulster County, New York	[DOC] = 1.55 * GPP32 ^(0.08)	0.128	0.000
01434498	Sullivan County, New York	[DOC] = 1.085 * GPP32 ^(0.048)	0.111	0.016
01445900	Warren County, New Jersey	[DOC] = 2.436 * GPP32 ^(0.101)	0.588	0.016
01455700	Sussex County, New Jersey	[DOC] = 2.411 * GPP32 ^(0.059)	0.529	0.025
01458570	Hunterdon County, New Jersey	[DOC] = 1.104 * GPP32 ^(0.097)	0.241	0.001
01460870	Hunterdon County, New Jersey	[DOC] = 11.242 * GPP32 ^(-0.172)	0.419	0.049

01464380	Burlington County, New Jersey	[DOC] = 1.13 * GPP32^(0.194)	0.423	0.048
01464460	Monmouth County, New Jersey	[DOC] = 1.592 * GPP32^(0.145)	0.360	0.006
01464515	Monmouth County, New Jersey	[DOC] = 1.215 * GPP32^(0.227)	0.600	0.000
01464527	Burlington County, New Jersey	[DOC] = 1.459 * GPP32^(0.205)	0.477	0.000
01465808	Burlington County, New Jersey	[DOC] = 3.06 * GPP32^(0.447)	0.819	0.003
01465950	Burlington County, New Jersey	[DOC] = 0.333 * GPP32^(0.473)	0.849	0.017
01467150	Camden County, New Jersey	[DOC] = 2.689 * GPP32^(0.074)	0.073	0.024
01467359	Camden County, New Jersey	[DOC] = 1.633 * GPP32^(0.145)	0.349	0.000
01475042	Gloucester County, New Jersey	[DOC] = 2.201 * GPP32^(0.116)	0.423	0.048
01476625	Gloucester County, New Jersey	[DOC] = 1.129 * GPP32^(0.283)	0.521	0.026
01490116	Dorchester County, Maryland	[DOC] = 3.172 * GPP32^(0.332)	0.665	0.016
01591000	Montgomery County, Maryland	[DOC] = 0.722 * GPP32^(0.188)	0.198	0.048
01660490	Stafford County, Virginia	[DOC] = 2.928 * GPP32^(0.076)	0.530	0.007
01673638	King William County, Virginia	[DOC] = 0.759 * GPP32^(0.379)	0.794	0.004
0204279240	Newport News City, Virginia	[DOC] = 131.263 * GPP32^(-0.493)	0.604	0.005
02087580	Wake County, North Carolina	[DOC] = 3.545 * GPP32^(0.085)	0.132	0.017
0209096970	Wayne County, North Carolina	[DOC] = 3.519 * GPP32^(0.192)	0.465	0.003
0209173190	Greene County, North Carolina	[DOC] = 1.086 * GPP32^(0.402)	0.493	0.000
0209173200	Greene County, North Carolina	[DOC] = 7.969 * GPP32^(0.128)	0.230	0.022
03353637	Marion County, Indiana	[DOC] = 2.511 * GPP32^(0.098)	0.120	0.025
03361638	Hancock County, Indiana	[DOC] = 2.135 * GPP32^(0.2)	0.072	0.046
04080791	Portage County, Wisconsin	[DOC] = 0 * GPP32^(10.394)	0.345	0.002
04084429	Outagamie County, Wisconsin	[DOC] = 4.162 * GPP32^(0.094)	0.723	0.020
04087204	Milwaukee County, Wisconsin	[DOC] = 5.427 * GPP32^(0.049)	0.152	0.001
05014300	Glacier County, Montana	[DOC] = 0.642 * GPP32^(0.041)	0.095	0.000
05540275	Du Page County, Illinois	[DOC] = 4.42 * GPP32^(0.038)	0.118	0.012
06187915	Park County, Montana	[DOC] = 0.822 * GPP32^(0.088)	0.311	0.006
06893564	Jackson County, Missouri	[DOC] = 48396.765 * GPP32^(-1.479)	0.514	0.000
07083000	Lake County, Colorado	[DOC] = 0.674 * GPP32^(0.071)	0.065	0.010
072632982	Pulaski County, Arkansas	[DOC] = 2.455 * GPP32^(0.182)	0.188	0.046
09013000	Larimer County, Colorado	[DOC] = 2.487 * GPP32^(0.08)	0.212	0.048
09013500	Grand County, Colorado	[DOC] = 5.059 * GPP32^(-0.176)	0.062	0.010
09306242	Rio Blanco County, Colorado	[DOC] = 4.707 * GPP32^(0.052)	0.326	0.003
10336778	El Dorado County, California	[DOC] = 37649.148 * GPP32^(-1.989)	0.516	0.012
10343500	Nevada County, California	[DOC] = 8.275 * GPP32^(-0.359)	0.206	0.000
11067000	San Bernardino County, California	[DOC] = 4.139 * GPP32^(-0.337)	0.726	0.019
12070000	Kitsap County, Washington	[DOC] = 68.73 * GPP32^(-0.472)	0.771	0.032
12072380	Kitsap County, Washington	[DOC] = 7.353 * GPP32^(-0.285)	0.853	0.016
12128000	King County, Washington	[DOC] = 20.642 * GPP32^(-0.34)	0.831	0.020
12178080	Skagit County, Washington	[DOC] = 1.411 * GPP32^(-0.145)	0.268	0.019
12178730	Whatcom County, Washington	[DOC] = 1.413 * GPP32^(-0.13)	0.318	0.021
14206435	Washington County, Oregon	[DOC] = 2.724 * GPP32^(0.094)	0.296	0.000
14206950	Washington County, Oregon	[DOC] = 2.34 * GPP32^(0.096)	0.114	0.025
352108077490901	Lenoir County, North Carolina	[DOC] = 0.404 * GPP32^(0.34)	0.649	0.001
353212077392801	Greene County, North Carolina	[DOC] = 1.058 * GPP32^(0.259)	0.406	0.015
353308077340301	Pitt County, North Carolina	[DOC] = 0.981 * GPP32^(0.196)	0.497	0.014
353351077342001	Pitt County, North Carolina	[DOC] = 1.162 * GPP32^(0.197)	0.662	0.003
353356077342901	Pitt County, North Carolina	[DOC] = 1.332 * GPP32^(0.209)	0.734	0.002

355453092061301	Stone County, Arkansas	[DOC] = 0.138 * GPP32^(0.696)	0.421	0.010
393944084120700	Montgomery County, Ohio	[DOC] = 2.788 * GPP32^(0.091)	0.166	0.002
401707105395000	Larimer County, Colorado	[DOC] = 2.039 * GPP32^(-0.23)	0.242	0.000
401723105400000	Larimer County, Colorado	[DOC] = 0.79 * GPP32^(-0.076)	0.042	0.000
401733105392404	Larimer County, Colorado	[DOC] = 2.526 * GPP32^(-0.168)	0.163	0.000
01022800	Hancock County, Maine	[DOC] = 1.434 * GPP32^(0.17)	-0.011	0.378
01022810	Hancock County, Maine	[DOC] = 1.202 * GPP32^(0.37)	0.250	0.224
01022815	Hancock County, Maine	[DOC] = 8.646 * GPP32^(0.002)	-0.333	0.997
01022825	Hancock County, Maine	[DOC] = 1.872 * GPP32^(0.033)	-0.194	0.880
01022845	Hancock County, Maine	[DOC] = 3.092 * GPP32^(-0.076)	-0.185	0.812
01022850	Hancock County, Maine	[DOC] = 100.259 * GPP32^(-0.604)	0.306	0.115
01022865	Hancock County, Maine	[DOC] = 2.703 * GPP32^(0.061)	-0.187	0.822
01022890	Hancock County, Maine	[DOC] = 4.947 * GPP32^(0.079)	-0.172	0.743
01090477	Hillsborough County, New Hampshire	[DOC] = 1.263 * GPP32^(0.238)	-0.017	0.387
01095220	Worcester County, Massachusetts	[DOC] = 7.889 * GPP32^(-0.096)	0.026	0.251
01102345	Essex County, Massachusetts	[DOC] = 5.806 * GPP32^(0.055)	0.027	0.242
01102500	Middlesex County, Massachusetts	[DOC] = 4.39 * GPP32^(0.019)	-0.026	0.834
011032058	Norfolk County, Massachusetts	[DOC] = 1.745 * GPP32^(0.196)	-0.208	0.728
01105000	Norfolk County, Massachusetts	[DOC] = 3.598 * GPP32^(0.11)	-0.012	0.373
01112262	Worcester County, Massachusetts	[DOC] = 1.724 * GPP32^(0.173)	-0.237	0.846
01311990	Hamilton County, New York	[DOC] = 2.621 * GPP32^(0.176)	0.199	0.149
0131199040	Hamilton County, New York	[DOC] = 2.739 * GPP32^(0.189)	0.243	0.182
0131199050	Essex County, New York	[DOC] = 4.669 * GPP32^(0.03)	-0.019	0.567
01367625	Sussex County, New Jersey	[DOC] = 2.701 * GPP32^(0.008)	-0.021	0.621
01367880	Sussex County, New Jersey	[DOC] = 2.324 * GPP32^(0.119)	0.278	0.103
01378387	Bergen County, New Jersey	[DOC] = 4.316 * GPP32^(-0.054)	-0.049	0.443
01378583	Bergen County, New Jersey	[DOC] = 2.39 * GPP32^(0.08)	-0.110	0.599
01378660	Morris County, New Jersey	[DOC] = 1.45 * GPP32^(0.143)	0.209	0.142
01379870	Morris County, New Jersey	[DOC] = 1.049 * GPP32^(0.181)	0.352	0.071
01380098	Morris County, New Jersey	[DOC] = 2.505 * GPP32^(0.092)	0.347	0.073
01381260	Morris County, New Jersey	[DOC] = 1.137 * GPP32^(0.094)	-0.066	0.479
01381330	Morris County, New Jersey	[DOC] = 0.84 * GPP32^(0.123)	0.279	0.102
01381498	Morris County, New Jersey	[DOC] = 2.567 * GPP32^(-0.001)	-0.167	0.979
01390800	Bergen County, New Jersey	[DOC] = 3.216 * GPP32^(0.04)	-0.012	0.375
01393960	Essex County, New Jersey	[DOC] = 1.965 * GPP32^(0.161)	0.306	0.090
01394200	Union County, New Jersey	[DOC] = 2.992 * GPP32^(-0.014)	-0.160	0.856
01394500	Union County, New Jersey	[DOC] = 3.089 * GPP32^(0)	-0.029	0.997
01396588	Hunterdon County, New Jersey	[DOC] = 1.287 * GPP32^(0.062)	0.060	0.115
01396900	Hunterdon County, New Jersey	[DOC] = 0.482 * GPP32^(0.284)	0.396	0.056
01397950	Hunterdon County, New Jersey	[DOC] = 1.401 * GPP32^(0.144)	0.323	0.082
01398000	Hunterdon County, New Jersey	[DOC] = 2.374 * GPP32^(0.062)	0.044	0.106
01398060	Hunterdon County, New Jersey	[DOC] = 1.405 * GPP32^(0.114)	0.267	0.109
01398090	Somerset County, New Jersey	[DOC] = 1.359 * GPP32^(0.121)	0.347	0.073
01399200	Morris County, New Jersey	[DOC] = 3.002 * GPP32^(0.13)	0.271	0.106
01399520	Somerset County, New Jersey	[DOC] = 2.999 * GPP32^(-0.107)	0.024	0.320
01399820	Somerset County, New Jersey	[DOC] = 1.657 * GPP32^(0.141)	0.268	0.108
01400560	Middlesex County, New Jersey	[DOC] = 1.702 * GPP32^(0.08)	-0.093	0.548
01400823	Middlesex County, New Jersey	[DOC] = 4.806 * GPP32^(0.128)	0.018	0.329

01401400	Middlesex County, New Jersey	[DOC] = 2.947 * GPP32^(0.058)	-0.001	0.337
01401520	Mercer County, New Jersey	[DOC] = 1.216 * GPP32^(0.113)	0.115	0.216
01401560	Somerset County, New Jersey	[DOC] = 3.333 * GPP32^(0.056)	-0.087	0.532
01403171	Somerset County, New Jersey	[DOC] = 5.303 * GPP32^(-0.02)	-0.177	0.765
01403190	Somerset County, New Jersey	[DOC] = 1.255 * GPP32^(0.154)	0.347	0.073
01403575	Somerset County, New Jersey	[DOC] = 1.165 * GPP32^(0.148)	0.062	0.272
01404400	Middlesex County, New Jersey	[DOC] = 6.583 * GPP32^(-0.076)	-0.061	0.468
01405003	Middlesex County, New Jersey	[DOC] = 4.564 * GPP32^(0.066)	0.140	0.194
01405180	Monmouth County, New Jersey	[DOC] = 1.164 * GPP32^(0.206)	0.323	0.083
01407012	Monmouth County, New Jersey	[DOC] = 1.109 * GPP32^(0.126)	-0.081	0.517
01407253	Monmouth County, New Jersey	[DOC] = 1.248 * GPP32^(0.079)	-0.046	0.437
01407520	Monmouth County, New Jersey	[DOC] = 10.19 * GPP32^(-0.214)	0.099	0.232
01407538	Monmouth County, New Jersey	[DOC] = 1.213 * GPP32^(0.128)	0.167	0.172
01407900	Monmouth County, New Jersey	[DOC] = 1.845 * GPP32^(-0.011)	-0.165	0.919
01408100	Ocean County, New Jersey	[DOC] = 3.631 * GPP32^(0.075)	0.036	0.135
01408110	Monmouth County, New Jersey	[DOC] = 3.66 * GPP32^(0.15)	0.013	0.336
01408152	Ocean County, New Jersey	[DOC] = 3.607 * GPP32^(0.043)	-0.152	0.795
01408290	Ocean County, New Jersey	[DOC] = 4.911 * GPP32^(0.085)	-0.061	0.469
01408460	Ocean County, New Jersey	[DOC] = 4.114 * GPP32^(0.039)	-0.031	0.474
01408830	Ocean County, New Jersey	[DOC] = 3.808 * GPP32^(0.026)	-0.027	0.795
01409030	Ocean County, New Jersey	[DOC] = 4.626 * GPP32^(0.121)	0.139	0.195
0140940200	Camden County, New Jersey	[DOC] = 4.675 * GPP32^(-0.04)	-0.159	0.853
0140941070	Atlantic County, New Jersey	[DOC] = 2.515 * GPP32^(0.157)	-0.093	0.548
0140941075	Atlantic County, New Jersey	[DOC] = 1.934 * GPP32^(0.142)	-0.034	0.415
01409416	Atlantic County, New Jersey	[DOC] = 3.89 * GPP32^(0.025)	-0.021	0.625
01409435	Burlington County, New Jersey	[DOC] = 7.148 * GPP32^(-0.173)	-0.102	0.574
01409600	Atlantic County, New Jersey	[DOC] = 7.997 * GPP32^(-0.088)	0.032	0.309
01409601	Atlantic County, New Jersey	[DOC] = 9.261 * GPP32^(0.056)	-0.061	0.468
01409930	Burlington County, New Jersey	[DOC] = 4.993 * GPP32^(0.14)	0.064	0.269
01410150	Burlington County, New Jersey	[DOC] = 9.054 * GPP32^(-0.159)	0.031	0.152
01410455	Atlantic County, New Jersey	[DOC] = 11.107 * GPP32^(-0.257)	0.241	0.123
01410810	Camden County, New Jersey	[DOC] = 4.973 * GPP32^(-0.018)	-0.123	0.905
01410820	Camden County, New Jersey	[DOC] = 65676.494 * GPP32^(-1.567)	0.016	0.323
01411035	Gloucester County, New Jersey	[DOC] = 3.905 * GPP32^(0.032)	-0.023	0.696
01411208	Atlantic County, New Jersey	[DOC] = 51.171 * GPP32^(-0.422)	0.049	0.287
01411290	Atlantic County, New Jersey	[DOC] = 3.295 * GPP32^(0.087)	-0.113	0.611
01411295	Atlantic County, New Jersey	[DOC] = 18.097 * GPP32^(-0.246)	-0.074	0.499
01411300	Cape May County, New Jersey	[DOC] = 6.89 * GPP32^(-0.028)	-0.165	0.925
01411427	Cape May County, New Jersey	[DOC] = 3.798 * GPP32^(-0.06)	-0.068	0.598
01411440	Cape May County, New Jersey	[DOC] = 3.138 * GPP32^(0.25)	0.312	0.087
01411452	Gloucester County, New Jersey	[DOC] = 1.915 * GPP32^(0.104)	-0.046	0.437
01411457	Gloucester County, New Jersey	[DOC] = 4.5 * GPP32^(0.18)	-0.070	0.489
01411458	Gloucester County, New Jersey	[DOC] = 2.63 * GPP32^(0.291)	0.126	0.206
01411466	Gloucester County, New Jersey	[DOC] = 10.95 * GPP32^(-0.034)	-0.025	0.705
01411487	Salem County, New Jersey	[DOC] = 5.884 * GPP32^(-0.177)	0.071	0.262
01411495	Cumberland County, New Jersey	[DOC] = 11.742 * GPP32^(-0.276)	0.192	0.154
01411955	Cumberland County, New Jersey	[DOC] = 5.73 * GPP32^(-0.104)	0.006	0.278
01412800	Cumberland County, New Jersey	[DOC] = 3.683 * GPP32^(-0.048)	-0.011	0.444

01434097	Ulster County, New York	[DOC] = 1.046 * GPP32^(0.102)	0.388	0.080
01440097	Warren County, New Jersey	[DOC] = 1.566 * GPP32^(-0.083)	0.019	0.327
01443250	Sussex County, New Jersey	[DOC] = 5.78 * GPP32^(0.062)	0.078	0.254
01444990	Sussex County, New Jersey	[DOC] = 2.287 * GPP32^(0.041)	-0.104	0.582
01445160	Warren County, New Jersey	[DOC] = 1.933 * GPP32^(-0.007)	-0.030	0.890
01455240	Warren County, New Jersey	[DOC] = 1.975 * GPP32^(0.019)	-0.092	0.547
01458300	Hunterdon County, New Jersey	[DOC] = 1.153 * GPP32^(0.174)	0.325	0.082
01458710	Hunterdon County, New Jersey	[DOC] = 1.728 * GPP32^(0.072)	0.078	0.221
01460860	Hunterdon County, New Jersey	[DOC] = 7.659 * GPP32^(-0.098)	0.229	0.130
01461250	Hunterdon County, New Jersey	[DOC] = 1.312 * GPP32^(0.283)	0.230	0.129
01461282	Hunterdon County, New Jersey	[DOC] = 2.115 * GPP32^(0.081)	-0.127	0.664
01462800	Mercer County, New Jersey	[DOC] = 1.786 * GPP32^(0.055)	0.129	0.165
01463610	Mercer County, New Jersey	[DOC] = 3.012 * GPP32^(0.086)	0.176	0.165
01463661	Mercer County, New Jersey	[DOC] = 4.187 * GPP32^(-0.077)	-0.093	0.550
01463810	Mercer County, New Jersey	[DOC] = 2.326 * GPP32^(0.06)	0.274	0.069
01463850	Mercer County, New Jersey	[DOC] = 4.351 * GPP32^(0.035)	-0.022	0.635
01464280	Burlington County, New Jersey	[DOC] = 8.168 * GPP32^(-0.146)	0.054	0.282
01464532	Burlington County, New Jersey	[DOC] = 3.348 * GPP32^(0.016)	-0.152	0.794
01464907	Bucks County, Pennsylvania	[DOC] = 3.953 * GPP32^(0.022)	-0.033	0.631
01465857	Burlington County, New Jersey	[DOC] = 2.939 * GPP32^(0.08)	-0.049	0.443
01465893	Burlington County, New Jersey	[DOC] = 10.84 * GPP32^(0.03)	-0.024	0.683
01465965	Burlington County, New Jersey	[DOC] = 2.752 * GPP32^(0.178)	0.355	0.070
01466100	Burlington County, New Jersey	[DOC] = 1.396 * GPP32^(0.172)	-0.036	0.418
01466500	Burlington County, New Jersey	[DOC] = 5.862 * GPP32^(0.081)	0.005	0.171
01467066	Burlington County, New Jersey	[DOC] = 1.807 * GPP32^(0.111)	-0.059	0.464
01467325	Gloucester County, New Jersey	[DOC] = 2.913 * GPP32^(-0.023)	-0.158	0.840
01475090	Gloucester County, New Jersey	[DOC] = 1.432 * GPP32^(0.263)	0.252	0.116
01476640	Gloucester County, New Jersey	[DOC] = 2.032 * GPP32^(0.176)	0.315	0.086
01477110	Gloucester County, New Jersey	[DOC] = 3.932 * GPP32^(-0.066)	-0.131	0.798
01477440	Salem County, New Jersey	[DOC] = 6.514 * GPP32^(-0.058)	-0.070	0.609
01479820	Chester County, Pennsylvania	[DOC] = 1.351 * GPP32^(0.238)	0.104	0.313
01482500	Salem County, New Jersey	[DOC] = 5.771 * GPP32^(0.027)	-0.012	0.457
01482520	Salem County, New Jersey	[DOC] = 7.149 * GPP32^(-0.059)	-0.036	0.419
01482530	Salem County, New Jersey	[DOC] = 1.834 * GPP32^(0.233)	0.319	0.084
01482645	Salem County, New Jersey	[DOC] = 9.347 * GPP32^(-0.194)	0.078	0.254
01490108	Dorchester County, Maryland	[DOC] = 5.524 * GPP32^(0.263)	0.069	0.307
01490112	Dorchester County, Maryland	[DOC] = 20.175 * GPP32^(-0.02)	-0.164	0.908
01490120	Dorchester County, Maryland	[DOC] = 16.274 * GPP32^(0.02)	-0.159	0.849
01490130	Dorchester County, Maryland	[DOC] = 14.114 * GPP32^(0.042)	-0.157	0.684
01493112	Kent County, Maryland	[DOC] = 1.736 * GPP32^(0.022)	-0.086	0.828
01493500	Kent County, Maryland	[DOC] = 5.067 * GPP32^(0.036)	-0.012	0.538
01610400	Hardy County, West Virginia	[DOC] = 1.011 * GPP32^(0.064)	0.104	0.053
01659500	Stafford County, Virginia	[DOC] = 0.252 * GPP32^(0.509)	0.515	0.106
0208500600	Orange County, North Carolina	[DOC] = 2.46 * GPP32^(0.071)	-0.183	0.659
0208524090	Durham County, North Carolina	[DOC] = 78167497059111518218 * GPP32^(-7.397)	0.101	0.253
0208725055	Wake County, North Carolina	[DOC] = 1.692 * GPP32^(0.16)	-0.040	0.420
0208726370	Wake County, North Carolina	[DOC] = 3.238 * GPP32^(-0.008)	-0.249	0.967
0208726995	Wake County, North Carolina	[DOC] = 3.561 * GPP32^(0.062)	-0.202	0.710

0208923650	Lenoir County, North Carolina	[DOC] = 1.192 * GPP32^(0.124)	0.060	0.211
02090960	Wayne County, North Carolina	[DOC] = 3.923 * GPP32^(0.184)	0.293	0.121
0209171225	Greene County, North Carolina	[DOC] = 2.325 * GPP32^(0.176)	-0.004	0.356
0209171725	Greene County, North Carolina	[DOC] = 1.855 * GPP32^(0.101)	-0.091	0.780
0209172000	Greene County, North Carolina	[DOC] = 6.826 * GPP32^(0.13)	0.350	0.072
0209173070	Greene County, North Carolina	[DOC] = 7.539 * GPP32^(0.201)	-0.011	0.423
0209173150	Greene County, North Carolina	[DOC] = 4.209 * GPP32^(0.078)	-0.040	0.696
02091734	Greene County, North Carolina	[DOC] = 2.362 * GPP32^(0.003)	-0.059	0.986
02096846	Orange County, North Carolina	[DOC] = 1.414 * GPP32^(0.277)	0.060	0.259
0209741955	Durham County, North Carolina	[DOC] = 19.032 * GPP32^(-0.111)	-0.140	0.527
02097464	Orange County, North Carolina	[DOC] = 2.571 * GPP32^(0.108)	-0.010	0.371
0209782609	Wake County, North Carolina	[DOC] = 3.242 * GPP32^(0.184)	0.052	0.301
02172300	Aiken County, South Carolina	[DOC] = 1.41 * GPP32^(0.294)	0.042	0.331
02172304	Aiken County, South Carolina	[DOC] = 36.375 * GPP32^(-0.329)	-0.150	0.780
02172305	Aiken County, South Carolina	[DOC] = 0.381 * GPP32^(0.494)	0.036	0.072
02176734	Beaufort County, South Carolina	[DOC] = 29959.109 * GPP32^(-1.433)	0.607	0.075
02306774	Hillsborough County, Florida	[DOC] = 56.6 * GPP32^(-0.25)	0.009	0.274
02314274	Charlton County, Georgia	[DOC] = 20.834 * GPP32^(0.146)	0.361	0.122
02336635	Cobb County, Georgia	[DOC] = 0.367 * GPP32^(0.33)	0.250	0.178
02338523	Heard County, Georgia	[DOC] = 0.612 * GPP32^(0.126)	0.024	0.184
02344480	Spalding County, Georgia	[DOC] = 1.373 * GPP32^(0.098)	-0.125	0.542
03448800	Buncombe County, North Carolina	[DOC] = 0.116 * GPP32^(0.397)	-0.106	0.588
04081897	Winnebago County, Wisconsin	[DOC] = 5.907 * GPP32^(0.02)	-0.096	0.495
040851325	Brown County, Wisconsin	[DOC] = 8.887 * GPP32^(0.105)	0.072	0.304
04085188	Kewaunee County, Wisconsin	[DOC] = 12.311 * GPP32^(0.043)	0.096	0.284
040853145	Kewaunee County, Wisconsin	[DOC] = 11.171 * GPP32^(0.04)	-0.038	0.417
040870195	Washington County, Wisconsin	[DOC] = 7.161 * GPP32^(-0.033)	-0.015	0.383
04087030	Waukesha County, Wisconsin	[DOC] = 7.598 * GPP32^(-0.001)	-0.071	0.985
04087070	Milwaukee County, Wisconsin	[DOC] = 7.112 * GPP32^(-0.013)	-0.059	0.575
04087088	Milwaukee County, Wisconsin	[DOC] = 5.758 * GPP32^(0.006)	-0.098	0.888
04087118	Milwaukee County, Wisconsin	[DOC] = 3.938 * GPP32^(0.04)	0.533	0.099
04087159	Milwaukee County, Wisconsin	[DOC] = 11.536 * GPP32^(-0.155)	0.241	0.060
04087214	Milwaukee County, Wisconsin	[DOC] = 5.771 * GPP32^(0.017)	-0.039	0.460
04288230	Lamoille County, Vermont	[DOC] = 2644.239 * GPP32^(-1.092)	0.221	0.135
05451080	Hamilton County, Iowa	[DOC] = 5.33 * GPP32^(0.008)	-0.011	0.735
05544371	Waukesha County, Wisconsin	[DOC] = 4.192 * GPP32^(0.01)	-0.093	0.808
06893557	Jackson County, Missouri	[DOC] = 4.688 * GPP32^(0.044)	-0.008	0.468
06893560	Jackson County, Missouri	[DOC] = 21986.769 * GPP32^(-1.371)	0.130	0.164
06893562	Jackson County, Missouri	[DOC] = 5.176 * GPP32^(0.037)	-0.010	0.500
07060894	Independence County, Arkansas	[DOC] = 0.517 * GPP32^(0.128)	0.034	0.285
072632962	Pulaski County, Arkansas	[DOC] = 2.186 * GPP32^(0.173)	0.009	0.301
072632971	Pulaski County, Arkansas	[DOC] = 4.674 * GPP32^(0.065)	-0.051	0.648
072632981	Pulaski County, Arkansas	[DOC] = 6.73 * GPP32^(0.027)	-0.199	0.959
0726329911	Pulaski County, Arkansas	[DOC] = 1.296 * GPP32^(0.387)	0.217	0.084
07288625	Bolivar County, Mississippi	[DOC] = 6.574 * GPP32^(0.062)	-0.203	0.713
07288636	Bolivar County, Mississippi	[DOC] = 6.2 * GPP32^(-0.005)	-0.015	0.943
07362587	Saline County, Arkansas	[DOC] = 13.731 * GPP32^(-0.253)	0.023	0.147
07379960	East Baton Rouge Parish, Louisiana	[DOC] = 7.488 * GPP32^(0.043)	-0.033	0.691

07381590	St. Mary Parish, Louisiana	[DOC] = 4.571 * GPP32^(0.002)	-0.024	0.976
09018000	Grand County, Colorado	[DOC] = 3.792 * GPP32^(0.031)	-0.032	0.672
10167800	Salt Lake County, Utah	[DOC] = 4.27 * GPP32^(-0.108)	-0.070	0.538
103367786	El Dorado County, California	[DOC] = 4136.139 * GPP32^(-1.501)	0.145	0.122
11058500	San Bernardino County, California	[DOC] = 34.952 * GPP32^(-0.631)	-0.029	0.406
11073470	San Bernardino County, California	[DOC] = 0.697 * GPP32^(0.083)	-0.227	0.797
11206800	Tulare County, California	[DOC] = 1.111 * GPP32^(-0.012)	-0.006	0.522
11262900	Merced County, California	[DOC] = 518.209 * GPP32^(-0.849)	0.386	0.111
12073520	Pierce County, Washington	[DOC] = 9.344 * GPP32^(-0.22)	-0.013	0.402
12119705	King County, Washington	[DOC] = 3.483 * GPP32^(-0.055)	-0.063	0.447
12120500	King County, Washington	[DOC] = 3.803 * GPP32^(0.016)	-0.329	0.927
12127100	King County, Washington	[DOC] = 11.784 * GPP32^(-0.147)	0.069	0.338
12154000	Snohomish County, Washington	[DOC] = 20.192 * GPP32^(-0.184)	0.244	0.227
12155050	Snohomish County, Washington	[DOC] = 5.378 * GPP32^(-0.045)	-0.016	0.405
12447390	Okanogan County, Washington	[DOC] = 1.276 * GPP32^(0.032)	0.033	0.180
13088510	Cassia County, Idaho	[DOC] = 1.433 * GPP32^(0.081)	0.255	0.078
13150200	Blaine County, Idaho	[DOC] = 2.06 * GPP32^(-0.029)	-0.047	0.461
14161500	Lane County, Oregon	[DOC] = 1.133 * GPP32^(-0.051)	0.013	0.116
14201300	Marion County, Oregon	[DOC] = 3.255 * GPP32^(0.023)	-0.024	0.662
14205400	Washington County, Oregon	[DOC] = 1.47 * GPP32^(-0.054)	0.035	0.118
14224570	Lewis County, Washington	[DOC] = 1.001 * GPP32^(0.029)	-0.056	0.750
280828082062900	Hillsborough County, Florida	[DOC] = 0.011 * GPP32^(1.27)	-0.043	0.425
301520092491800	Jefferson Davis Parish, Louisiana	[DOC] = 75.341 * GPP32^(-0.272)	-0.063	0.459
333150090530400	Bolivar County, Mississippi	[DOC] = 11.774 * GPP32^(-0.117)	0.032	0.078
3343250813616	Aiken County, South Carolina	[DOC] = 0 * GPP32^(1.85)	0.445	0.133
3344250813538	Aiken County, South Carolina	[DOC] = 1.083 * GPP32^(0.303)	0.041	0.333
3344280813547	Aiken County, South Carolina	[DOC] = 1.101 * GPP32^(0.338)	0.119	0.265
3344580813559	Aiken County, South Carolina	[DOC] = 41.89 * GPP32^(-0.274)	-0.277	0.741
3345100813509	Aiken County, South Carolina	[DOC] = 1.222 * GPP32^(0.273)	0.091	0.288
341014116494801	San Bernardino County, California	[DOC] = 0.047 * GPP32^(0.658)	0.141	0.248
352053077483001	Lenoir County, North Carolina	[DOC] = 0.357 * GPP32^(0.402)	0.284	0.053
353107077383001	Greene County, North Carolina	[DOC] = 1.899 * GPP32^(0.025)	-0.085	0.722
353111077330501	Greene County, North Carolina	[DOC] = 1.484 * GPP32^(0.268)	0.177	0.165
353111077334901	Greene County, North Carolina	[DOC] = 1.001 * GPP32^(0.153)	0.091	0.178
353220077392401	Greene County, North Carolina	[DOC] = 4.534 * GPP32^(-0.116)	-0.041	0.444
353354077343401	Pitt County, North Carolina	[DOC] = 0.456 * GPP32^(0.323)	0.539	0.059
353354077343402	Pitt County, North Carolina	[DOC] = 1.669 * GPP32^(0.087)	0.114	0.217
353530092053201	Stone County, Arkansas	[DOC] = 15.494 * GPP32^(-0.152)	-0.065	0.615
374248107324501	San Juan County, Colorado	[DOC] = 61.142 * GPP32^(-1.041)	0.138	0.095
382752123003401	Sonoma County, California	[DOC] = 0.414 * GPP32^(0.106)	-0.318	0.862
385431119574201	El Dorado County, California	[DOC] = 1.592 * GPP32^(0.48)	0.215	0.054
391116120562501	Nevada County, California	[DOC] = 0.993 * GPP32^(-0.04)	-0.035	0.873
391344105133601	Douglas County, Colorado	[DOC] = 1.543 * GPP32^(0.155)	0.007	0.265
392023105070601	Douglas County, Colorado	[DOC] = 2.046 * GPP32^(0.093)	-0.011	0.435
394409105020501	Denver County, Colorado	[DOC] = 2.869 * GPP32^(0.077)	0.341	0.131
394921105015701	Adams County, Colorado	[DOC] = 2.916 * GPP32^(0.138)	-0.097	0.497
400812106254800	Grand County, Colorado	[DOC] = 8.418 * GPP32^(-0.029)	-0.086	0.730
400855105090501	Boulder County, Colorado	[DOC] = 20.342 * GPP32^(-0.512)	0.272	0.166

403048105042701	Larimer County, Colorado	[DOC] = 6.896 * GPP32 [^] (-0.11)	-0.151	0.589
404750106454200	Routt County, Colorado	[DOC] = 4.573 * GPP32 [^] (-0.013)	-0.243	0.890
405344106405101	Jackson County, Colorado	[DOC] = 0.496 * GPP32 [^] (0.394)	0.103	0.057
415642074343101	Ulster County, New York	[DOC] = 0.567 * GPP32 [^] (0.009)	-0.049	0.803
445551123015800	Marion County, Oregon	[DOC] = 0.806 * GPP32 [^] (0.12)	0.309	0.146
450022123012400	Marion County, Oregon	[DOC] = 3.065 * GPP32 [^] (0.01)	-0.248	0.944
452231122200000	Clackamas County, Oregon	[DOC] = 0.927 * GPP32 [^] (0.123)	0.025	0.348
452414122213200	Clackamas County, Oregon	[DOC] = 1.239 * GPP32 [^] (0.052)	-0.005	0.379
452526122364400	Clackamas County, Oregon	[DOC] = 2.683 * GPP32 [^] (-0.031)	-0.164	0.709
454510122424900	Clark County, Washington	[DOC] = 3.825 * GPP32 [^] (-0.021)	-0.152	0.590
454549122295800	Clark County, Washington	[DOC] = 1.478 * GPP32 [^] (0.004)	-0.249	0.965
455122122310600	Clark County, Washington	[DOC] = 2.145 * GPP32 [^] (0.093)	0.118	0.266
455550113432001	Ravalli County, Montana	[DOC] = 5.947 * GPP32 [^] (-0.102)	-0.070	0.611
483256113590201	Flathead County, Montana	[DOC] = 1.488 * GPP32 [^] (-0.034)	0.003	0.292

Table A.3. Table showing the regression equations, R^2 , and p -value for dissolved organic carbon concentration (DOC) vs. stormflow ratio (S_R) in individual basins.

USGS Station	Location	Regression equation	R^2	p
01095220	Worcester County, Massachusetts	[DOC] = 3.744 * exp[SR*(0.586)]	0.210	0.003
01172680	Worcester County, Massachusetts	[DOC] = 3.01 * exp[SR*(0.83)]	0.650	0.002
01174565	Franklin County, Massachusetts	[DOC] = 2.46 * exp[SR*(0.49)]	0.129	0.002
01184490	Hartford County, Connecticut	[DOC] = 2.454 * exp[SR*(1.341)]	0.271	0.000
01187800	Litchfield County, Connecticut	[DOC] = 2.492 * exp[SR*(1.356)]	0.600	0.001
01362380	Ulster County, New York	[DOC] = 1.082 * exp[SR*(1.171)]	0.530	0.000
01381500	Morris County, New Jersey	[DOC] = 2.674 * exp[SR*(0.822)]	0.389	0.000
01390500	Bergen County, New Jersey	[DOC] = 1.879 * exp[SR*(1.127)]	0.488	0.000
01394500	Union County, New Jersey	[DOC] = 2.902 * exp[SR*(0.59)]	0.179	0.000
01398000	Hunterdon County, New Jersey	[DOC] = 2.556 * exp[SR*(0.509)]	0.167	0.000
01399690	Hunterdon County, New Jersey	[DOC] = 2.8 * exp[SR*(0.66)]	0.085	0.040
01410784	Camden County, New Jersey	[DOC] = 7.781 * exp[SR*(0.981)]	0.098	0.010
01410810	Camden County, New Jersey	[DOC] = 5.617 * exp[SR*(1.474)]	0.292	0.006
01412800	Cumberland County, New Jersey	[DOC] = 2.231 * exp[SR*(1.529)]	0.248	0.008
01421618	Delaware County, New York	[DOC] = 1.955 * exp[SR*(0.932)]	0.486	0.000
01422747	Delaware County, New York	[DOC] = 1.201 * exp[SR*(1.016)]	0.531	0.000
01434013	Ulster County, New York	[DOC] = 1.053 * exp[SR*(1.102)]	0.226	0.000
01434017	Ulster County, New York	[DOC] = 1.079 * exp[SR*(1.099)]	0.239	0.000
0143402265	Ulster County, New York	[DOC] = 0.712 * exp[SR*(0.752)]	0.199	0.000
01434025	Ulster County, New York	[DOC] = 1.371 * exp[SR*(0.99)]	0.429	0.000
01434105	Ulster County, New York	[DOC] = 0.885 * exp[SR*(1.713)]	0.507	0.000
01434176	Ulster County, New York	[DOC] = 0.671 * exp[SR*(1.296)]	0.364	0.000
01434498	Sullivan County, New York	[DOC] = 0.849 * exp[SR*(1.272)]	0.427	0.000
01464907	Bucks County, Pennsylvania	[DOC] = 4.188 * exp[SR*(0.418)]	0.301	0.000
01478000	New Castle County, Delaware	[DOC] = 5.172 * exp[SR*(0.5)]	0.221	0.012
01480095	New Castle County, Delaware	[DOC] = 5.485 * exp[SR*(0.436)]	0.105	0.049
01480300	Chester County, Pennsylvania	[DOC] = 4.172 * exp[SR*(1.34)]	0.597	0.000
01480675	Chester County, Pennsylvania	[DOC] = 4.903 * exp[SR*(0.723)]	0.459	0.002
01493112	Kent County, Maryland	[DOC] = 1.97 * exp[SR*(1.194)]	0.460	0.000
01493500	Kent County, Maryland	[DOC] = 4.676 * exp[SR*(0.593)]	0.181	0.001
01527050	Steuben County, New York	[DOC] = 3.256 * exp[SR*(0.464)]	0.038	0.019
01571490	Cumberland County, Pennsylvania	[DOC] = 1.428 * exp[SR*(1.428)]	0.102	0.010
01572000	Schuylkill County, Pennsylvania	[DOC] = 1.853 * exp[SR*(1.048)]	0.383	0.000
01591000	Montgomery County, Maryland	[DOC] = 1.63 * exp[SR*(1.294)]	0.340	0.000
01594710	St Mary	[DOC] = 3.141 * exp[SR*(1.237)]	0.507	0.000
01621050	Rockingham County, Virginia	[DOC] = 3.119 * exp[SR*(0.773)]	0.112	0.016
01654000	Fairfax County, Virginia	[DOC] = 2.712 * exp[SR*(0.987)]	0.349	0.001
02083833	Pitt County, North Carolina	[DOC] = 5.078 * exp[SR*(-0.511)]	0.077	0.042
02087580	Wake County, North Carolina	[DOC] = 5.457 * exp[SR*(0.208)]	0.133	0.045
02097464	Orange County, North Carolina	[DOC] = 4.459 * exp[SR*(1.015)]	0.680	0.007
02143040	Burke County, North Carolina	[DOC] = 1.3 * exp[SR*(0.985)]	0.073	0.040
021603257	Greenville County, South Carolina	[DOC] = 1.471 * exp[SR*(0.948)]	0.382	0.000
02172300	Aiken County, South Carolina	[DOC] = 4.268 * exp[SR*(0.549)]	0.187	0.005
02174250	Orangeburg County, South Carolina	[DOC] = 4.076 * exp[SR*(0.385)]	0.103	0.006

02332830	Hall County, Georgia	[DOC] = 1.046 * exp[SR*(2.317)]	0.800	0.000
02335870	Cobb County, Georgia	[DOC] = 1.514 * exp[SR*(1.341)]	0.637	0.000
02337500	Carroll County, Georgia	[DOC] = 1.169 * exp[SR*(1.614)]	0.629	0.000
02338523	Heard County, Georgia	[DOC] = 1.061 * exp[SR*(1.297)]	0.286	0.001
03015795	Warren County, Pennsylvania	[DOC] = 1.321 * exp[SR*(0.987)]	0.355	0.001
03037525	Indiana County, Pennsylvania	[DOC] = 1.352 * exp[SR*(0.921)]	0.468	0.000
03282100	Estill County, Kentucky	[DOC] = 1.946 * exp[SR*(1.422)]	0.587	0.004
03283370	Powell County, Kentucky	[DOC] = 1.72 * exp[SR*(2.041)]	0.578	0.011
03353551	Marion County, Indiana	[DOC] = 4.487 * exp[SR*(0.344)]	0.305	0.019
03353600	Marion County, Indiana	[DOC] = 4 * exp[SR*(0.472)]	0.348	0.001
03353637	Marion County, Indiana	[DOC] = 2.886 * exp[SR*(0.569)]	0.484	0.000
03373530	Orange County, Indiana	[DOC] = 1.802 * exp[SR*(2.197)]	0.696	0.000
03448800	Buncombe County, North Carolina	[DOC] = 1.1 * exp[SR*(1.947)]	0.595	0.015
04087030	Waukesha County, Wisconsin	[DOC] = 6.476 * exp[SR*(0.6)]	0.205	0.045
05014300	Glacier County, Montana	[DOC] = 0.738 * exp[SR*(0.581)]	0.162	0.000
05288705	Hennepin County, Minnesota	[DOC] = 7.146 * exp[SR*(-0.389)]	0.159	0.001
05451080	Hamilton County, Iowa	[DOC] = 3.88 * exp[SR*(0.727)]	0.488	0.000
06061900	Jefferson County, Montana	[DOC] = 2.284 * exp[SR*(0.679)]	0.510	0.043
06340540	Mercer County, North Dakota	[DOC] = 9.413 * exp[SR*(0.746)]	0.537	0.023
06929315	Texas County, Missouri	[DOC] = 1.084 * exp[SR*(0.749)]	0.121	0.034
07083000	Lake County, Colorado	[DOC] = 0.738 * exp[SR*(1.468)]	0.200	0.000
07248620	Le Flore County, Oklahoma	[DOC] = 2.108 * exp[SR*(1.207)]	0.498	0.004
07362587	Saline County, Arkansas	[DOC] = 1.107 * exp[SR*(1.883)]	0.570	0.000
10167499	Salt Lake County, Utah	[DOC] = 4.458 * exp[SR*(-1.061)]	0.937	0.004
10167800	Salt Lake County, Utah	[DOC] = 1.387 * exp[SR*(1.362)]	0.532	0.002
10336778	El Dorado County, California	[DOC] = 1.036 * exp[SR*(2.481)]	0.484	0.050
12103380	King County, Washington	[DOC] = 0.659 * exp[SR*(1.607)]	0.617	0.000
12108500	King County, Washington	[DOC] = 2.817 * exp[SR*(1.624)]	0.308	0.000
12128000	King County, Washington	[DOC] = 3.082 * exp[SR*(0.699)]	0.291	0.000
12416000	Kootenai County, Idaho	[DOC] = 2.898 * exp[SR*(2.782)]	0.769	0.003
14161500	Lane County, Oregon	[DOC] = 0.725 * exp[SR*(1.101)]	0.453	0.000
14201300	Marion County, Oregon	[DOC] = 3.267 * exp[SR*(0.422)]	0.128	0.011
14203750	Washington County, Oregon	[DOC] = 0.53 * exp[SR*(1.175)]	0.391	0.002
14205400	Washington County, Oregon	[DOC] = 1.022 * exp[SR*(0.889)]	0.208	0.003
14206950	Washington County, Oregon	[DOC] = 3.586 * exp[SR*(0.471)]	0.177	0.001
14211500	Multnomah County, Oregon	[DOC] = 0.474 * exp[SR*(2.63)]	0.714	0.021
01097480	Middlesex County, Massachusetts	[DOC] = 4.494 * exp[SR*(0.565)]	0.237	0.074
01102345	Essex County, Massachusetts	[DOC] = 6.975 * exp[SR*(-0.028)]	-0.029	0.843
01102500	Middlesex County, Massachusetts	[DOC] = 4.542 * exp[SR*(0.052)]	-0.010	0.651
01104460	Middlesex County, Massachusetts	[DOC] = 4.292 * exp[SR*(0.201)]	0.445	0.089
01105000	Norfolk County, Massachusetts	[DOC] = 6.778 * exp[SR*(-0.055)]	-0.028	0.740
01172800	Worcester County, Massachusetts	[DOC] = 10.516 * exp[SR*(0.019)]	-0.083	0.954
01174050	Worcester County, Massachusetts	[DOC] = 5.626 * exp[SR*(0.042)]	-0.017	0.732
01174575	Franklin County, Massachusetts	[DOC] = 3.261 * exp[SR*(0.022)]	-0.047	0.936
01208873	Fairfield County, Connecticut	[DOC] = 2.183 * exp[SR*(0.354)]	0.044	0.139
01304000	Suffolk County, New York	[DOC] = 2.036 * exp[SR*(1.506)]	-0.033	0.470
01356190	Schenectady County, New York	[DOC] = 4.751 * exp[SR*(0.139)]	-0.003	0.351
01367800	Sussex County, New Jersey	[DOC] = 3.28 * exp[SR*(0.264)]	-0.026	0.505

01372051	Dutchess County, New York	[DOC] = 4.088 * exp[SR*(0.115)]	-0.041	0.657
01376500	Westchester County, New York	[DOC] = 3.545 * exp[SR*(0.5)]	0.033	0.268
01377500	Bergen County, New Jersey	[DOC] = 3.632 * exp[SR*(-0.202)]	-0.168	0.725
01393450	Union County, New Jersey	[DOC] = 4.321 * exp[SR*(-0.119)]	-0.029	0.663
01399500	Morris County, New Jersey	[DOC] = 4.011 * exp[SR*(0.072)]	-0.032	0.819
01399700	Hunterdon County, New Jersey	[DOC] = 2.316 * exp[SR*(0.88)]	0.086	0.060
01403400	Somerset County, New Jersey	[DOC] = 2.631 * exp[SR*(0.84)]	-0.078	0.461
01407760	Monmouth County, New Jersey	[DOC] = 3.21 * exp[SR*(0.346)]	0.023	0.198
01410150	Burlington County, New Jersey	[DOC] = 4.078 * exp[SR*(-0.255)]	-0.008	0.546
01410787	Camden County, New Jersey	[DOC] = 6.388 * exp[SR*(-0.206)]	-0.079	0.576
01410820	Camden County, New Jersey	[DOC] = 7.585 * exp[SR*(0.938)]	-0.036	0.545
01411300	Cape May County, New Jersey	[DOC] = 3.677 * exp[SR*(2.064)]	0.029	0.314
01463620	Mercer County, New Jersey	[DOC] = 4.009 * exp[SR*(0.287)]	0.050	0.152
01466500	Burlington County, New Jersey	[DOC] = 11.303 * exp[SR*(-0.088)]	0.004	0.207
01467021	Burlington County, New Jersey	[DOC] = 7.943 * exp[SR*(0.01)]	-0.042	0.967
01467081	Burlington County, New Jersey	[DOC] = 4.527 * exp[SR*(0.105)]	-0.016	0.468
01467150	Camden County, New Jersey	[DOC] = 3.55 * exp[SR*(0.134)]	0.007	0.186
01478137	Chester County, Pennsylvania	[DOC] = 17.963 * exp[SR*(0.052)]	-0.046	0.776
01479820	Chester County, Pennsylvania	[DOC] = 2.396 * exp[SR*(1.444)]	0.232	0.234
014806318	Chester County, Pennsylvania	[DOC] = 4.158 * exp[SR*(0.768)]	0.008	0.283
01482500	Salem County, New Jersey	[DOC] = 6.539 * exp[SR*(0.012)]	-0.040	0.957
01559795	Bedford County, Pennsylvania	[DOC] = 1.674 * exp[SR*(-0.275)]	-0.078	0.725
01573095	Lebanon County, Pennsylvania	[DOC] = 1.291 * exp[SR*(-0.341)]	-0.030	0.559
01576771	Lancaster County, Pennsylvania	[DOC] = 5.75 * exp[SR*(0.582)]	0.032	0.127
01673638	King William County, Virginia	[DOC] = 5.75 * exp[SR*(0.166)]	-0.184	0.661
02082731	Franklin County, North Carolina	[DOC] = 5.106 * exp[SR*(0.051)]	-0.028	0.651
02084164	Pitt County, North Carolina	[DOC] = 5.395 * exp[SR*(0.596)]	0.123	0.056
02084540	Beaufort County, North Carolina	[DOC] = 26.934 * exp[SR*(-0.678)]	0.065	0.269
02086849	Durham County, North Carolina	[DOC] = 14.224 * exp[SR*(-0.507)]	-0.051	0.436
0209096970	Wayne County, North Carolina	[DOC] = 8.607 * exp[SR*(-0.108)]	-0.170	0.629
0209173190	Greene County, North Carolina	[DOC] = 5.18 * exp[SR*(0.689)]	0.042	0.313
0209173200	Greene County, North Carolina	[DOC] = 15.05 * exp[SR*(0.004)]	-0.059	0.972
02091970	Craven County, North Carolina	[DOC] = 18.741 * exp[SR*(-0.188)]	-0.213	0.743
0209741955	Durham County, North Carolina	[DOC] = 7.082 * exp[SR*(0.606)]	0.276	0.210
02123567	Montgomery County, North Carolina	[DOC] = 2.991 * exp[SR*(1.661)]	0.323	0.186
02172305	Aiken County, South Carolina	[DOC] = 4.999 * exp[SR*(0.66)]	0.013	0.189
02300700	Hillsborough County, Florida	[DOC] = 11.36 * exp[SR*(0.116)]	-0.020	0.605
02306774	Hillsborough County, Florida	[DOC] = 17.925 * exp[SR*(0.212)]	0.031	0.232
02314274	Charlton County, Georgia	[DOC] = 53.146 * exp[SR*(-0.407)]	0.438	0.091
02315392	Columbia County, Florida	[DOC] = 45.283 * exp[SR*(-0.369)]	0.323	0.082
02336635	Cobb County, Georgia	[DOC] = 1.619 * exp[SR*(1.411)]	0.480	0.077
02358685	Liberty County, Florida	[DOC] = 3.645 * exp[SR*(0.504)]	-0.042	0.459
03039925	Somerset County, Pennsylvania	[DOC] = 0.973 * exp[SR*(-0.16)]	-0.005	0.413
03144270	Coshocton County, Ohio	[DOC] = 4.169 * exp[SR*(0.512)]	0.072	0.164
03144289	Coshocton County, Ohio	[DOC] = 4.412 * exp[SR*(0.301)]	0.036	0.239
03201600	Vinton County, Ohio	[DOC] = 4.653 * exp[SR*(-0.168)]	-0.316	0.857
03201700	Vinton County, Ohio	[DOC] = 1.787 * exp[SR*(0.313)]	-0.127	0.663
03207965	Pike County, Kentucky	[DOC] = 3.858 * exp[SR*(-0.513)]	-0.022	0.407

03282075	Lee County, Kentucky	[DOC] = 2.808 * exp[SR*(0.424)]	0.092	0.119
03361638	Hancock County, Indiana	[DOC] = 7.86 * exp[SR*(-0.336)]	0.023	0.181
03450000	Buncombe County, North Carolina	[DOC] = 1.728 * exp[SR*(0.489)]	-0.015	0.383
04026349	Bayfield County, Wisconsin	[DOC] = 3.998 * exp[SR*(2.01)]	0.080	0.330
04071795	Shawano County, Wisconsin	[DOC] = 14.573 * exp[SR*(-0.353)]	0.071	0.122
04086175	Sheboygan County, Wisconsin	[DOC] = 13.678 * exp[SR*(-0.175)]	0.000	0.343
04087088	Milwaukee County, Wisconsin	[DOC] = 4.738 * exp[SR*(0.512)]	0.178	0.096
04087159	Milwaukee County, Wisconsin	[DOC] = 6.266 * exp[SR*(0.015)]	-0.100	0.983
04087204	Milwaukee County, Wisconsin	[DOC] = 6.725 * exp[SR*(0.028)]	-0.017	0.784
04087214	Milwaukee County, Wisconsin	[DOC] = 6.324 * exp[SR*(0.094)]	-0.095	0.555
05288470	Anoka County, Minnesota	[DOC] = 19.484 * exp[SR*(0.012)]	-0.250	0.973
05357225	Vilas County, Wisconsin	[DOC] = 5.48 * exp[SR*(0.394)]	0.035	0.077
05427948	Dane County, Wisconsin	[DOC] = 7.923 * exp[SR*(0.485)]	0.035	0.339
05487550	Jasper County, Iowa	[DOC] = 3.998 * exp[SR*(0.949)]	0.105	0.312
05540275	Du Page County, Illinois	[DOC] = 4.801 * exp[SR*(0.12)]	0.023	0.183
05595226	St Clair County, Illinois	[DOC] = 5.276 * exp[SR*(0.925)]	0.474	0.121
06058900	Jefferson County, Montana	[DOC] = 2.773 * exp[SR*(0.802)]	-0.069	0.487
06187915	Park County, Montana	[DOC] = 1.033 * exp[SR*(-0.084)]	-0.024	0.653
06279790	Park County, Wyoming	[DOC] = 4.368 * exp[SR*(0.569)]	-0.074	0.747
06279795	Park County, Wyoming	[DOC] = 1.681 * exp[SR*(2.238)]	0.231	0.055
06339560	Mercer County, North Dakota	[DOC] = 11.265 * exp[SR*(0.496)]	0.218	0.071
06340580	Mercer County, North Dakota	[DOC] = 16.281 * exp[SR*(-0.099)]	-0.233	0.824
06340780	Mercer County, North Dakota	[DOC] = 25.135 * exp[SR*(-0.445)]	0.241	0.085
06342040	Oliver County, North Dakota	[DOC] = 14.232 * exp[SR*(0.357)]	-0.198	0.699
06355310	Bowman County, North Dakota	[DOC] = 16.598 * exp[SR*(0.289)]	0.114	0.109
06611800	Jackson County, Colorado	[DOC] = 6.629 * exp[SR*(-0.304)]	-0.011	0.390
06714400	Clear Creek County, Colorado	[DOC] = 1.61 * exp[SR*(3.398)]	-0.027	0.401
06720415	Adams County, Colorado	[DOC] = 11.106 * exp[SR*(0.229)]	-0.025	0.516
06879650	Riley County, Kansas	[DOC] = 1.903 * exp[SR*(0.784)]	-0.041	0.427
07031692	Shelby County, Tennessee	[DOC] = 5.955 * exp[SR*(0.131)]	0.034	0.125
07232024	Pittsburg County, Oklahoma	[DOC] = 11.053 * exp[SR*(0.285)]	0.150	0.117
07246615	Le Flore County, Oklahoma	[DOC] = 8.644 * exp[SR*(-0.444)]	-0.069	0.603
07247550	Latimer County, Oklahoma	[DOC] = 6.864 * exp[SR*(0.508)]	0.158	0.139
072632962	Pulaski County, Arkansas	[DOC] = 2.439 * exp[SR*(0.829)]	-0.096	0.734
072632971	Pulaski County, Arkansas	[DOC] = 4.213 * exp[SR*(0.479)]	-0.033	0.429
07381590	St. Mary Parish, Louisiana	[DOC] = 4.805 * exp[SR*(-0.193)]	-0.014	0.517
09046530	Summit County, Colorado	[DOC] = 0.58 * exp[SR*(0.244)]	0.016	0.172
09153290	Mesa County, Colorado	[DOC] = 4.288 * exp[SR*(-0.078)]	-0.014	0.602
09243700	Routt County, Colorado	[DOC] = 6.082 * exp[SR*(0.268)]	-0.154	0.596
09250600	Moffat County, Colorado	[DOC] = 5.958 * exp[SR*(0.841)]	0.416	0.070
09306242	Rio Blanco County, Colorado	[DOC] = 8.067 * exp[SR*(0.013)]	-0.029	0.949
09310600	Carbon County, Utah	[DOC] = 3.999 * exp[SR*(-0.507)]	-0.119	0.632
09310700	Carbon County, Utah	[DOC] = 4.483 * exp[SR*(-0.21)]	-0.061	0.775
09313975	Carbon County, Utah	[DOC] = 3.834 * exp[SR*(-0.565)]	-0.117	0.821
09317919	Emery County, Utah	[DOC] = 2.514 * exp[SR*(0.745)]	0.008	0.343
09367685	San Juan County, New Mexico	[DOC] = 5.325 * exp[SR*(0.409)]	-0.015	0.391
10170250	Salt Lake County, Utah	[DOC] = 8.709 * exp[SR*(0.046)]	-0.071	0.957
10172000	Salt Lake County, Utah	[DOC] = 5.944 * exp[SR*(1.04)]	-0.006	0.381

10244950	White Pine County, Nevada	[DOC] = 1.653 * exp[SR*(1.206)]	0.109	0.115
10249300	Nye County, Nevada	[DOC] = 2.298 * exp[SR*(0.485)]	0.172	0.062
10249900	Esmeralda County, Nevada	[DOC] = 2.344 * exp[SR*(0.934)]	0.003	0.327
10254970	Imperial County, California	[DOC] = 3.731 * exp[SR*(4.41)]	0.201	0.174
10336626	El Dorado County, California	[DOC] = 1.406 * exp[SR*(0.878)]	-0.180	0.783
10343500	Nevada County, California	[DOC] = 1.658 * exp[SR*(-0.138)]	0.002	0.243
11262900	Merced County, California	[DOC] = 10.215 * exp[SR*(-0.236)]	-0.033	0.597
11447360	Sacramento County, California	[DOC] = 7.514 * exp[SR*(0.17)]	-0.019	0.414
11482468	Humboldt County, California	[DOC] = 2.945 * exp[SR*(0.36)]	-0.034	0.487
11532620	Del Norte County, California	[DOC] = 2.067 * exp[SR*(0.58)]	0.000	0.334
12185300	Snohomish County, Washington	[DOC] = 0.731 * exp[SR*(0.196)]	-0.001	0.342
14222980	Cowlitz County, Washington	[DOC] = 2.435 * exp[SR*(-3.319)]	0.091	0.120

Table A.4. Table showing the regression equations, R^2 , and p -value for specific ultraviolet absorbance at 254nm (SUVA₂₅₄) vs. discharge (Q) in individual basins.

USGS Station	Location	Regression equation	R^2	p
01377500	Bergen County, New Jersey	SUVA = 1.017*ln(Q) + 3.003	0.544	0.036
01394500	Union County, New Jersey	SUVA = 0.253*ln(Q) + 3.148	0.231	0.000
01398000	Hunterdon County, New Jersey	SUVA = 0.072*ln(Q) + 2.956	0.061	0.050
01467150	Camden County, New Jersey	SUVA = 0.998*ln(Q) + 4.573	0.377	0.000
03361638	Hancock County, Indiana	SUVA = 0.211*ln(Q) + 2.941	0.206	0.002
05451080	Hamilton County, Iowa	SUVA = 0.201*ln(Q) + 2.874	0.511	0.000
01367800	Sussex County, New Jersey	SUVA = 0.076*ln(Q) + 3.727	0.014	0.265
01407760	Monmouth County, New Jersey	SUVA = -0.007*ln(Q) + 3.97	-0.030	0.967
01410150	Burlington County, New Jersey	SUVA = -0.076*ln(Q) + 4.85	-0.017	0.632
01411300	Cape May County, New Jersey	SUVA = -0.302*ln(Q) + 4.672	-0.084	0.525
01412800	Cumberland County, New Jersey	SUVA = 0.024*ln(Q) + 3.631	-0.045	0.916
01466500	Burlington County, New Jersey	SUVA = 0.062*ln(Q) + 4.44	-0.020	0.767
01482500	Salem County, New Jersey	SUVA = 0.119*ln(Q) + 3.578	0.021	0.222
01493500	Kent County, Maryland	SUVA = 0.038*ln(Q) + 2.911	-0.013	0.412
02172300	Aiken County, South Carolina	SUVA = -0.066*ln(Q) + 3.917	-0.231	0.818
02172305	Aiken County, South Carolina	SUVA = -0.153*ln(Q) + 3.897	0.000	0.322
04087204	Milwaukee County, Wisconsin	SUVA = 0.111*ln(Q) + 3.166	0.060	0.059
14161500	Lane County, Oregon	SUVA = 0.158*ln(Q) + 2.722	0.012	0.207
14205400	Washington County, Oregon	SUVA = 0.03*ln(Q) + 3.554	-0.132	0.806

Table A.5. Table showing the regression equations, R^2 , and p -value for specific ultraviolet absorbance at 254nm ($SUVA_{254}$) vs. antecedent gross primary production (GPP_{32}) in individual basins.

USGS Station	Location	Regression equation	R^2	p
01367625	Sussex County, New Jersey	$SUVA = 0.073 \ln(GPP_{32}) + 2.033$	0.114	0.023
01367800	Sussex County, New Jersey	$SUVA = 0.068 \ln(GPP_{32}) + 3.305$	0.110	0.025
01367880	Sussex County, New Jersey	$SUVA = 0.208 \ln(GPP_{32}) + 2.705$	0.459	0.039
01380100	Morris County, New Jersey	$SUVA = 0.206 \ln(GPP_{32}) + 2.789$	0.260	0.001
01381498	Morris County, New Jersey	$SUVA = 0.163 \ln(GPP_{32}) + 2.347$	0.419	0.049
01399200	Morris County, New Jersey	$SUVA = 0.31 \ln(GPP_{32}) + 2.559$	0.651	0.010
01400808	Mercer County, New Jersey	$SUVA = 0.211 \ln(GPP_{32}) + 3.398$	0.296	0.017
01400823	Middlesex County, New Jersey	$SUVA = 0.361 \ln(GPP_{32}) + 3.035$	0.424	0.048
01405340	Middlesex County, New Jersey	$SUVA = 0.394 \ln(GPP_{32}) + 2.072$	0.200	0.004
01408100	Ocean County, New Jersey	$SUVA = 0.229 \ln(GPP_{32}) + 3.457$	0.196	0.004
01408152	Ocean County, New Jersey	$SUVA = 0.552 \ln(GPP_{32}) + 2.002$	0.593	0.015
01409387	Burlington County, New Jersey	$SUVA = 0.252 \ln(GPP_{32}) + 3.543$	0.116	0.034
01409416	Atlantic County, New Jersey	$SUVA = 0.221 \ln(GPP_{32}) + 3.14$	0.210	0.003
01410150	Burlington County, New Jersey	$SUVA = 0.19 \ln(GPP_{32}) + 3.884$	0.180	0.005
01411196	Atlantic County, New Jersey	$SUVA = 0.302 \ln(GPP_{32}) + 3.132$	0.334	0.000
01411440	Cape May County, New Jersey	$SUVA = 0.675 \ln(GPP_{32}) + 0.919$	0.683	0.007
01411444	Cumberland County, New Jersey	$SUVA = 0.255 \ln(GPP_{32}) + 3.167$	0.136	0.015
01411955	Cumberland County, New Jersey	$SUVA = 0.284 \ln(GPP_{32}) + 3.127$	0.262	0.001
01463810	Mercer County, New Jersey	$SUVA = 0.379 \ln(GPP_{32}) + 1.597$	0.711	0.005
01464460	Monmouth County, New Jersey	$SUVA = 0.414 \ln(GPP_{32}) + 2.456$	0.299	0.020
01464515	Monmouth County, New Jersey	$SUVA = 0.302 \ln(GPP_{32}) + 2.13$	0.275	0.001
01465893	Burlington County, New Jersey	$SUVA = 0.178 \ln(GPP_{32}) + 3.968$	0.104	0.040
01467150	Camden County, New Jersey	$SUVA = -0.309 \ln(GPP_{32}) + 5.264$	0.120	0.026
01476625	Gloucester County, New Jersey	$SUVA = 0.42 \ln(GPP_{32}) + 2.376$	0.485	0.033
01477110	Gloucester County, New Jersey	$SUVA = 0.403 \ln(GPP_{32}) + 2.452$	0.457	0.039
02172300	Aiken County, South Carolina	$SUVA = 1.188 \ln(GPP_{32}) + -2.168$	0.697	0.024
02172305	Aiken County, South Carolina	$SUVA = 0.406 \ln(GPP_{32}) + 1.882$	0.084	0.035
03361638	Hancock County, Indiana	$SUVA = 0.472 \ln(GPP_{32}) + 0.361$	0.234	0.001
04087204	Milwaukee County, Wisconsin	$SUVA = 0.19 \ln(GPP_{32}) + 2.311$	0.413	0.000
05451080	Hamilton County, Iowa	$SUVA = 0.107 \ln(GPP_{32}) + 2.288$	0.119	0.001
07288636	Bolivar County, Mississippi	$SUVA = 0.181 \ln(GPP_{32}) + 1.685$	0.128	0.002
3344280813547	Aiken County, South Carolina	$SUVA = 1.103 \ln(GPP_{32}) + -1.763$	0.757	0.015
01311990	Hamilton County, New York	$SUVA = 0.095 \ln(GPP_{32}) + 3.267$	0.303	0.091
0131199010	Hamilton County, New York	$SUVA = 0.033 \ln(GPP_{32}) + 4.182$	0.052	0.147
0131199022	Hamilton County, New York	$SUVA = 0.028 \ln(GPP_{32}) + 3.894$	-0.153	0.802
0131199040	Hamilton County, New York	$SUVA = 0.085 \ln(GPP_{32}) + 3.427$	0.297	0.152
0131199050	Essex County, New York	$SUVA = 0.016 \ln(GPP_{32}) + 3.718$	-0.005	0.370
01367780	Sussex County, New Jersey	$SUVA = 0.082 \ln(GPP_{32}) + 2.81$	-0.011	0.373
01367902	Sussex County, New Jersey	$SUVA = 0.043 \ln(GPP_{32}) + 3.428$	0.012	0.337
01368825	Sussex County, New Jersey	$SUVA = 0.207 \ln(GPP_{32}) + 3.875$	0.130	0.203
01378387	Bergen County, New Jersey	$SUVA = -0.06 \ln(GPP_{32}) + 3.219$	-0.022	0.393
01378583	Bergen County, New Jersey	$SUVA = 0.104 \ln(GPP_{32}) + 2.342$	-0.056	0.458

01378660	Morris County, New Jersey	$SUVA = 0.125 \cdot \ln(GPP32) + 2.904$	-0.001	0.358
01379200	Somerset County, New Jersey	$SUVA = -0.045 \cdot \ln(GPP32) + 3.296$	-0.005	0.368
01379870	Morris County, New Jersey	$SUVA = 0.138 \cdot \ln(GPP32) + 3.35$	0.355	0.070
01380098	Morris County, New Jersey	$SUVA = 0.224 \cdot \ln(GPP32) + 2.479$	-0.018	0.385
01381260	Morris County, New Jersey	$SUVA = 0.14 \cdot \ln(GPP32) + 2.324$	-0.013	0.378
01381330	Morris County, New Jersey	$SUVA = 0.098 \cdot \ln(GPP32) + 2.795$	-0.057	0.460
01382960	Passaic County, New Jersey	$SUVA = 0.158 \cdot \ln(GPP32) + 2.473$	0.415	0.050
01388720	Morris County, New Jersey	$SUVA = -0.038 \cdot \ln(GPP32) + 4.92$	-0.011	0.435
01390800	Bergen County, New Jersey	$SUVA = 0.024 \cdot \ln(GPP32) + 3.539$	-0.135	0.697
01393960	Essex County, New Jersey	$SUVA = 0.085 \cdot \ln(GPP32) + 2.3$	0.024	0.320
01394200	Union County, New Jersey	$SUVA = 0.023 \cdot \ln(GPP32) + 2.964$	-0.139	0.718
01394500	Union County, New Jersey	$SUVA = -0.005 \cdot \ln(GPP32) + 3.03$	-0.028	0.907
01396588	Hunterdon County, New Jersey	$SUVA = 0.023 \cdot \ln(GPP32) + 3.096$	-0.018	0.465
01396900	Hunterdon County, New Jersey	$SUVA = 0.151 \cdot \ln(GPP32) + 2.221$	0.262	0.111
01397950	Hunterdon County, New Jersey	$SUVA = 0.031 \cdot \ln(GPP32) + 2.859$	-0.108	0.593
01398000	Hunterdon County, New Jersey	$SUVA = -0.086 \cdot \ln(GPP32) + 3.278$	0.033	0.141
01398060	Hunterdon County, New Jersey	$SUVA = 0.063 \cdot \ln(GPP32) + 2.377$	-0.033	0.412
01398090	Somerset County, New Jersey	$SUVA = 0.008 \cdot \ln(GPP32) + 2.655$	-0.159	0.846
01399295	Morris County, New Jersey	$SUVA = -0.01 \cdot \ln(GPP32) + 4.109$	-0.166	0.963
01399520	Somerset County, New Jersey	$SUVA = -0.079 \cdot \ln(GPP32) + 3.486$	-0.120	0.635
01399820	Somerset County, New Jersey	$SUVA = 0.06 \cdot \ln(GPP32) + 3.225$	-0.157	0.832
01400530	Monmouth County, New Jersey	$SUVA = 0.17 \cdot \ln(GPP32) + 4.164$	-0.270	0.724
01400560	Middlesex County, New Jersey	$SUVA = 0.09 \cdot \ln(GPP32) + 3.962$	0.314	0.111
01400860	Mercer County, New Jersey	$SUVA = -0.103 \cdot \ln(GPP32) + 4.304$	-0.013	0.394
01401400	Middlesex County, New Jersey	$SUVA = 0.127 \cdot \ln(GPP32) + 3.214$	0.074	0.052
01401520	Mercer County, New Jersey	$SUVA = 0.007 \cdot \ln(GPP32) + 2.891$	-0.166	0.949
01401560	Somerset County, New Jersey	$SUVA = 0.041 \cdot \ln(GPP32) + 3.463$	-0.130	0.675
01401700	Somerset County, New Jersey	$SUVA = -0.207 \cdot \ln(GPP32) + 4.331$	0.031	0.310
01403171	Somerset County, New Jersey	$SUVA = -0.098 \cdot \ln(GPP32) + 3.662$	-0.056	0.446
01403190	Somerset County, New Jersey	$SUVA = -0.022 \cdot \ln(GPP32) + 3.57$	-0.164	0.911
01403575	Somerset County, New Jersey	$SUVA = 0.01 \cdot \ln(GPP32) + 2.86$	-0.166	0.947
01404400	Middlesex County, New Jersey	$SUVA = -0.035 \cdot \ln(GPP32) + 4.128$	-0.158	0.837
01405003	Middlesex County, New Jersey	$SUVA = -0.041 \cdot \ln(GPP32) + 4.434$	-0.100	0.570
01405180	Monmouth County, New Jersey	$SUVA = 0.124 \cdot \ln(GPP32) + 2.659$	-0.081	0.517
01407210	Monmouth County, New Jersey	$SUVA = -0.065 \cdot \ln(GPP32) + 3.65$	-0.124	0.648
01407253	Monmouth County, New Jersey	$SUVA = 0.045 \cdot \ln(GPP32) + 2.888$	-0.155	0.817
01407520	Monmouth County, New Jersey	$SUVA = 0.215 \cdot \ln(GPP32) + 3.533$	0.220	0.136
01407538	Monmouth County, New Jersey	$SUVA = -0.072 \cdot \ln(GPP32) + 5.413$	-0.189	0.841
01407760	Monmouth County, New Jersey	$SUVA = 0.171 \cdot \ln(GPP32) + 3.151$	0.036	0.142
01407900	Monmouth County, New Jersey	$SUVA = 0.07 \cdot \ln(GPP32) + 2.946$	-0.155	0.815
01408009	Monmouth County, New Jersey	$SUVA = 0.305 \cdot \ln(GPP32) + 2.998$	0.233	0.054
01408110	Monmouth County, New Jersey	$SUVA = 0.039 \cdot \ln(GPP32) + 4.34$	0.020	0.326
01408290	Ocean County, New Jersey	$SUVA = 0.065 \cdot \ln(GPP32) + 4.587$	-0.201	0.707
01408460	Ocean County, New Jersey	$SUVA = -0.047 \cdot \ln(GPP32) + 5.298$	-0.070	0.782
01408598	Ocean County, New Jersey	$SUVA = -0.24 \cdot \ln(GPP32) + 6.207$	-0.050	0.471
01408830	Ocean County, New Jersey	$SUVA = -0.154 \cdot \ln(GPP32) + 5.578$	0.020	0.201
01409030	Ocean County, New Jersey	$SUVA = -0.016 \cdot \ln(GPP32) + 4.475$	-0.162	0.888
0140940200	Camden County, New Jersey	$SUVA = 0.234 \cdot \ln(GPP32) + 3.652$	0.071	0.261

0140940950	Camden County, New Jersey	SUVA = 0*ln(GPP32) + 5	-0.038	0.999
0140941070	Atlantic County, New Jersey	SUVA = 0.111*ln(GPP32) + 2.995	-0.144	0.743
0140941075	Atlantic County, New Jersey	SUVA = 0.232*ln(GPP32) + 2.506	0.406	0.053
01409435	Burlington County, New Jersey	SUVA = 0.506*ln(GPP32) + 1.772	0.141	0.193
01409600	Atlantic County, New Jersey	SUVA = 0.199*ln(GPP32) + 3.468	-0.166	0.620
01409601	Atlantic County, New Jersey	SUVA = 0.193*ln(GPP32) + 3.295	0.218	0.137
01409930	Burlington County, New Jersey	SUVA = -0.035*ln(GPP32) + 4.858	-0.162	0.880
01410455	Atlantic County, New Jersey	SUVA = -0.057*ln(GPP32) + 4.05	-0.126	0.659
01410810	Camden County, New Jersey	SUVA = 0.002*ln(GPP32) + 4.747	-0.200	0.984
01410820	Camden County, New Jersey	SUVA = 1.726*ln(GPP32) + -6.449	-0.215	0.626
01411035	Gloucester County, New Jersey	SUVA = 0.02*ln(GPP32) + 4.852	-0.043	0.837
01411208	Atlantic County, New Jersey	SUVA = 0.264*ln(GPP32) + 3.502	0.073	0.260
01411290	Atlantic County, New Jersey	SUVA = -0.189*ln(GPP32) + 5.011	0.132	0.200
01411295	Atlantic County, New Jersey	SUVA = 0.123*ln(GPP32) + 4.291	0.019	0.328
01411300	Cape May County, New Jersey	SUVA = 0.162*ln(GPP32) + 3.919	-0.074	0.500
01411400	Cape May County, New Jersey	SUVA = 0.07*ln(GPP32) + 4.272	-0.015	0.503
01411427	Cape May County, New Jersey	SUVA = -0.073*ln(GPP32) + 3.969	-0.087	0.736
01411452	Gloucester County, New Jersey	SUVA = 0.307*ln(GPP32) + 2.897	0.126	0.206
01411457	Gloucester County, New Jersey	SUVA = 0.21*ln(GPP32) + 3.492	0.004	0.369
01411458	Gloucester County, New Jersey	SUVA = -0.444*ln(GPP32) + 6.095	-0.145	0.533
01411466	Gloucester County, New Jersey	SUVA = 0.046*ln(GPP32) + 4.835	-0.025	0.542
01411487	Salem County, New Jersey	SUVA = 0.094*ln(GPP32) + 4.263	-0.103	0.579
01411495	Cumberland County, New Jersey	SUVA = 0.084*ln(GPP32) + 4.22	-0.135	0.695
01412005	Cumberland County, New Jersey	SUVA = -0.017*ln(GPP32) + 4.343	-0.164	0.915
01412800	Cumberland County, New Jersey	SUVA = 0.126*ln(GPP32) + 3.071	0.052	0.094
01413013	Cumberland County, New Jersey	SUVA = -0.154*ln(GPP32) + 4	-0.120	0.576
01440097	Warren County, New Jersey	SUVA = 0.117*ln(GPP32) + 2.26	-0.001	0.357
01443250	Sussex County, New Jersey	SUVA = -0.005*ln(GPP32) + 3.322	-0.166	0.954
01444990	Sussex County, New Jersey	SUVA = -0.046*ln(GPP32) + 3.34	-0.046	0.437
01445160	Warren County, New Jersey	SUVA = -0.053*ln(GPP32) + 2.987	-0.004	0.357
01445900	Warren County, New Jersey	SUVA = 0.078*ln(GPP32) + 2.957	-0.013	0.377
01455240	Warren County, New Jersey	SUVA = -0.191*ln(GPP32) + 2.622	0.116	0.215
01455700	Sussex County, New Jersey	SUVA = 0.057*ln(GPP32) + 2.44	-0.084	0.524
01458300	Hunterdon County, New Jersey	SUVA = 0.086*ln(GPP32) + 3.029	0.032	0.310
01458570	Hunterdon County, New Jersey	SUVA = 0.02*ln(GPP32) + 2.941	-0.025	0.740
01458710	Hunterdon County, New Jersey	SUVA = 0.059*ln(GPP32) + 2.442	0.020	0.308
01460860	Hunterdon County, New Jersey	SUVA = 0.078*ln(GPP32) + 3.149	0.006	0.346
01460870	Hunterdon County, New Jersey	SUVA = 0.159*ln(GPP32) + 2.921	-0.061	0.469
01461250	Hunterdon County, New Jersey	SUVA = 0.243*ln(GPP32) + 2.793	-0.055	0.456
01461282	Hunterdon County, New Jersey	SUVA = -0.01*ln(GPP32) + 3.475	-0.166	0.955
01462800	Mercer County, New Jersey	SUVA = 0.076*ln(GPP32) + 2.487	0.003	0.351
01463610	Mercer County, New Jersey	SUVA = 0.284*ln(GPP32) + 2.692	0.033	0.308
01463661	Mercer County, New Jersey	SUVA = -0.116*ln(GPP32) + 4.612	-0.102	0.575
01463850	Mercer County, New Jersey	SUVA = 0.121*ln(GPP32) + 3.663	0.033	0.150
01464280	Burlington County, New Jersey	SUVA = 0.058*ln(GPP32) + 2.977	-0.188	0.832
01464380	Burlington County, New Jersey	SUVA = -0.004*ln(GPP32) + 3.855	-0.167	0.984
01464527	Burlington County, New Jersey	SUVA = -0.14*ln(GPP32) + 5.302	0.041	0.142
01464532	Burlington County, New Jersey	SUVA = 0.235*ln(GPP32) + 2.909	0.183	0.186

01465808	Burlington County, New Jersey	$SUVA = 0.392 \cdot \ln(GPP32) + 3.042$	0.404	0.074
01465857	Burlington County, New Jersey	$SUVA = -0.177 \cdot \ln(GPP32) + 4.329$	0.058	0.276
01465950	Burlington County, New Jersey	$SUVA = 0.338 \cdot \ln(GPP32) + 2.372$	-0.126	0.511
01465965	Burlington County, New Jersey	$SUVA = 0.249 \cdot \ln(GPP32) + 3.778$	0.388	0.059
01466100	Burlington County, New Jersey	$SUVA = 0.261 \cdot \ln(GPP32) + 2.878$	-0.025	0.398
01466500	Burlington County, New Jersey	$SUVA = 0.184 \cdot \ln(GPP32) + 3.292$	0.060	0.078
01467066	Burlington County, New Jersey	$SUVA = -0.346 \cdot \ln(GPP32) + 5.188$	0.223	0.160
01467325	Gloucester County, New Jersey	$SUVA = -0.041 \cdot \ln(GPP32) + 4.041$	-0.128	0.668
01467359	Camden County, New Jersey	$SUVA = 0.076 \cdot \ln(GPP32) + 4.72$	0.001	0.321
01475042	Gloucester County, New Jersey	$SUVA = 0.067 \cdot \ln(GPP32) + 4.043$	-0.038	0.422
01475090	Gloucester County, New Jersey	$SUVA = 0.034 \cdot \ln(GPP32) + 3.375$	-0.159	0.847
01476640	Gloucester County, New Jersey	$SUVA = 0.027 \cdot \ln(GPP32) + 4.01$	-0.160	0.859
01477440	Salem County, New Jersey	$SUVA = 0.109 \cdot \ln(GPP32) + 3.442$	-0.040	0.441
01482500	Salem County, New Jersey	$SUVA = 0.051 \cdot \ln(GPP32) + 3.149$	-0.002	0.340
01482520	Salem County, New Jersey	$SUVA = 0.262 \cdot \ln(GPP32) + 2.144$	0.414	0.051
01482530	Salem County, New Jersey	$SUVA = -0.033 \cdot \ln(GPP32) + 2.778$	-0.193	0.874
01482645	Salem County, New Jersey	$SUVA = -0.097 \cdot \ln(GPP32) + 3.591$	-0.147	0.759
01493500	Kent County, Maryland	$SUVA = -0.008 \cdot \ln(GPP32) + 2.963$	-0.045	0.948
02172304	Aiken County, South Carolina	$SUVA = -4.939 \cdot \ln(GPP32) + 31.744$	-0.041	0.421
07288625	Bolivar County, Mississippi	$SUVA = 0.004 \cdot \ln(GPP32) + 2.699$	-0.250	0.985
14161500	Lane County, Oregon	$SUVA = 0.062 \cdot \ln(GPP32) + 2.47$	-0.015	0.651
14205400	Washington County, Oregon	$SUVA = -0.031 \cdot \ln(GPP32) + 3.703$	-0.139	0.887
14206435	Washington County, Oregon	$SUVA = 0.097 \cdot \ln(GPP32) + 2.543$	0.045	0.072
333150090530400	Bolivar County, Mississippi	$SUVA = 0.182 \cdot \ln(GPP32) + 1.579$	0.025	0.105
3343250813616	Aiken County, South Carolina	$SUVA = 1.178 \cdot \ln(GPP32) + -3.113$	0.101	0.315
3344250813538	Aiken County, South Carolina	$SUVA = 0.711 \cdot \ln(GPP32) + 0.135$	0.094	0.285
3344580813559	Aiken County, South Carolina	$SUVA = 0.093 \cdot \ln(GPP32) + 3.749$	-0.329	0.931
3345100813509	Aiken County, South Carolina	$SUVA = 0.061 \cdot \ln(GPP32) + 3.544$	-0.245	0.909

Table A.6. Table showing the regression equations, R^2 , and p -value for specific ultraviolet absorbance at 254nm ($SUVA_{254}$) vs. stormflow ratio (S_R) in individual basins.

USGS Station	Location	Regression equation	R^2	p
01493500	Kent County, Maryland	$SUVA = 0.41 \cdot SR + 14.402$	0.136	0.043
05451080	Hamilton County, Iowa	$SUVA = 0.74 \cdot SR + 12.125$	0.297	0.000
01367800	Sussex County, New Jersey	$SUVA = -0.132 \cdot SR + 40.954$	-0.043	0.726
01377500	Bergen County, New Jersey	$SUVA = -1.92 \cdot SR + 21.476$	0.285	0.125
01394500	Union County, New Jersey	$SUVA = 0.279 \cdot SR + 18.421$	0.003	0.296
01398000	Hunterdon County, New Jersey	$SUVA = 0.424 \cdot SR + 16.113$	0.040	0.111
01407760	Monmouth County, New Jersey	$SUVA = -0.44 \cdot SR + 60.387$	-0.007	0.384
01410150	Burlington County, New Jersey	$SUVA = -0.007 \cdot SR + 136.214$	-0.022	0.988
01411300	Cape May County, New Jersey	$SUVA = -1.687 \cdot SR + 173.279$	0.030	0.312
01412800	Cumberland County, New Jersey	$SUVA = -0.395 \cdot SR + 40.42$	-0.031	0.587
01466500	Burlington County, New Jersey	$SUVA = -0.408 \cdot SR + 90.77$	0.124	0.071
01467150	Camden County, New Jersey	$SUVA = 1.146 \cdot SR + 36.227$	0.023	0.161
01482500	Salem County, New Jersey	$SUVA = 0.068 \cdot SR + 31.414$	-0.038	0.834
02172300	Aiken County, South Carolina	$SUVA = -0.746 \cdot SR + 64.448$	-0.140	0.568
02172305	Aiken County, South Carolina	$SUVA = -0.376 \cdot SR + 60.379$	0.003	0.299
03361638	Hancock County, Indiana	$SUVA = -0.573 \cdot SR + 24.696$	0.040	0.136
04087204	Milwaukee County, Wisconsin	$SUVA = -0.029 \cdot SR + 21.761$	-0.027	0.915
14161500	Lane County, Oregon	$SUVA = 0.61 \cdot SR + 15.07$	-0.001	0.330
14205400	Washington County, Oregon	$SUVA = 0.612 \cdot SR + 32.762$	-0.091	0.581